

TALLINN UNIVERSITY OF TECHNOLOGY
DOCTORAL THESIS
25/2018

Structure and Regulation of Arachidonate 11R-lipoxygenase

PRIIT EEK



TALLINN UNIVERSITY OF TECHNOLOGY
School of Science
Department of Chemistry and Biotechnology

This dissertation was accepted for the defense of the degree of Doctor of Philosophy in Chemistry on 11 May, 2018.

Supervisor: Nigulas Samel, PhD
Department of Chemistry and Biotechnology,
Tallinn University of Technology, Estonia

Co-supervisor: Ivar Järving, PhD
Department of Chemistry and Biotechnology,
Tallinn University of Technology, Estonia

Opponents: Hartmut Kühn, MD, DSc
Institute of Biochemistry,
Charité — University Medicine Berlin, Germany

Juhan Sedman, PhD
Institute of Molecular and Cell Biology,
University of Tartu, Estonia

Defense of the thesis: 13 June, 2018, Tallinn

Declaration:

I hereby declare that this doctoral thesis, submitted for the doctoral degree at Tallinn University of Technology, is my original investigation and achievement and has not been previously submitted for a doctoral or an equivalent academic degree.

Priit Eek

Copyright: Priit Eek, 2018, Creative Commons Attribution-NonCommercial-NoDerivatives 4.0 International License

Colophon: This thesis was typeset with \LaTeX 2 ϵ using André Miede's *classicthesis* style with modifications by David Schryer, Ardo Illaste, Martin Laasmaa, and Priit Eek to conform with the style guidelines provided by Tallinn University of Technology. The main font is Carlito.



European Union
European Regional
Development Fund



Investing
in your future

ISSN 2585-6898 (publication)

ISBN 978-9949-83-265-1 (publication)

ISSN 2585-6901 (PDF)

ISBN 978-9949-83-266-8 (PDF)

TALLINNA TEHNIKAÜLIKOO
DOKTORITÖÖ
25/2018

Arahhidoonhappe 11R-lipoksügenaasi struktuur ja regulatsioon

PRIIT EEK

CONTENTS

LIST OF PUBLICATIONS	7
INTRODUCTION	9
ABBREVIATIONS	11
1 LITERATURE REVIEW	13
1.1 Concerning nomenclature	13
1.2 Diversity and biological functions	15
1.3 Overall tertiary structure	17
1.3.1 PLAT domain	17
1.3.2 Catalytic domain	18
1.4 Lipoxygenation mechanism	21
1.5 Determinants of catalytic specificity	22
1.5.1 Positioning of the substrate	22
1.5.2 Oxygen channeling	23
1.6 Post-translational and allosteric regulation	24
1.6.1 Regulation of ALOX5	25
1.6.2 Allosteric effectors of other lipoxygenases	26
1.6.3 Dimerization	26
1.7 Arachidonate 11R-lipoxygenase	27
2 AIMS OF THE STUDY	29
3 MATERIALS AND METHODS	31
4 RESULTS	33
4.1 Overall crystal structure (Publication I)	33
4.2 Mode of substrate binding (Publication I)	35
4.3 Allosteric regulation (Publications I and II)	35
4.4 Dimer assembly (Publication III)	36
5 DISCUSSION	37
5.1 Regulation at the active site	37
5.1.1 Limiting access to the active site	38
5.1.2 Substrate tethering	38
5.2 Allosteric regulation	39
5.2.1 Role of the PLAT domain	39
5.2.2 Allostery related to quaternary structure	40
CONCLUSIONS	43
REFERENCES	45
ACKNOWLEDGMENTS	57
ABSTRACT	59
KOKKUVÖTE	61

CONTENTS

PUBLICATION I	63
PUBLICATION II	81
PUBLICATION III	91
CURRICULUM VITAE	105
ELULOOKIRJELDUS	109

LIST OF PUBLICATIONS

THIS THESIS IS BASED ON THE FOLLOWING PUBLICATIONS, which are cited in the text using the corresponding Roman numerals:

- I **P. Eek**, R. Järving, I. Järving, N.C. Gilbert, M.E. Newcomer, N. Samel, Structure of a calcium-dependent 11R-lipoxygenase suggests a mechanism for Ca²⁺ regulation., *J. Biol. Chem.* 287 (2012) 22377–22386.
- II **P. Eek**, M.-A. Piht, M. Rätsep, A. Freiberg, I. Järving, N. Samel, A conserved π -cation and an electrostatic bridge are essential for 11R-lipoxygenase catalysis and structural stability., *Biochim. Biophys. Acta* 1851 (2015) 1377–1382.
- III **P. Eek**, K. Pöldemaa, S. Kasvandik, I. Järving, N. Samel, A PDZ-like domain mediates the dimerization of 11R-lipoxygenase., *Biochim. Biophys. Acta* 1862 (2017) 1121–1128.

SUMMARY OF THE AUTHOR'S CONTRIBUTIONS

- I The author contributed to designing the experiments, performed the experimental work, analyzed and interpreted the data, and wrote the manuscript.
- II The author designed the experiments, participated in experimental work, performed the thermal stability assays, analyzed and interpreted the data, and wrote the manuscript.
- III The author designed the experiments, participated in the experimental work, performed the small-angle X-ray scattering experiment and structure modeling, analyzed and interpreted the data, and wrote the manuscript.

INTRODUCTION

LIPXYGENASES (LOXs) are a family of polyunsaturated fatty acid peroxidizing enzymes that have been of interest as pharmacological targets for decades. This is hardly surprising since deviations in the functioning of the several LOX isoforms in humans manifest in pathologies ranging from inflammation-related conditions like asthma and atherosclerosis to genetic disorders like ichthyosis. In recent years, LOXs have also been concerned with the dispute about healthy diet: depending on the fatty acid substrate species, either ω 3 or ω 6, lipoxygenation products tend to be anti-inflammatory and pro-resolving in one case, but the opposite in the other, thus a balance between these nutrients needs to be maintained. Failure to do so can contribute, for instance, to the progress of chronic vascular disorders.

Despite the prevalence of LOXs, only one LOX-targeting drug has actually reached the market at the time of writing this thesis: the 5-LOX inhibitor Zileuton for asthma treatment. One of the hurdles in designing specific inhibitors for LOXs is the relative similarity of the active sites among distinct isoforms—there are six of them in humans—that perform completely different functions. These enzymes differ not only in catalysis specificity or tissue localization, but also in activation and allosteric regulation. The latter could provide another means of pharmacological intervention besides active site ligands.

Research on human LOXs, especially structural work, has been arduous largely because of the instability of these enzymes. Interestingly, some very distant relatives of ours in the animal kingdom, Octocorals, have proven to be a valuable source of more stable LOXs, suitable for extensive experimentation. One such enzyme is the arachidonate 11R-LOX from the Arctic soft coral *Gersemia fruticosa*.

In the present thesis, the structure and regulatory mechanisms of 11R-LOX were investigated. The crystal structure of the enzyme was solved, which gave rise to new hypotheses regarding its molecular machinery. More specifically, binding of the substrate into the active site, interdomain communications, and quaternary interfaces were studied. The roles of possibly significant residues were probed by site-directed mutagenesis. Mutant enzymes were subjected to various assays to evaluate the effect on the functionality of the enzyme. Additional in-solution structural data was obtained with small-angle X-ray scattering and chemical cross-linking. This allowed to determine the dimeric assembly of 11R-LOX, which makes it the first LOX with a known quaternary structure at a near-atomic resolution.

These data provide novel insight into the workings of LOXs, and have already contributed to widen our understanding of these enzymes. Hopefully, this knowledge can be put into good use to design better pharmaceuticals or to comprehend allosteric mechanisms and protein-protein interactions.

ABBREVIATIONS

AA	arachidonic acid
AOS	allene oxide synthase
CD	circular dichroism
CLP	coactosin-like protein
DSF	differential scanning fluorimetry
FLAP	5-LOX activating protein
HpETE	hydroperoxyeicosatetraenoic acid
HPLC	high-performance liquid chromatography
HpODE	hydroperoxyoctadecadienoic acid
LA	linoleic acid
LOX	lipoxygenase
LT	leukotriene
MS	mass spectrometry
OS	oleyl sulfate
PC	phosphatidylcholine
PE	phosphatidylethanolamine
PS	phosphatidylserine
PUFA	polyunsaturated fatty acid
SAXS	small-angle X-ray scattering
SEC	size exclusion chromatography

LITERATURE REVIEW

LIPOXYGENASES (LOXs) are oxidoreductases that catalyze the peroxidation of polyunsaturated fatty acids (PUFAs) by the addition of dioxygen. The reaction specificity is generally under strict regio- and stereocontrol, so a single predominant fatty acid hydroperoxide is produced from any suitable substrate [1]. These enzymes are widely spread among living organisms, being endogenous to most eukaryotes, including animals, plants and fungi, but also to some bacteria [2]. The main substrate in animals is arachidonic acid (AA), which is converted into hydroperoxyeicosatetraenoic acids (HpETEs). In plants, linoleic acid (LA) is utilized to yield hydroperoxyoctadecadienoic acids (HpODEs). The products can serve as precursors for the synthesis of various lipid mediators, or can act as such on their own [3-5].

The principal method for determining protein structures at (near-)atomic resolution is X-ray crystallography. To date, there are 62 crystal structure models of various LOXs published in the PDB database (www.rcsb.org), though that number also includes mutated variants of already known structures. If we disregard those duplicates, we are left with 33 models of 16 unique LOXs, listed collectively in Table 1. Four of these are plant LOXs, all from soybean (*Glycine max*), another three are from bacteria, two from fungi, and seven of animal origin.

Animal LOXs generally consist of a single polypeptide chain that folds into two distinct domains: a smaller N-terminal regulatory domain, and a larger C-terminal catalytic domain [33]. Although plant LOXs are built upon the same two-domain framework, they contain several insertions that form additional loops and helices on the protein surface [15, 18, 26]. These alterations do not necessarily affect the enclosed active site and catalytic activity, but changes in the activation and regulation of the enzyme are likely. Bacterial and fungal LOXs tend to lack the common regulatory domain altogether, and feature alternative α -helical N-termini instead [27-29].

The extensive structural and functional research conducted on LOXs from plants and microorganisms provides valuable information about the active site and actual catalysis, since the inner core of the enzyme is rather conserved. However, in order to draw reasonable conclusions on the regulatory aspects of human LOXs, which are potential drug targets, enzymes that bear more similar features in peripheral regions need to be studied.

1.1 CONCERNING NOMENCLATURE

Historically, LOXs have been named according to the catalytic specificity towards their primary endogenous substrate. For example, human 5-LOX oxygenates AA at the 5th carbon,

LITERATURE REVIEW

Table 1 – LOX structures published in the PDB. Mutant enzyme variants have been omitted.

Organism	Protein	PDB ID	Resolution (Å)	Reference and remarks
Animals				
<i>Gerseemia fruticosa</i>	11R-LOX	3VF1	2.47	Publication I
<i>Homo sapiens</i>	ALOX5	3O8Y	2.39	[6], stabilized mutant
	ALOX12	3D3L	2.6	-, mutated catalytic domain only
	ALOX15B	4NRE	2.63	[7], detergent C8E4 complex
<i>Oryctolagus cuniculus</i>	ALOX15	1LOX	2.4	[8], inhibitor RS75091 complex
		2POM	2.4	[9], reinterpretation of 1LOX data
<i>Plexaura homomalla</i>	8R-LOX	2FNQ	3.2	[10], part of AOS-LOX fusion protein
		3FG1	1.85	[11], PLAT domain loop truncation
		4QWT	2.0	[12], substrate AA complex
<i>Sus scrofa</i>	ALOX15	3RDE	1.89	[13], catalytic domain with inhibitor OPP
Plants				
<i>Glycine max</i>	LOX-1	2SBL	2.6	[14]
		1YGE	1.4	[15]
		1F8N	1.4	[16], re-refinement of 1YGE data
		3PZW	1.4	[17], re-refinement of 1YGE data
		1LNH	2.6	[18]
	LOX-3	1IK3	2.0	[19], 13(S)-HODE complex
		1HU9	2.2	[20], curcumin complex
		1JNQ	2.1	[21], EGCG complex
		1N8Q	2.1	[22], protocatechuic acid complex
		1NO3	2.15	[23], 4-nitrocatechol complex
		1ROV	2.0	[24], oxidized active site
		1RRH, 1RRL	2.0, 2.09	[25], ambient vs cryo-temperature
		2IUJ	2.4	[26]
	LOX-B	2IUJ	2.4	[26]
	LOX-D	2IUK	2.4	[26]
Bacteria				
<i>Cyanothece</i> sp. PCC 8801	Csp-LOX-1	5EK8	2.7	[27]
	Csp-LOX-2	5MED	1.8	[28]
<i>Pseudomonas aeruginosa</i>	Pa-LOX	4G32, 4G33	1.75, 2.03	[29], phospholipid complex
		5IR4, 5IR5	1.48, 1.9	[30], phospholipid complex
Fungi				
<i>Gaeumannomyces graminis</i>	Gg-MnLOX	5FX8	2.6	[31], manganese LOX
<i>Magnaporthe oryzae</i>	Mo-MnLOX	5FNO	2.04	[32], manganese LOX

producing 5(S)-HpETE. *S*-stereospecificity is often omitted from the name, since the first LOXs studied were all *S*-specific. *R*-LOXs, which were discovered later, are usually labeled explicitly. This is also practiced if two LOXs with the same regio-, but different stereospecificity are under discussion (e.g. human 12*S*- and 12*R*-LOX). Stating the source tissue or cell type has been another means for distinguishing paralogs, i.e., distinct LOX isoforms in an organism.

This system is rational in a purely functional sense, but falls short once homologous enzymes need to be compared in an evolutionary aspect. The catalytic specificity is not always constant over genetic lineages: while the enzyme trivially called 15-LOX-2 catalyzes 15*S*-lipoxygenation in humans, its murine ortholog is in fact an arachidonate 8*S*-LOX [34]. To overcome this source of confusion, at least among mammalian LOXs, it has been suggested to address these enzymes by their respective gene names [33, 35]. In the previous example, both human and murine enzymes would be referred to as ALOX15B.

Since catalytic specificity is one of the subjects of this study, the product-based nomenclature is provided in the thesis wherever applicable and necessary to convey the message. For mammalian LOXs, however, the gene-based names are preferred.

1.2 DIVERSITY AND BIOLOGICAL FUNCTIONS

The mechanism of LOX catalysis, viewed in detail in Section 1.4 Lipoxygenation mechanism, enables the production of multiple different peroxy-derivatives from a single substrate PUFA. This creates a possibility of having alternative enzyme forms with differing product specificities. Indeed, there are six functional LOX isoforms in humans, encoded by genes ALOX5, ALOX12, ALOX12B, ALOXE3, ALOX15 and ALOX15B, each with a unique set of properties summarized in Table 2. The role of LOX catalysis by the different enzyme variants—not only in humans, but all LOX-containing organisms—spans from the synthesis of lipid mediators to the modification of biomembranes [2, 3, 36, 37]. These affect regulation of inflammation, cell differentiation and proliferation, and oxidative stress. Consequently, the pathologies that can be related to or modified by LOX activity include a wide range of conditions such as asthma, atherosclerosis, ichthyosis, atherothrombosis, carcinogenesis, diabetes, and neurodegenerative disorders. In general, the actions LOXs perform in an organism can be classified into three categories, illustrated in Figure 1.

Table 2 – Human LOXs and their properties [36].

Gene	Common names	Main substrates	Main products	Biological functions
ALOX5	5-LOX	AA	5(S)-HpETE, LTA ₄	leukotriene production, inflammatory mediators
ALOX12	platelet 12-LOX	AA	12(S)-HpETE	modulation of platelet aggregation
ALOX12B	12 <i>R</i> -LOX	linoleoyl- ω -hydroxyceramide	9(<i>R</i>)-hydroperoxy-linoleoyl- ω -hydroxyceramide	maintenance of epidermal permeability barrier
ALOXE3	eLOX3	9(<i>R</i>)-hydroperoxy-linoleoyl- ω -hydroxyceramide	9(<i>R</i>),10(<i>R</i>)-epoxy-13(<i>R</i>)-hydroxy-linoleoyl- ω -hydroxyceramide	maintenance of epidermal permeability barrier
ALOX15	15-LOX-1, 12/15-LOX, leukocyte 12-LOX	free and esterified PUFAs	15(S)- and 12(S)-HpETE (from AA)	inflammatory mediators, membrane oxidation
ALOX15B	15-LOX-2	AA	15(S)-HpETE	negative cell cycle regulation, tumor suppression

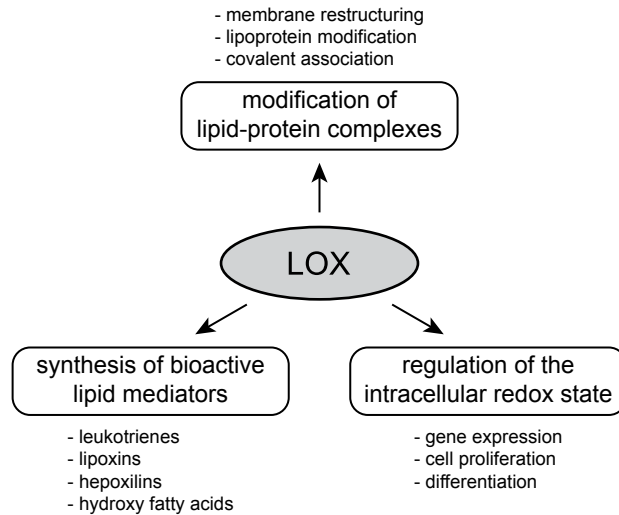


Figure 1 – Biological functions of LOXs. Figure reproduced from [3].

The most well-established and studied function is the production of hydroperoxy derivatives of PUFAs that serve as precursors for a myriad of bioactive compounds like leukotrienes (LTs), lipoxins, hepxilins, eoxins and resolvins in mammals [2, 3], volatile aldehydes and jasmonates in plants [38], and other oxylipins in fungi and bacteria [39]. These lipid mediators participate in inflammatory processes—both inducing and resolving—and in overall stress response. LTs and eoxins, for instance, are strong pro-inflammatory agents, whereas lipoxins and resolvins promote return to homeostasis [3]. Jasmonates mediate stress response in plants, e.g., to counter with wounding, insect attack, or other environmental sources of stress, but participate also in developmental processes like seed germination [40]. Similar functions have been attributed to eicosanoids in octocorals, where the expression of an allene oxide synthase (AOS)–LOX fusion protein was found to be up-regulated in response to wounding and thermal stress [41, 42].

While most LOXs prefer free fatty acids as substrates, some are also able to catalyze the oxygenation of PUFAs incorporated into complex lipids. By modifying the lipid membrane structure, these LOXs contribute to cell development, e.g., erythropoiesis, epidermal differentiation, and skin development [3]. In addition, it has recently been hypothesized that the secreted LOX from the opportunistic pathogen *Pseudomonas aeruginosa* could induce hemolysis by oxygenating erythrocyte membranes [43], or participate in biofilm growth on host tissue [44].

There are many factors that affect the intracellular redox state, but LOX-formed lipid peroxides are nevertheless important contributors to the oxidative side of the equilibrium [3]. The redox state regulates cell proliferation and gene expression, hence LOX catalysis can impact these processes. Some of the pro-carcinogenic effects of LOXs can be attributed to the increased oxidative stress, as can be their role in neurodegenerative disorders like Alzheimer's and Parkinson's disease [45, 46].

In addition to canonical lipoxygenation, some LOXs display slightly alternative catalytic activities. Enzymes with lipohydroperoxidase (or hydroperoxide isomerase) activity catalyze the conversion of fatty acid peroxides, i.e., products of previous lipoxygenation, into secondary peroxidation products like ketodienes, epoxy hydroxy compounds, short chain aldehydes, etc. [35]. A remarkable example of this is human ALOXE3, expressed in the epidermis, that predominantly converts esterified 12(*R*)-HpODE, the product of ALOX12B catalysis, into a corresponding epoxyalcohol derivative [47]. This process is necessary in the skin water-barrier formation, as individuals with a loss-of-function mutation suffer from severe ichthyosis. Another alternative mode of LOX action is LT synthase activity. ALOX5, also known as 5-LOX and LTA₄ synthase, is the key enzyme in LT synthesis [2, 36, 48]. ALOX5 firstly converts AA into 5(*S*)-HpETE and subsequently catalyzes the dehydration of the hydroperoxide into an allylic epoxide, LTA₄. The highly unstable LTA₄ is then further converted by downstream enzymes into various LTs, which act as potent pro-inflammatory mediators.

1.3 OVERALL TERTIARY STRUCTURE

In 1993, Boyington et al. published the first LOX crystal structure of soybean (*G. max*) LOX-1 [14]. The resolution was improved a few years later to 1.4 Å by Minor et al. [15]. Rabbit (*Oryctolagus cuniculus*) reticulocyte 15S-LOX (ALOX15) was the first mammalian enzyme to follow in 1997 by Gillmor et al. [8], though the solution of the crystal structure was flawed due to overlooked crystal twinning. The data was reinterpreted only in 2008 to reveal the enzyme in two different conformations, with and without a bound inhibitor [9]. Despite this, the soybean and rabbit enzyme models laid the foundation for structure-based functional studies of LOXs already in the 90s.

The canonical tertiary structure of a LOX comprises of an N-terminal β-sandwich called the PLAT domain, which acts as a regulatory and membrane-binding module, and a C-terminal mostly α-helical catalytic domain, which harbors the active site [1, 5]. The enzyme is cylindrical in shape with the catalytic domain constituting the majority, and the smaller, relatively loosely attached β-sandwich at one end of the cylinder (Figure 2). The single polypeptide chain of an animal LOX is about 660 residues long (~110 in PLAT and ~540 in catalytic domain). Plant enzymes are considerably larger (~900 amino acids) thanks to several additional loops.

1.3.1 PLAT domain

The N-terminal β-fold was at first called a C2-like domain due to its similarity to the structure found in lipases, but is now classified as PLAT domain, the acronym deriving from three representative proteins: polycystin-1, lipoxygenase, and α-toxin [50]. It is a β-sandwich of two four-strand antiparallel sheets, and it constitutes about a sixth of the whole protein chain. The domain functions as a Ca²⁺-activated membrane-targeting module in several animal LOXs including human ALOX5 [51, 52], ALOX15 [53, 54] and ALOX15B [55].

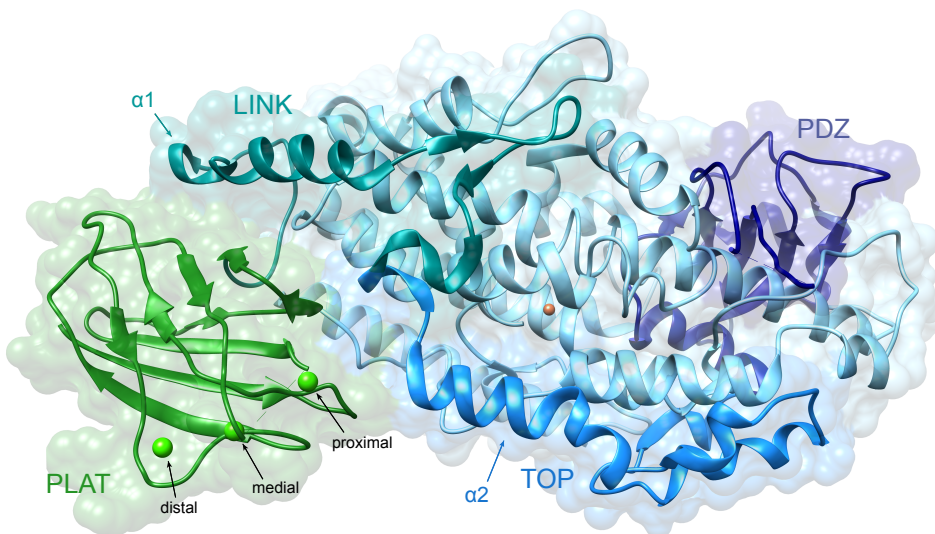


Figure 2 – Crystal structure model of the coral 8R-LOX (PDB ID: 2FNQ). The PLAT domain (green) binds three calcium ions, labeled “distal”, “medial”, and “proximal”. The catalytic domain (hues of blue) is divided into subregions as in [49]. Moving along the chain from N- towards C-terminus, the LINK region connects the N-terminal PLAT domain to the catalytic part, the following TOP region envelopes the entrance to the active site with helix $\alpha 2$, and the PDZ-like subdomain constitutes another potential regulatory unit. The rest of the catalytic domain is the core that defines the active site with the prosthetic iron (brown sphere).

The crystal structure of the arachidonate 8R-LOX from the soft coral *Plexaura homomalla* revealed three Ca^{2+} -binding sites between the loops on one edge of the domain (Figure 2) [10]. In the thesis, these are referred to as “distal”, “medial”, and “proximal” sites with respect to their position relative to the catalytic domain. The binding clusters are defined by negatively charged or polar (Asp, Asn, Glu) side chains and carbonylic oxygens from the backbone. The sites coincide with the ones identified in *Clostridium perfringens* α -toxin [56]. Despite that, the coordinating residues are not highly conserved; for instance, only two sites (distal and proximal) can be found in human ALOX15B [7].

The same loops that constitute Ca^{2+} -binding sites may also contain bulky hydrophobic residues that can submerge into a lipid bilayer. In the 8R-LOX model, two tryptophanes are exposed on extended loops, and replacing them with alanines impaired membrane binding [10]. Likewise, human ALOX15B displays a hydrophobic proline-rich β -hairpin that protrudes from the PLAT domain and is stabilized by the proximal Ca^{2+} site [7]. Deletion of this loop hindered membrane association, so the hairpin likely acts as a membrane-insertion motif [57]. In ALOX5, three exposed tryptophanes (Trp¹³, Trp⁷⁵, Trp¹⁰²) have been implicated in membrane anchoring [52].

1.3.2 Catalytic domain

In contrast to the PLAT domain, the catalytic domain is largely a helical bundle, the two longest helices containing over 40 amino acid residues. The active site is inside a deep and narrow cavity situated roughly in the center of the domain, where it harbors a prosthetic

non-heme iron [1] (Figure 3A). The iron is pseudo-octagonally coordinated by three invariant histidines, provided by the two longest helices that constitute the core of the LOX fold, and the carboxyl group of the invariant C-terminal isoleucine (Figure 3B). Another weaker ligand is an Asn/His/Ser residue, which is more distant to the metal ion, but fits into the distorted coordination sphere [5, 15]. In crystallographic models, the sixth ligand to the iron is a water molecule that is also necessary for bridging the redox reaction during catalysis [16].

The exact binding mode of the fatty acid substrate in the LOX active site was a matter of debate for a long time, since in order to halt the enzyme:substrate complex in the productive conformation, one had to completely remove the second substrate, O₂, from the environment. Neau et al. succeeded in that in 2014 by soaking AA into coral 8R-LOX crystals in a glovebox, which had been thoroughly equilibrated with nitrogen [12]. The resulting crystal structure confirmed the prevalent hypothesis: the active site is mainly defined by four helices oriented roughly in an antiparallel fashion along the axis of the cylindrical protein [12, 15] (Figure 3). The two longest helical segments of the catalytic domain, which provide His-ligands to the non-heme iron, wall the site on the core side. On the surface side, an arched or discontinuous helix features a reverse turn just over the site to form the main cavity. Lastly, the penultimate helix of the protein seals the bottom part of the substrate channel. The entrance to the substrate-binding channel is between the arched and the penultimate helix, and is lined by helix α_2 . The channel continues to the catalytic site by the non-heme iron, then makes a sharp turn away from the PLAT domain, and ends with a hydrophobic pocket. Another narrow discontinuous tunnel reaches from the catalytic center to the surface on the other side of the arched helix. This is the putative O₂ access route [12, 28, 58].

Jankun et al. proposed that the N-terminal portion of the catalytic domain could be divided into smaller subdomains, each with a distinct role [49]. The hypothesis was prompted by small-angle X-ray scattering (SAXS) analysis of human ALOX12 that suggested the relative mobility of not only the N-terminal PLAT domain, but also the $\alpha+\beta$ formation in the other end of the catalytic domain [59]. This subdomain consists of a five-strand antiparallel β -sheet flanked by two to three helices. The CATH database lists an NTF2 topology in that region of several LOXs, but the authors concluded that the fold bears notably greater resemblance to PDZ domains—a family of heterologous folds that are known to participate in protein-protein interactions mostly by binding the C-termini of peptides [60, 61]. According to their model, the chain segment between PLAT and PDZ domains is split into two sections: first, the ~50 residues directly following the PLAT domain including helix α_1 comprise the LINK region; and second, the chain including helix α_2 , which passes the entrance to the substrate channel, constitutes the TOP region (Figure 2). The rest of the C-terminal part of the enzyme is the true catalytic domain, a helical bundle that forms the catalytic site together with the iron coordination sphere. The role of LINK and TOP segments would be to connect the regulatory PLAT and PDZ domains with the active site to convey their regulatory effect to the catalytic apparatus.

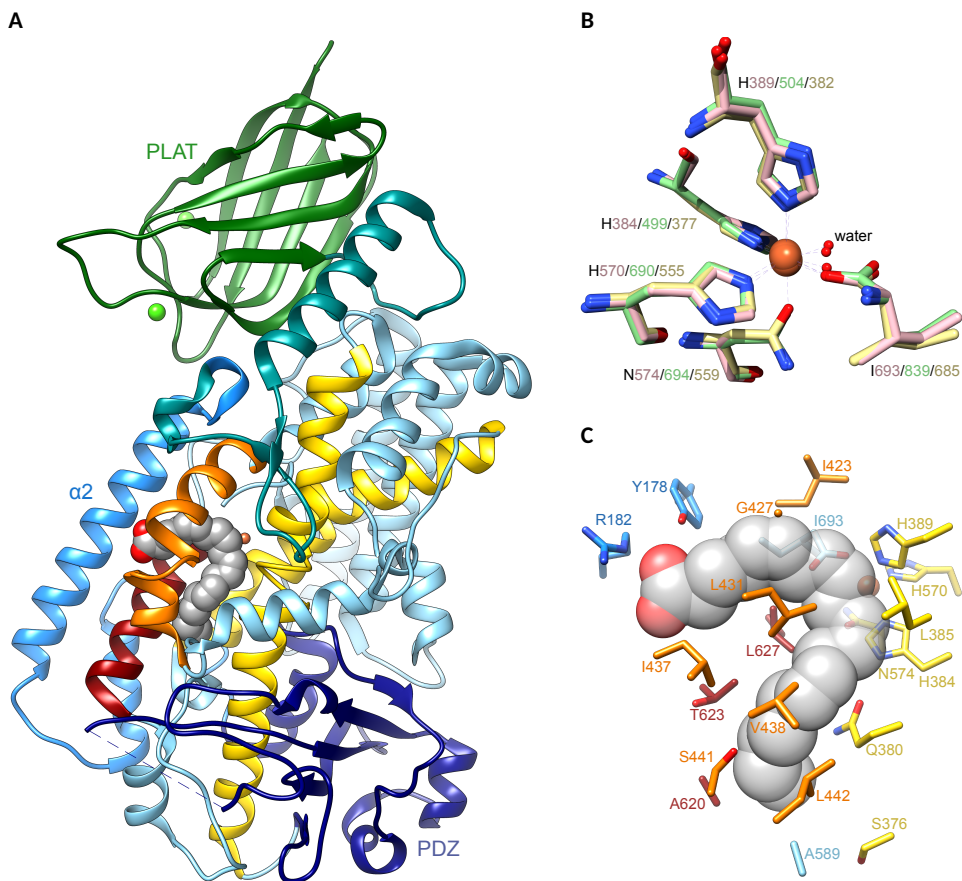


Figure 3 – Crystal structure model of the coral 8R-LOX with AA bound in its active site (PDB ID: 4QWT). (A) The helices that define the substrate-binding channel are highlighted: the core helices are in yellow, the discontinuous arched helix in orange, and the penultimate helix in red. AA is depicted as a *space-filling molecule* and the non-heme iron in the active site is a *brown sphere*. Helix $\alpha 2$ passes the entrance to the substrate channel. The rest of the structure is colored as in Figure 2. (B) Coordination sphere of the prosthetic iron in the catalytic center. In addition to 8R-LOX (pink), which is of animal origin, a plant (soybean LOX-1, 3PZW, green) and a bacterial LOX (Pa-LOX, 5IR4, yellow) have been superposed. (C) Active site of 8R-LOX with AA. The residues that outline the active site together with the substrate-binding channel are displayed. The colors of the residues and the rough orientation correspond to panel A.

1.4 LIPOXYGENATION MECHANISM

The non-heme iron, coordinated in the active site of a LOX, initiates the catalytic cycle [1, 33, 62]. The iron must be oxidized to its ferric form (Fe^{3+}) beforehand, which is likely carried out by any peroxides available in the solution. The substrate PUFA is then bound to the active site so that a bisallylic sp^3 carbon is tethered near the iron. This alignment is the first specificity-determining step since the following radical reaction is confined to the selected pentadiene fragment of the PUFA. The determinants behind substrate positioning are viewed in detail in Section 1.5 Determinants of catalytic specificity.

The first step of the conversion is hydrogen abstraction from the bisallylic methylene group, leading to radical formation (Figure 4a). This process utilizes proton-coupled electron transfer: an electron from the breaking C–H bond is tunneled to the iron over the leaving proton and the oxygen of a hydroxide ion, which is chelated to the iron [16, 63, 64]. As a result, the iron is reduced to Fe^{2+} . In the newly formed conjugated pentadienyl system, the radical can relocate either to -2 or $+2$ carbon relative to the point of abstraction (Figure 4b). Next, molecular oxygen merges to one of those positions, giving a peroxy radical (Figure 4c). The choice between the two alternatives is mainly determined by a single Gly/Ala residue [65, 66], also discussed in Section 1.5 Determinants of catalytic specificity. As hydrogen abstraction and oxygen insertion are strictly in an antarafacial relationship, i.e., these events take place on the opposite sides of the substrate, the position of O_2 insertion also determines the absolute configuration of the product [67]. Lastly, the radical

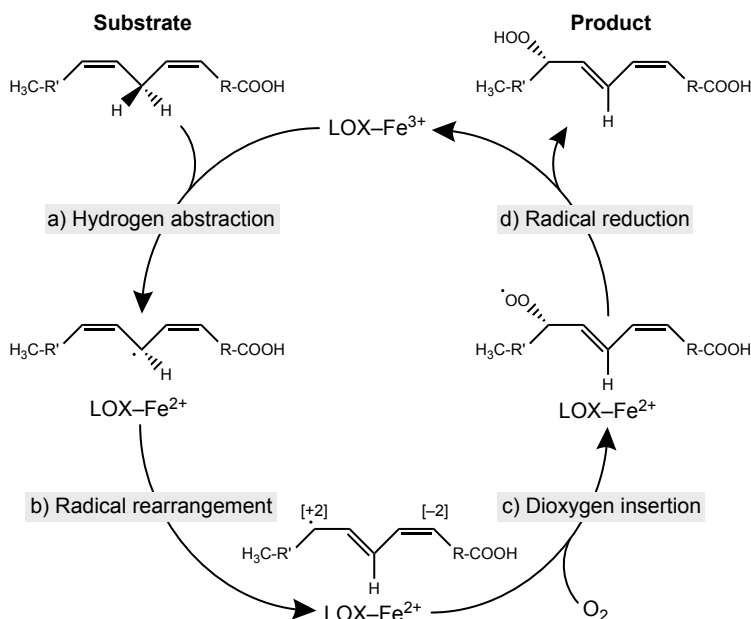


Figure 4 – Catalytic cycle of LOXs is driven by the $\text{Fe}^{2+}/\text{Fe}^{3+}$ redox reaction. The substrate PUFA is converted into a hydroperoxide by a radical mechanism, which involves hydrogen abstraction from the bisallylic methylene of a pentadiene fragment, and subsequent dioxygen insertion either at -2 or $+2$ position. Figure reproduced from [33].

is reduced to yield a hydroperoxy fatty acid (Figure 4d). The iron is simultaneously oxidized to Fe^{3+} , returning the enzyme ready for the next catalytic cycle.

1.5 DETERMINANTS OF CATALYTIC SPECIFICITY

There are two elementary reactions in LOX catalysis that determine the final configuration of the PUFA hydroperoxy derivative: firstly, the homolytic hydrogen abstraction from a bisallylic methylene group, and secondly, the antarafacial addition of molecular oxygen to either end of the newly-formed pentadienyl radical [1]. These steps are controlled by the shape of the active site, that is, directed by the residues which line the substrate-binding channel and interact with the fatty acid. In theory, it is possible to obtain twelve different hydroperoxy derivatives from AA by lipoxygenation, provided that enzymes with each specificity exist (Figure 5). An overview of the key residues that determine the course of catalysis is given below.

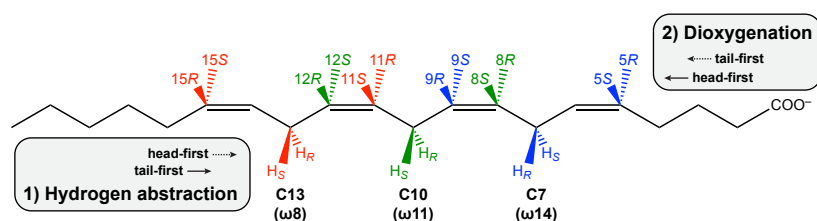


Figure 5 - Twelve possibilities of AA lipoxygenation. Initially, either *proS* or *proR* hydrogen is removed from a bisallylic methylene (C7, C10 or C13). The reactive side of the molecule is determined by the orientation of the substrate in the binding channel, either aliphatic tail- or carboxylate head-first. Then, O_2 merges to either -2 or +2 carbon (grouped by colors) on the other side of the molecule. For example, the removal of *proS* hydrogen from C13 can lead to either 11(R)- or 15(S)-HpETE formation.

1.5.1 Positioning of the substrate

Extensive studies employing mutations in the active site revealed that the depth of the substrate-binding channel is a major factor for determining the positional specificity in several LOXs [68–70]. A “frameshift” in hydrogen abstraction was induced in different ALOX15 orthologs by reducing the size of side chain moieties in the bottom of the cavity, the key residues in rabbit ALOX15 being Phe³⁵³, Ile⁴¹⁸, Met⁴¹⁹ and Ile⁵⁹³. Using site-directed mutagenesis, a 15S-lipoxygenating enzyme was transformed into a 12S-LOX. This indicated that the fatty acid enters the substrate channel of ALOX15 hydrophobic tail-first, and once more room is available, it can slide in deeper and expose the *proS* hydrogen at ω 11 instead of ω 8 for abstraction. It should be mentioned that both 12S- and 15S-lipoxygenating ALOX15 orthologs exist in nature, hence the trivial name 12/15-LOX. Frameshift-inducing mutations have been performed on several ALOX15 enzymes and also in the 12 → 15 direction [71, 72]. However, not all LOXs yield to this type of manipulation, that is, alterations to the depth of the binding pocket, so there are other factors that also affect substrate positioning [71]. For example, additional π - π and van der Waals interactions with the central part of the substrate also contribute to the correct productive placement [73].

A study on plant LOXs with a tritium-labeled substrate proved already in the 1970s that hydrogen removal can occur on both sides of the pentadiene fragment [74]. It was logically reasoned that the fatty acid may bind into the active site in opposite orientations. As already mentioned before, the murine version of ALOX15B is an 8S-LOX, whereas the human counterpart is a pure 15S-LOX. It was discovered that a pair of residues is mainly responsible for this variation: in the mouse ortholog these are Tyr⁶⁰³ and His⁶⁰⁴, which in the human enzyme correspond to Asp and Val [34]. Swapping these residues caused an exchange of specificity in both enzyme variants. The authors suggested that the effect is caused by a switch in binding the substrate head- vs tail-first. In 8S-LOX, the aromatic Tyr and positively charged His can tether the carboxylate group of the fatty acid and support head-first binding, while in 15S-LOX the negatively charged Asp causes repulsion and the hydrophobic Val favors aliphatic tail-first entry. Similarly, His⁶⁰⁰ of human ALOX5 participates in coordinating the fatty acid head in the bottom of the cavity [75]. pH-dependent reaction specificity has been observed in LOXs with charged side chains in the binding pocket, and the variations correlate with the charge state of the residues that might interact with the negative carboxylate in head-first binding mode [76, 77]. Furthermore, double dioxygenation of AA by some LOXs can be explained by the enzyme acting on the substrate twice in opposite orientations [78, 79]. The carboxylate group of the free fatty acid can be tethered also in the aliphatic tail-first binding orientation. For instance, Arg⁴⁰² near the active site entrance of human ALOX15 is important for proper substrate binding [73, 80]. In general, the orientation hypothesis is consistent with antarafacial hydrogen abstraction and oxygen insertion, and does not contradict with the frameshift concept, but complements it.

The most definitive evidence regarding substrate positioning comes from the co-crystal of the coral 8R-LOX with AA bound in its active site [12]. The binding mode and the residues that make up the active site are illustrated in Figure 3C. The fatty acid has entered the channel tail-first, so its methyl end is buried deep inside the pocket. The key residues that determine the 12/15-specificity of ALOX15 are Ser³⁷⁶, Ser⁴⁴¹, Leu⁴⁴² and Thr⁶²³ in 8R-LOX. These are rather compact and allow the substrate to penetrate deeper like in 12-lipoxygenating ALOX15 enzymes. At the entrance there is Arg¹⁸² that tethers the carboxylate head. Removing the positive charge from this position resulted in pronounced substrate inhibition [12]. In addition, there are several crystal structures available with substrate-mimicking inhibitors or phospholipids bound in the active site [7, 9, 13, 29, 30]. The binding modes in these models are all in agreement, so there is little doubt regarding the positioning of the substrate in LOXs.

1.5.2 Oxygen channeling

After hydrogen abstraction, O₂ can merge with the radical, and this happens preferentially two carbons away from the initial catalysis step. Whether it is -2 or +2, is determined by the so called Coffa determinant, a Gly/Ala switch that sterically directs the oxygen to the correct position [65–67]. Since the addition follows an antarafacial geometry, the residue concurrently dictates the stereoconfiguration of the product—an Ala directs the oxygen to *S*-configuration, while Gly enables the formation of an *R*-product. In the 8R-LOX model, this determinant is aptly Gly⁴²⁷. It is situated on the arched helix opposite to the iron, so

it is positioned just above the pentadienyl radical during catalysis (Figure 3C). The penta-diene system is surrounded by invariant leucines and isoleucines that aid to fasten the substrate and also shield its suprafacial side [12].

Although oxygen could infiltrate the active site using the same entrance as the substrate, there is also a visible tunnel in the model that begins from the surface on the other side of the arched helix and extends conveniently to Gly⁴²⁷. This putative oxygen channel has been observed in other LOX crystal structures as well [7, 28, 58]. Several mutagenesis studies coupled with computational modeling have substantiated the role of this specific access route in contrast to non-specific diffusion [81–84]. Once the oxygen reaches the active site, the Gly/Ala switch directs it to the correct end of the pentadienyl radical: a Gly residue enables access to the carbon closer to the active site entrance, whereas an Ala blocks it and guides the oxygen deeper into the binding pocket. There are exceptions, for instance, the determinant in a structurally atypical 12S-LOX (or LOX-1) from zebrafish (*Danio reio*) is Gly⁴¹⁰, yet the main product of AA conversion is 12(*S*)-HpETE [85, 86]. Furthermore, site-directed mutagenesis of the switch in several mammalian enzymes has resulted in only minor changes in catalysis specificity [85]. This suggests that oxygen addition is orchestrated in a more complex manner, and the Gly/Ala switch is only a part of the machinery, although an important one.

1.6 POST-TRANSLATIONAL AND ALLOSTERIC REGULATION

While most LOXs are able to acquire their substrate, a free fatty acid, from the solution, many prefer to work on the surface of a lipid bilayer. Association with lipid membranes is induced by Ca²⁺ binding in the N-terminal PLAT domain, which then mediates localization to the membrane. The activating effect of Ca²⁺-induced membrane binding has been demonstrated in various mammalian LOXs [7, 51–55], but also in enzymes from other animals [10, 87, 88] and plants [89, 90]. Despite this, neither the Ca²⁺ sites nor the membrane-binding loops are highly conserved.

Truncation of the N-terminal PLAT domain impairs, but does not abolish the catalytic activity in several mammalian LOXs, indicating that the domain does not participate in catalysis, but confers regulatory functions [59, 91, 92]. Although the two domains interact tightly in crystal structures, this does not necessarily hold true in solution. SAXS measurements of both ALOX12 and ALOX15 imply that there is a high degree of motional freedom between the domains, meaning the PLAT domain can swing away from the catalytic portion and expose the otherwise shielded interface [59, 93, 94]. The process of domain association/dissociation may induce further conformational changes that, in turn, impact enzymatic activity. However, not all LOXs display such flexibility—no major conformational changes were detected in soybean LOX-1 [95]. These results were confirmed by dynamic fluorescence measurements demonstrating the more flexible nature of rabbit ALOX15 in contrast to the plant enzyme [96].

1.6.1 Regulation of ALOX5

The most thoroughly studied LOX in terms of regulatory aspects is ALOX5 due to its prominent role in inflammation signaling [36, 48, 97, 98]. The PLAT domain of ALOX5 can bind two calcium ions with a K_D of about $6 \mu\text{M}$ [51, 99]. Ca^{2+} -binding likely stabilizes the coinciding membrane insertion loops and exposes bulky tryptophanes (Trp¹³, Trp⁷⁵, Trp¹⁰²) for membrane anchoring [52]. ALOX5 preferentially binds the nuclear envelope, rich with phosphatidylcholine (PC), and this selectivity is dictated by the aforementioned tryptophanes [52, 100, 101]. Additionally, some mono- and diglycerides (e.g. 1-oleyl-2-acetylglycerol) can stimulate ALOX5 catalysis *in vitro* in the absence of Ca^{2+} and phospholipid membranes by interacting through the same residues [102]. ATP stimulates ALOX5 activity and its association is sufficiently strong to enable purification of the enzyme by ATP-affinity chromatography. Covalent labeling identified two residues, Trp⁷⁵ and Trp²⁰¹, that likely interact with the adenine ring of ATP [103]. These are respectively situated in the PLAT domain in a membrane-binding loop, and in the TOP region between helix $\alpha 2$ and the PDZ-like subdomain. While the distance between these residues implies that two distinct binding sites exist, quantitation of the label indicated an equimolar binding ratio.

ALOX5 can be phosphorylated by various protein kinases [97]. Phosphorylations at Ser²⁷¹ and Ser⁶⁶³ can induce ALOX5 activity *in vitro*, affect intracellular localization, and may also lower the Ca^{2+} threshold necessary for enzyme activation. Phosphorylation of Ser⁵²³, on the other hand, suppresses ALOX5 catalysis and prevents its import into the nucleus. A phosphorylation-mimicking point mutation (S663D) was shown to convert ALOX5 to a 15-lipoxygenating enzyme, and consequently promote the synthesis of pro-resolving lipoxins [104]. However, these results could not be reproduced by others [105], and it was speculated that the conversion might have been partly due to additional stabilizing mutations present in the 5-LOX variant used in the study.

There are a number of scaffold proteins that bind ALOX5 and regulate its activity. 5-LOX activating protein (FLAP) is a transmembrane protein associated mainly with the nuclear envelope. Although it possesses no catalytic activity *per se*, nor is it obligatory for ALOX5 activity, FLAP is thought to facilitate catalysis by presenting AA to ALOX5, and it also promotes the conversion of the formed 5(S)-HpETE further into LTA_4 [106, 107]. Moreover, FLAP can form a complex with LTC_4 synthase, which is the next enzyme in the LT pathway utilizing LTA_4 as a substrate. These proteins and phospholipase A_2 , which liberates the fatty acid substrate from the membrane, are colocalized at the nuclear membrane in an orchestrated fashion to create a compartmentalized framework for LT synthesis [108]. A coactosin-like protein (CLP), which binds actin filaments, can also function as a scaffold to substitute PC, and it stimulates LTA_4 formation in the presence of lipid membranes [109]. Trp¹⁰² of ALOX5 was found essential for interaction with CLP, so the interface of the complex resides at the interdomain cleft of ALOX5 [110]. The C-terminal end of Dicer, a multidomain ribonuclease III that participates in microRNA biogenesis, can bind the PLAT domain at the membrane-insertion tryptophanes [111, 112]. The stimulatory effect is similar to CLP, but not as pronounced.

The crystal structure of a stabilized version of ALOX5 revealed that the entrance to the active site is blocked by a “cork” made up of Phe¹⁷⁷ and Tyr¹⁸¹ on helix $\alpha 2$ [6]. In most LOX structures, including coral 8R-LOX (Figure 3A), this helix is several turns long, but in ALOX5

it is short and flanked by extended loops enabling the blockage of the active site. This clearly indicates that extensive conformational changes must occur to facilitate substrate binding and catalysis. In recent years, the essence of this cleft and the interdomain cleft that binds the many effectors has been under active investigation in ALOX5 as well as in other LOXs [75, 113–115]. These studies are analyzed in more detail in Chapter 5 DISCUSSION.

1.6.2 *Allosteric effectors of other lipoxygenases*

To date, no ligand proteins have been identified for LOXs other than ALOX5. Besides activation by Ca^{2+} and lipid membranes, allosteric binding of fatty acid derivatives has been observed. Measurements of steady-state kinetics and kinetic isotope effects indicate that inhibition of soybean LOX-1 and human ALOX15 by oleyl sulfate (OS) does not follow a competitive mechanism, but suggest the existence of an alternative allosteric binding site instead [116]. Catalysis products of ALOX15 and ALOX15B, such as 15(S)-HpETE and 13(S)-HpODE, can affect these enzymes allosterically and impact their substrate selectivity (AA vs LA) [117, 118]. The allosteric site of ALOX15B was proposed to lie in the cleft between PLAT and catalytic domains, and involve His⁶²⁷ [119], but this has been questioned—a site in the catalytic domain has also been suggested [120].

Recently, a rational computational approach was used to design novel ligands that act as allosteric activators of ALOX15 [121]. The binding pocket of these compounds resides in the catalytic domain between the active site and the putative PDZ-like subdomain involving highly conserved residues Arg²⁴² and Asp²⁷⁷. Hence, the PLAT domain and the interdomain cleft are not the only locations that allow allosteric manipulation.

1.6.3 *Dimerization*

LOXs were considered to function strictly as monomeric units for a long time, but recent results concerning a number of mammalian enzymes have shifted this paradigm. ALOX5 [122], ALOX12 [59, 94] and ALOX15 [94, 123] all have been observed to assemble into dimers. The proposed quaternary structures are illustrated in Figure 6.

Under oxidizing conditions human ALOX5 is susceptible to dimerization via disulfide bridge formation [122]. The suggested assembly forms in a head-to-tail fashion, and interestingly, utilizes ATP-binding sites (residues 73–83 in the PLAT domain and 193–209 in the TOP region of the catalytic domain). This can explain the observed enzyme:ATP stoichiometry of 1:1 even with two identified binding sites [103]. However, the catalytically active unit of ALOX5 is the monomer as dimerization hinders both catalysis and Ca^{2+} -induced membrane binding [122, 124]. Controversially, an inactive ALOX5 isoform that lacks the majority of the TOP region was shown to stimulate the activity of the full-length enzyme at low protein concentrations [125]. It was speculated that this could be due to heterodimer formation, since ATP-binding sites are still intact in the deletion isoform.

SAXS studies revealed that ALOX12 functions minimally as a dimer, its monomers associate by their catalytic domains, and the assembly could involve either the TOP region including helix $\alpha 2$ or the putative PDZ-like domain [59, 94]. The PLAT domains face outwards away from each other, and loosely interact with the catalytic part. The dimers are prone

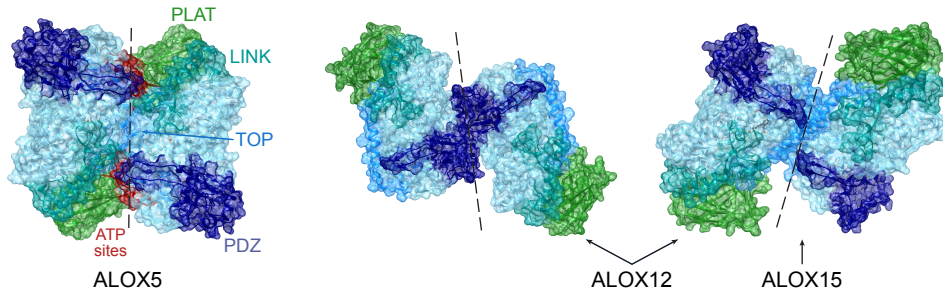


Figure 6 – Proposed dimer assemblies of mammalian LOXs. **ALOX5**: two crystallographic ALOX5 models (PDB ID: 3O8Y) are positioned so that their ATP-binding sites (red) overlap. **ALOX15**: the crystal structure model (PDB ID: 2POM) is a conformational heterodimer, connected mainly through $\alpha 2$ helices (TOP region). It should be noted that according to SAXS, PLAT domains can swing away from the catalytic part—this is not illustrated here. **ALOX12**: SAXS data indicate that ALOX12 dimer either is similar to ALOX15 assembly, or associates using PDZ-like domains. In both cases, PLAT and PDZ domains are flexible in their relative positioning like in ALOX15. The model of ALOX15 was used for visualization.

to cluster into higher oligomers, but this was diminished by replacing surface-exposed cysteines with serines, indicating the involvement of disulfide bridges in further aggregation.

By reinterpreting the crystallographic data of rabbit ALOX15, it was discovered that the asymmetric unit of the crystal contains the enzyme in two different conformations: one conformer with a ligand bound to an enclosed active site, and the other, an apo-conformer, with an open active site [9]. The molecules interact by their $\alpha 2$ helices, which are notably the most differing features of the two conformers. The $\alpha 2$ of the open apo-form has less turns which allows it to swing away from the core, expanding the active site orifice. Although mostly monomeric in solution according to SAXS, the share of dimeric ALOX15 is somewhat increased at near-physiological salt concentrations (in contrast to no salt), or by increasing the concentration of the enzyme [94]. Strikingly, the addition of 13(S)-HODE into the solution induces nearly full dimerization of rabbit ALOX15 [123]. A double mutation of W181E + H585E (situated on $\alpha 2$ and penultimate helices, respectively) abolished this property, suggesting that these structural features participate in binding of the ligand, the other monomer, or both. As mentioned above, ALOX15 can be allosterically affected by its own products. Apparently the mechanistic explanation to this phenomenon could very well be the conformational changes caused by dimerization.

1.7 ARACHIDONATE 11R-LIPOXYGENASE

The discovery of 11(R)-HETE in incubations of AA with the extract of the White Sea soft coral *Gersemia fruticosa* [126] eventually led to the first cloning and characterization of an arachidonate 11R-LOX [127]. As the name suggests, AA is the preferred substrate of the enzyme, the main product being 11(R)-HpETE with a minor amount of byproduct 15-HpETE (about 2%). It is a 77 kDa protein and its closest known relative is the 8R-LOX part of the AOS-LOX fusion protein from the Caribbean sea whip coral *P. homomalla*, sharing 42% of the primary sequence. In mammals the closest homolog is ALOX5 with sequence identity of about 33%. The identity with plant enzymes falls below 20%. Little is known about the biological role of 11R-LOX, but studies regarding another soft coral, *Capnella imbricata*,

have linked the AOS-LOX pathway to response against wounding and thermal stress [41, 42]; thus, there is an analogy with the jasmonate pathway in plants and inflammatory eicosanoids in mammals. It is reasonable to speculate that 11R-LOX could fulfill a similar function in *G. fruticosa* as well.

The Gly/Ala switch that controls the position of oxygen addition and *R/S*-stereospecificity [67] is Gly⁴¹⁶ in 11R-LOX, which conforms to the concept. By using alternative substrates with differing lengths and double bond positions, it was found that the location of hydrogen abstraction is relative to the distance from the methyl-end of the substrate, hence it was reasoned that the fatty acid likely enters the substrate channel tail-first [127].

A striking feature of 11R-LOX is its absolute dependence on Ca²⁺ and lipid membranes: no enzymatic activity was detected in the absence of either component [127]. The three Ca²⁺-binding sites observed in *P. homomalla* 8R-LOX seem to be conserved in 11R-LOX, however, the Trp residues that can be found in the membrane insertion loops of 8R-LOX and ALOX5 are missing, suggesting a different mode of membrane interactions. A systematic analysis using model membranes with varying compositions revealed that activation of 11R-LOX is dependent on the combination of phospholipid head groups that make up the membrane surface [87]. 11R-LOX can interact with membranes that contain anionic phospholipids like phosphatidylserine (PS) even in the absence of Ca²⁺, but for productive binding, i.e., catalytic activity, involvement of Ca²⁺ is a must (Figure 7). Additionally, phosphatidylethanolamine (PE) works synergistically together with anionic phospholipids to lower the concentration of Ca²⁺ needed for activation. While 10 mM CaCl₂ provides the maximal reaction rate with bacterial cell membranes, lipid vesicles with an optimized composition reduce this to about 1 mM. Data indicate that Ca²⁺ binding, too, is a cooperative procedure, affected by membrane surface components. In short, productive association of 11R-LOX with lipid membranes is a synergistic procedure dependent on Ca²⁺ concentration and the properties of the membrane surface.

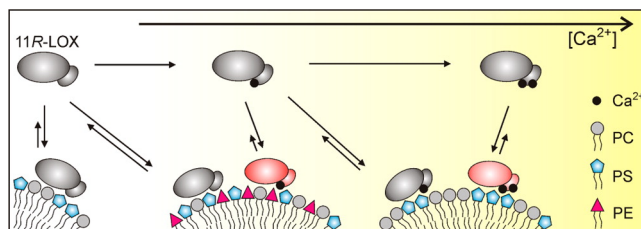


Figure 7 – Membrane binding of 11R-LOX. The inactive and active enzyme forms are in gray and red, respectively. 11R-LOX can unproductively bind anionic membranes in the absence of Ca²⁺, but Ca²⁺ is needed for productive binding. The activating concentration of Ca²⁺ is dependent on membrane composition [87].

Although the active site of LOXs has been studied thoroughly by now, and the catalytic apparatus is rather well-established, there is still much to learn about the regulatory mechanisms in LOXs that affect actual enzymatic activity. These include activation by Ca²⁺-mediated lipid membrane association, but also other allosteric effectors. Thanks to its unique strict requirement for Ca²⁺ and lipid membranes, and relative similarity to mammalian LOXs, 11R-LOX provides novel opportunities for investigating these regulatory aspects.

AIMS OF THE STUDY

BEING RELATIVELY SIMILAR to pharmacologically relevant human LOXs, 11R-LOX represents a promising model enzyme to explore the regulation of LOXs by structural and functional studies. On this account, the following key points were set as the aims of the thesis:

- to solve the three-dimensional structure of 11R-LOX;
- to establish the mode of substrate binding in the active site;
- to investigate the activation of the enzyme by Ca^{2+} -induced membrane association;
- to compare its structure and regulatory mechanisms to mammalian LOXs.

MATERIALS AND METHODS

LISTED HERE ARE THE BRIEF DESCRIPTIONS of the materials and methods used in the thesis. More detailed protocols can be found in the corresponding publications.

- Recombinant *G. fruticosa* 11R-LOX with an N-terminal His-tag was expressed in *Escherichia coli* BL21(DE3) cells. The protein was purified from cell lysate in three chromatographic stages: Ni-affinity, anion exchange and size exclusion chromatography (SEC).
- 11R-LOX was crystallized using the hanging-drop vapor diffusion method. Diffraction data was collected at the NE-CAT beamline 24-ID-E at the Advanced Photon Source (Argonne, IL, USA). The crystal structure was solved by molecular replacement.
- Whole plasmid PCR with mutagenic primers was used to introduce mutations for structure-function studies.
- Kinetic properties of enzyme variants were assayed spectrophotometrically, and catalysis products were analyzed by high-performance liquid chromatography (HPLC)-mass spectrometry (MS).
- Thermal stability assays were conducted using a hydrophobic fluorophore as a denaturation indicator in differential scanning fluorimetry (DSF) experiments or by monitoring circular dichroism (CD) while continuously ramping the temperature.
- The quaternary structure of 11R-LOX was studied using SAXS coupled with inline SEC on the SWING beamline at synchrotron SOLEIL (Gif-sur-Yvette, France), and also by chemical cross-linking.
- Site-directed mutagenesis was employed to create mutants with altered surface residues, and the oligomeric state of mutant variants was assessed by SEC.

RESULTS

THE ARACHIDONATE 11R-LOX from the soft coral *G. fruticosa* was subjected to various structural and functional experiments to investigate its unique catalytic and regulatory properties and better understand the enzymatic machinery of LOXs in general.

4.1 OVERALL CRYSTAL STRUCTURE (PUBLICATION I)

Recombinant 11R-LOX with an N-terminal T7 gene 10 leader peptide and His₄-tag was expressed in *E. coli* BL21(DE3) cells. The protein was purified from cell lysate in three stages with Ni-affinity, anion exchange and SEC. 11R-LOX was crystallized using the hanging-drop vapor-diffusion method. Diffraction data was collected at the Advanced Photon Source synchrotron (Argonne, Illinois, USA). The structure was solved with a resolution of 2.47 Å using molecular replacement, and the model was deposited to wwPDB under the accession code 3VF1.

Overall, 11R-LOX structure follows the canonical LOX framework consisting of a smaller N-terminal PLAT domain with a β -sandwich fold, and a larger C-terminal mainly α -helical catalytic domain. The region distal to the PLAT domain contains an α + β formation that could be considered a separate PDZ subdomain within the large LOX fold.

The crystallization cocktail did not contain any Ca²⁺, so the model depicts an apo-state that is likely catalytically inactive, since this enzyme requires Ca²⁺ for any activity. The PLAT domain loops that comprise the putative Ca²⁺-binding sites are extended, hence major restructuring would be needed to establish similar binding pockets like the ones found in other LOX structures. These differences are illustrated in Figure 8.

The active site of 11R-LOX is concealed in a cavity in the center of the catalytic domain, surrounded by helices that make up the core of the fold (Figure 9). The prosthetic iron is chelated by highly conserved His³⁷³, His³⁷⁸, His⁵⁵⁶, and the carboxyl-terminus of Ile⁶⁷⁹. Asn⁵⁶⁰ and a water molecule complete the octahedral coordination sphere. There are two possible passageways into the active site, one on either side of the conserved arched helix that covers the cavity. Both of these entrances are obstructed by bulky residues (Tyr¹⁵⁴ and Phe¹⁸⁵) rendering the active site inaccessible from the surface of the enzyme. The interior channel continues from the iron towards the peripheral PDZ-like domain and ends in a spacious hydrophobic pocket.

RESULTS

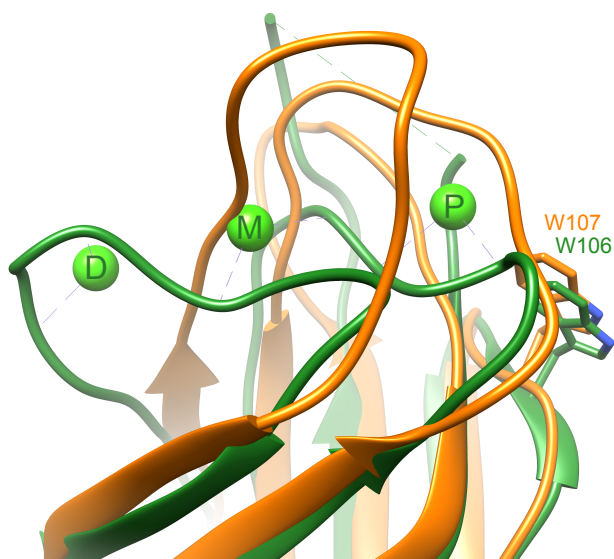


Figure 8 – Ca^{2+} -binding sites in PLAT domain. In the 8R-LOX model (2FNQ, *green*), there are three Ca^{2+} (Distal, Medial, and Proximal) bound between PLAT domain loops, whereas in the superposed 11R-LOX (*orange*), these loops are in a different conformation and do not constitute similar sites. The invariant tryptophan residing next to the interdomain cleft is also displayed in both models.

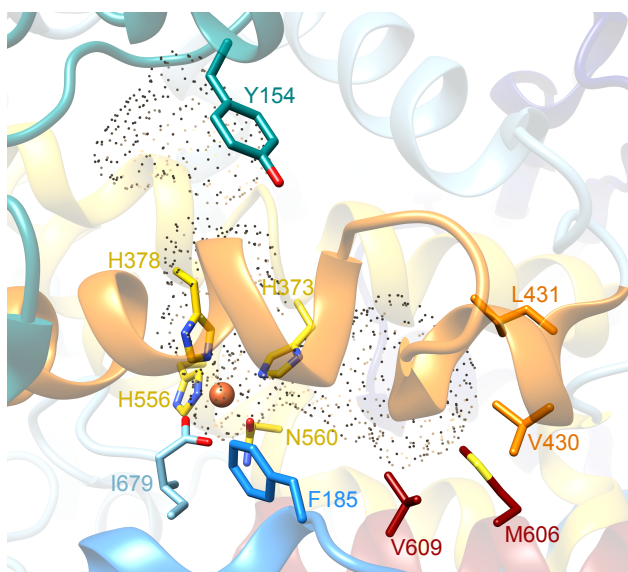


Figure 9 – Active site of 11R-LOX. The substrate-binding channel (cavities rendered in *dots*) is sealed off on both sides of the arched helix (*orange*): on one side by the TOP fragment with Phe¹⁸⁵, and on the other by LINK with Tyr¹⁵⁴. The coordination sphere of the iron is displayed along with the residues in the bottom of the hydrophobic pocket that were mutated in this study.

4.2 MODE OF SUBSTRATE BINDING (PUBLICATION I)

To elucidate the mode of fatty acid binding in the substrate channel, key residues that line the cavity were mutated to determine their potential role in substrate positioning. Mutant enzyme variants were expressed and purified, their kinetic parameters were assayed spectrophotometrically, and product profiles were determined by HPLC-MS analysis.

Val⁴³⁰, Leu⁴³¹, Met⁶⁰⁶ and Val⁶⁰⁹ are less-conserved bulky residues that form the bottom of the hydrophobic substrate-binding pocket (Figure 9). These were swapped for more compact alanines in the hope of enabling deeper penetration of the substrate. Of these substitutions, L431A and M606A had the strongest impact on catalysis specificity: up to 10% of AA peroxidation occurred at C8 instead of C11. This shift supports the previous impression that the substrate is bound into the channel aliphatic tail-first, not by the carboxylate head. As the fatty acid slides deeper into the pocket, methylenic C10 is partially exposed for hydrogen abstraction in addition to C13, which in turn leads to 8-HpETE formation as a side product. The effort to block the cavity with V609W mutation reduced the catalytic efficiency 50-fold, further substantiating the use of the hydrophobic pocket for productive substrate positioning.

4.3 ALLOSTERIC REGULATION (PUBLICATIONS I AND II)

A common feature among LOXs concerning the interface between PLAT and catalytic domains was discovered while analyzing the 11R-LOX model. There are π -cation (Trp¹⁰⁷-Lys¹⁷²) and electrostatic (Arg¹⁰⁶-Asp¹⁷³) bridges, both well-conserved, which connect the Ca²⁺-binding region in the PLAT domain to the helical segments (LINK and TOP) that cover the potential active site entrances (Figure 10). It was hypothesized that Ca²⁺-induced activation of 11R-LOX could be allosterically communicated from the PLAT domain to the active site, enabling access to the otherwise occluded substrate channel.

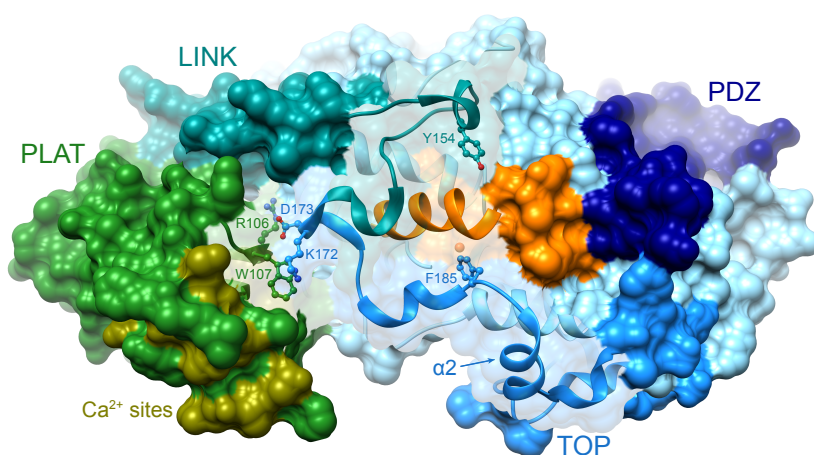


Figure 10 – Proposed components in the allosteric regulation of 11R-LOX. Two interdomain bridges connect the regulatory PLAT domain near the putative Ca²⁺-binding residues (*olive*) to LINK and TOP segments that seal the active site on both sides of the arched helix (*orange*).

RESULTS

The conserved interdomain bridges were severed by mutating the aforementioned residues. For instance, R106D substitution introduced electrostatic repulsion instead of attraction, and K172E abolished the π -cation interaction. Several such mutants were tested, and the majority displayed remarkably reduced turnover rates. Re-establishing the bridges in a swapped orientation restored catalytic activity, albeit not to the full extent. These results support the idea of allosteric communication between the two domains. Additionally, all performed mutations had a slight negative impact on the thermal stability of the enzyme as was demonstrated by DSF and CD analysis. Therefore, the two-domain interface is also important in stabilizing the protein structure.

4.4 DIMER ASSEMBLY (PUBLICATION III)

During preparative enzyme purification it was observed that 11R-LOX is a stable dimer in solution. However, none of the determined crystal contacts were deemed strong enough by *in silico* analysis. SAXS, chemical cross-linking, computational modeling, and site-directed mutagenesis were employed to resolve the correct quaternary structure.

The determined symmetric assembly is arranged so that contacts are made between the two catalytic domains with the sides distal to PLAT domains (Figure 11). In the crystal structure model, the interface includes two distinct charged clusters: one in the TOP region (Glu²¹¹, Arg²¹⁴, Glu²³⁰, Arg²³³) and the other in the PDZ-like subdomain (Lys²⁷⁰, Asp²⁷³, Arg²⁷⁴, Asp³²³). Mutant enzyme variants that were designed to impair electrostatic attraction in these clusters partially appeared as monomeric species in SEC analysis, proving their role in dimer formation.

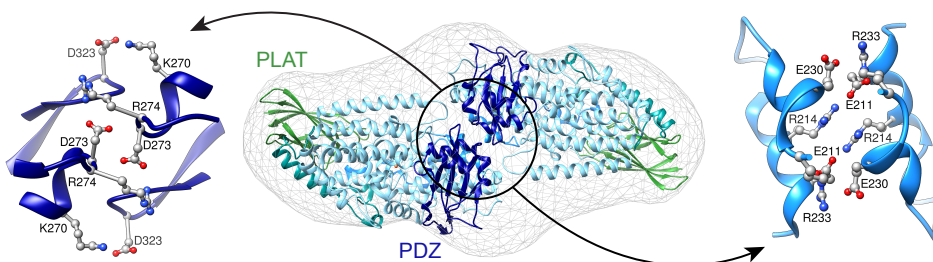


Figure 11 – Quaternary structure of 11R-LOX dimer. The two monomers interact by TOP and PDZ regions, which form two zipper-like electrostatic clusters with their counterparts. The particle model obtained by SAXS analysis is displayed in *wireframe*.

DISCUSSION

FOR 11R-LOX TO MANIFEST ITS ACTIVITY, a series of distinct molecular events must occur. Most LOXs display some basal activity *in vitro* whenever a suitable PUFA is available in solution, whereas 11R-LOX persists as an inactive dimer without the key components, Ca²⁺ and lipid membranes. Only when both of these are added, does catalysis commence. The crystal structure of 11R-LOX, obtained under restrictive conditions, reveals the likely reason behind this behavior: the active site is completely enclosed inside the protein fold. It is evident that significant conformational changes have to occur upon Ca²⁺-induced membrane association for the active site to open up and enable substrate binding.

5.1 REGULATION AT THE ACTIVE SITE

The crystal structure of 8R-LOX:AA complex by Neau et al. was a major milestone in understanding LOX catalysis, confirming the binding position of the substrate [12]. Previously, the way of substrate binding had been a matter of debate, and although the main theory contemplated the very same mode that was confirmed by Neau et al., there were alternative proposals. A few years earlier, the same authors had speculated that the substrate could position itself curved around the arched helix and use the cavity that is now believed to be the O₂ access channel instead of the hydrophobic pocket [11]. This hypothesis emerged because a 1.85-Å structure of the same 8R-LOX, which lacked the substrate, displayed a U-shaped tunnel curving under the arched helix with both of its ends open to solvent. Instead of the fatty acid entering the active site either head- or tail-first for different catalytic specificities, it was proposed that it could slide into the hydrophobic U-channel from either entrance and neglect the hydrophobic pocket altogether.

The structure of 11R-LOX featured a similar set of cavities, however, both entrances were sealed and a more pronounced hydrophobic pocket was present. In addition, mutational studies suggested that the pocket is still important for substrate binding and/or catalysis. Therefore, the two-entrance idea was studied further in Publication I in an attempt to explain the role of the pocket and the evident impact of channel bottom mutations. It was reasoned that depending on the particular LOX isoform, one or the other entrance could be used, but the aliphatic tail would still be bound into the hydrophobic pocket. Thanks to recent advances we now know that the fatty acid most likely employs the orifice next to helix α 2, and the one on the other side of the arched helix directs O₂ to the active site. These disputes illustrate fully the value of a crystal structure that characterizes an actual enzyme:substrate complex.

DISCUSSION

5.1.1 *Limiting access to the active site*

The putative active site entrance of 11R-LOX is covered by the TOP segment, which is positioned in a distinct conformation: the $\alpha 2$ helix is much shorter than in most other LOX models and is situated at a different angle (compare Figures 2 and 10). Consequently, the TOP chain takes a serpentine-like shape, which enables it to block the passageway with Phe¹⁸⁵. The structure of ALOX5 also displays similar deviating features: its $\alpha 2$ is only three turns long and seals the active site with an “FY cork” constituted by Phe¹⁷⁷ and Tyr¹⁸¹ [6]. Removal of the cork with Y181A mutation resulted in increased catalytic efficiency, which substantiates the cork hypothesis [75]. However, F177A substitution did not have that effect; instead, it abolished further conversion of 5(S)-HpETE into LTA₄. Additional mutations were made, including an effort to refold and elongate the $\alpha 2$ helix to open up the entrance. Based on the altered catalytic properties of the mutants it was concluded that the cork is there not just to block the passage to the active site, but once repositioned, it also contributes to defining the binding site and is necessary for correct substrate positioning.

Replacing the corresponding residues with smaller side chains in olive LOX-1 (F277A and Y280I mutations) decreased the K_m value and augmented catalytic efficiency [113], meaning a similar feature can exist in plant LOXs as well. It can be concluded that the cork and the underlying regulatory mechanisms could be widespread among LOXs of various species.

5.1.2 *Substrate tethering*

It has been shown that positively charged residues near the active site entrance can coordinate the carboxylate head of the substrate. For example, in coral 8R-LOX there is Arg¹⁸² on $\alpha 2$ instead of an aromatic plug. Replacing it with an alanine had a drastic impact on 8R-LOX catalysis: both substrate affinity and turnover rate were reduced [12]. Strikingly, the R182A mutant also started to exhibit strong substrate inhibition. The same effect was observed with human ALOX15 R403L mutant [80]. Although Arg⁴⁰³ is not located on the $\alpha 2$ helix, it is still in the vicinity of the substrate channel entrance, and it forms hydrogen bonds with $\alpha 2$. These possible interactions with both the substrate and the surrounding protein structure have been thoroughly modeled [128, 129]. Furthermore, it has been suggested that substrate binding can break the aforementioned H-bond network and cause a conformational shift of $\alpha 2$, which in turn induces dimerization of ALOX15 [80]. The dimerization of LOXs is discussed in detail further on.

Several LOXs suffer naturally from substrate inhibition, including human ALOX12 [59], ALOX15B [57], and coral 11R-LOX, which displays reduced turnover rates at AA concentrations higher than $\sim 30 \mu\text{M}$ as described in Publication II. In the position that corresponds to Arg¹⁸² of 8R-LOX, there is Gly¹⁸⁸ in 11R-LOX that begins the short $\alpha 2$ helix. Introducing a positive charge by mutating it to an arginine completely abolished inhibition by AA, while all other properties of the enzyme remained unchanged (unpublished results by K. Pöldermaa et al.). Hence it is evident that tethering of the carboxylate head of the fatty acid is important for productive substrate binding, and lack thereof can result in substrate inhibition, which *per se* could fulfill a biological function [130]. However, this has not been studied yet in the context of LOXs.

5.2 ALLOSTERIC REGULATION

Allosteric effects in 11R-LOX can be viewed from both intra-, and intermolecular aspects. On the one hand, Ca^{2+} -induced association with lipid membranes is essential for its activity. This means the membrane-binding PLAT domain must have some sort of influence over the catalytic domain, which most likely entails a cascade of conformational changes, conveyed allosterically from the periphery to the active site. On the other hand, the stability of 11R-LOX dimer raises the question whether the quaternary assembly also serves a regulatory purpose.

5.2.1 *Role of the PLAT domain*

While studying the 11R-LOX model, an interesting feature was discovered that is conserved among known LOX structures. There is a π -cation interaction (Trp¹⁰⁷-Lys¹⁷²) and an electrostatic bridge (Arg¹⁰⁶-Asp¹⁷³) between the PLAT domain and the TOP region that bind the two domains together. Mutational studies described in Publication II show that these interdomain connections are important for the enzymatic activity and also for the structural stability of 11R-LOX. Substitutions that disrupt the interactions hinder catalysis, but additional counter-mutations to restore the connections can salvage some of the activity.

A similar experiment was conducted on human ALOX5: the bridge (Arg¹⁰¹-Asp¹⁶⁶) was severed by introducing electrostatic repulsion, but surprisingly, this increased catalytic efficiency [114]. The authors reasoned that the disruption may have provided additional flexibility to the $\alpha 2$ region, allowing a shift of the FY cork and thereby promoting catalysis. CLP associates with ALOX5 at the interdomain cleft, and computational docking suggests that the same bridge-forming residues may participate in the interface with CLP [110]. New interactions upon CLP binding could likewise trigger such conformational changes, explaining the activating effect of this protein.

Zebrafish LOX-1 also displays Ca^{2+} -dependent membrane association and activation. SAXS experiments indicated that Ca^{2+} binding introduces flexibility to the protein structure, which can be interpreted as PLAT domain swinging away from the catalytic domain [88]. A mutant enzyme with an impaired distal Ca^{2+} site (zebrafish LOX-1 already lacks the medial site, like human ALOX15B) was no longer stimulated by Ca^{2+} —there was no increase in catalytic activity, and the dimensions of the enzyme particle expanded only by a fraction of the amount that was observed with the fully functional enzyme in the presence of Ca^{2+} . The versatile nature of relative domain positioning has also been observed in ALOX12 and ALOX15 in earlier SAXS studies [59, 93, 94]. Moreover, it has been shown that membrane-binding ability of soybean LOX-1 and rabbit ALOX15 is impaired by an active site ligand that stiffens the protein structure [131]. 11R-LOX tends to aggregate in the presence of Ca^{2+} , as was described in Publication I, which suggests that hydrophobic residues (either from PLAT domain loops or the interdomain cleft) are exposed due to Ca^{2+} -induced conformational changes. These data from multiple sources indicate that flexibility in PLAT domain positioning is integral to membrane association, and Ca^{2+} binding can be a means to achieve this freedom.

Soybean LOX-1 is inhibited by OS in a manner that cannot be explained by competitive mechanism. Hydrogen-deuterium exchange experiments coupled with MS indicated that

DISCUSSION

the allosteric binding site of OS is in the PLAT domain in the vicinity of the N-terminal β -strand [132]. Furthermore, the data showed that the presence of OS destabilizes helical peptides near the active site portal almost 30 Å away. It should be noted that compared to animal LOXs, the soybean enzyme contains large insertions in this region that form several additional helices and a small β -sheet. In animal LOXs, this would correspond to the TOP region including helix $\alpha 2$. The analysis of kinetic parameters implied that OS binding increases the rate of substrate association/dissociation, but disfavors further structural reorganization to a productive conformation. Therefore, it was deduced that binding of OS likely causes conformational changes that force the enzyme into a more flexible, open form, which is, however, catalytically less potent.

The recent results obtained with zebrafish and soybean enzymes correlate well with the ALOX5 mutation study in the sense that binding of an effector in PLAT domain, be it Ca^{2+} or a fatty acid, can increase the flexibility of the protein structure. In the case of ALOX5 and zebrafish LOX-1, these changes also stimulated catalysis. Interestingly, mutations that supposedly allowed 11R-LOX more conformational freedom hindered its activity. A possible explanation is that the lid structure in the TOP region of 11R-LOX is stable enough on its own, and additional forces are needed to displace it from the closed conformation. The fact that the coral 11R-LOX is the only known LOX with such strict Ca^{2+} - and membrane requirements complements this rationale. Be that as it may, the discussed findings demonstrate that Ca^{2+} binding is a distinct event capable of inducing major structural reorganization, which can transform the enzyme into an open, active conformation.

5.2.2 *Allostery related to quaternary structure*

Unlike most other LOXs that either are stable as monomers, dimerize only under certain conditions, or are prone to aggregate into larger clusters, 11R-LOX is a remarkably stable dimer in solution. The dimer is assembled together by the TOP and PDZ regions of both monomers, leaving PLAT domains free in the periphery. Although there is no direct evidence to date that dimerization somehow affects the functioning of 11R-LOX, studies on other LOXs with similar dimer interfaces, namely ALOX12 and ALOX15, have provided some clues regarding the role of these quaternary assemblies.

13(S)-HODE, which is the reduced product of LA conversion by ALOX15, induces dimerization of the very same enzyme [123]. It also shifts AA/LA substrate preference of ALOX15 towards AA [117]. These phenomena are likely related since helix $\alpha 2$ is involved in both dimer assembly and substrate tethering. Arg⁴⁰³ is a potential key residue in rabbit ALOX15 that participates in an H-bond network to stabilize $\alpha 2$ helix, but it can also interact with the carboxylate group of the fatty acid [80]. R403L mutation abolished product-induced dimerization and also destabilized the $\alpha 2$ region. Therefore, the authors hypothesized that the interaction between Arg⁴⁰³ and the substrate/product may promote conformational changes around $\alpha 2$ that lead to dimerization and modification of enzymatic activity.

The exact quaternary structure of an ALOX12 dimer is still unknown, but SAXS data and modeling indicate the involvement of the same surface region as in ALOX15 or 11R-LOX—either the TOP part with $\alpha 2$ helix or the PDZ-like subdomain [59, 94]. A naturally occurring Q261R mutation delays the activation of ALOX12 as characterized by a prominent lag-phase, but it has no effect on the membrane-binding properties of the enzyme [133]. This

effect may well be dimerization-related since Gln²⁶¹ is situated far from the active site in the PDZ-like domain, and is surface-exposed.

It has yet to be determined whether 11R-LOX is a functional dimer; in other words, does the quaternary assembly persist once the enzyme associates with a lipid membrane, or does it dissociate into separate functional monomers. Thanks to the crystal structure of an 11R-LOX dimer, it can be hypothesized that dimerization may be an additional stabilizing factor to enforce the enzyme into a closed conformation in solution. The TOP region can be envisaged squeezed together in a stable state, the PLAT domain on one side, and the countering TOP region from the second monomer on the other. Structural motions that occur on the lipid surface may alleviate these restrictions to allow conformational changes in $\alpha 2$, and consequently, substrate entry. This would make 11R-LOX a unique specimen since in ALOX12 and ALOX15 comparable assemblies seem to contribute to activity, not to preventing it. If this is the case, the knowledge provided by 11R-LOX structure could illuminate a novel means to pharmacologically intervene in LOX catalysis by allosterically affecting the accessibility of the active site.

CONCLUSIONS

STRUCTURAL AND FUNCTIONAL STUDIES were conducted to elucidate the regulatory mechanisms involved in catalysis by the arachidonate 11R-LOX, an enzyme unique in that Ca^{2+} -induced membrane association is an absolute prerequisite for its activity. Here are the main conclusions derived from this work:

- The 2.47-Å crystal structure of 11R-LOX follows the framework typical to other LOXs of animal origin, but features an active site that is completely sealed from the surrounding environment. This concealment is the most plausible reason for enzymatic inactivity in solution without Ca^{2+} and lipid membranes.
- The putative entrance to the substrate-binding channel is shielded by Phe¹⁸⁵ due to the distinct conformation of helix $\alpha 2$ and the adjoining part of the chain, contrasting thus with other LOX structures except for human ALOX5, which displays a similar broken $\alpha 2$ helix.
- In solution, 11R-LOX assembles into a dimer that may stabilize the inactive closed conformation, since the dimerization interface involves the immediate vicinity of the $\alpha 2$ region, and a PDZ-like subdomain in the catalytic portion of the enzyme.
- Conserved interactions between PLAT and catalytic domains (Trp¹⁰⁷-Lys¹⁷² and Arg¹⁰⁶-Asp¹⁷³) are needed for catalytic activity and structural stability, and therefore, participate in conveying the stimulatory effect of Ca^{2+} -induced membrane association to the active site.
- Once 11R-LOX has adopted an active conformation, the fatty acid enters the active site aliphatic tail-first, so its methyl end is cushioned by hydrophobic residues in the bottom of the substrate-binding channel.

REFERENCES

- [1] M. E. Newcomer, A. R. Brash, The structural basis for specificity in lipoxygenase catalysis., *Protein Sci.* 24 (2015) 298–309.
- [2] T. Horn, S. Adel, R. Schumann, S. Sur, K. R. Kakularam, A. Polamarasetty, P. Redanna, H. Kühn, D. Heydeck, Evolutionary aspects of lipoxygenases and genetic diversity of human leukotriene signaling., *Prog. Lipid Res.* 57 (2015) 13–39.
- [3] H. Kühn, S. Banthiya, K. van Leyen, Mammalian lipoxygenases and their biological relevance., *Biochim. Biophys. Acta* 1851 (2015) 308–330.
- [4] A. Liavonchanka, I. Feussner, Lipoxygenases: occurrence, functions and catalysis., *J. Plant Physiol.* 163 (2006) 348–357.
- [5] A. R. Brash, Lipoxygenases: occurrence, functions, catalysis, and acquisition of substrate., *J. Biol. Chem.* 274 (1999) 23679–23682.
- [6] N. C. Gilbert, S. G. Bartlett, M. T. Waight, D. B. Neau, W. E. Boeglin, A. R. Brash, M. E. Newcomer, The structure of human 5-lipoxygenase., *Science* 331 (2011) 217–219.
- [7] M. J. Kobe, D. B. Neau, C. E. Mitchell, S. G. Bartlett, M. E. Newcomer, The structure of human 15-lipoxygenase-2 with a substrate mimic., *J. Biol. Chem.* 289 (2014) 8562–8569.
- [8] S. A. Gillmor, A. Villaseñor, R. Fletterick, E. Sigal, M. F. Browner, The structure of mammalian 15-lipoxygenase reveals similarity to the lipases and the determinants of substrate specificity., *Nat. Struct. Biol.* 4 (1997) 1003–1009.
- [9] J. Choi, J. K. Chon, S. Kim, W. Shin, Conformational flexibility in mammalian 15S-lipoxygenase: Reinterpretation of the crystallographic data., *Proteins* 70 (2008) 1023–1032.
- [10] M. L. Oldham, A. R. Brash, M. E. Newcomer, Insights from the X-ray crystal structure of coral 8R-lipoxygenase: calcium activation via a C2-like domain and a structural basis of product chirality., *J. Biol. Chem.* 280 (2005) 39545–39552.
- [11] D. B. Neau, N. C. Gilbert, S. G. Bartlett, W. E. Boeglin, A. R. Brash, M. E. Newcomer, The 1.85 Å structure of an 8R-lipoxygenase suggests a general model for lipoxygenase product specificity., *Biochemistry* 48 (2009) 7906–7915.
- [12] D. B. Neau, G. Bender, W. E. Boeglin, S. G. Bartlett, A. R. Brash, M. E. Newcomer, Crystal structure of a lipoxygenase in complex with substrate: the arachidonic acid-binding site of 8R-lipoxygenase., *J. Biol. Chem.* 289 (2014) 31905–31913.

REFERENCES

- [13] S. Xu, T. C. Mueser, L. J. Marnett, M. O. Funk, Crystal structure of 12-lipoxygenase catalytic-domain-inhibitor complex identifies a substrate-binding channel for catalysis., *Structure* 20 (2012) 1490–1497.
- [14] J. C. Boyington, B. J. Gaffney, L. M. Amzel, The three-dimensional structure of an arachidonic acid 15-lipoxygenase., *Science* 260 (1993) 1482–1486.
- [15] W. Minor, J. Steczko, B. Stec, Z. Otwinowski, J. T. Bolin, R. Walter, B. Axelrod, Crystal structure of soybean lipoxygenase L-1 at 1.4 Å resolution., *Biochemistry* 35 (1996) 10687–10701.
- [16] D. R. Tomchick, P. Phan, M. Cymborowski, W. Minor, T. R. Holman, Structural and functional characterization of second-coordination sphere mutants of soybean lipoxygenase-1, *Biochemistry* 40 (2001) 7509–7517.
- [17] M. Chruszcz, A. Wlodawer, W. Minor, Determination of protein structures—a series of fortunate events., *Biophys. J.* 95 (2008) 1–9.
- [18] E. Skrzypczak-Jankun, L. M. Amzel, B. A. Kroa, M. O. Funk, Structure of soybean lipoxygenase L3 and a comparison with its L1 isoenzyme, *Proteins* 29 (1997) 15–31.
- [19] E. Skrzypczak-Jankun, R. A. Bross, R. T. Carroll, W. R. Dunham, M. O. Funk, Three-dimensional structure of a purple lipoxygenase., *J. Am. Chem. Soc.* 123 (2001) 10814–10820.
- [20] E. Skrzypczak-Jankun, K. Zhou, N. P. McCabe, S. H. Selman, J. Jankun, Structure of curcumin in complex with lipoxygenase and its significance in cancer., *Int. J. Mol. Med.* 12 (2003) 17–24.
- [21] E. Skrzypczak-Jankun, K. Zhou, J. Jankun, Inhibition of lipoxygenase by (-)-epigallocatechin gallate: X-ray analysis at 2.1 Å reveals degradation of EGCG and shows soybean LOX-3 complex with EGC instead, *Int. J. Mol. Med.* 12 (2003) 415–420.
- [22] O. Y. Borbulevych, J. Jankun, S. H. Selman, E. Skrzypczak-Jankun, Lipoxygenase interactions with natural flavonoid, quercetin, reveal a complex with protocatechuic acid in its X-ray structure at 2.1 Å resolution, *Proteins* 54 (2004) 13–19.
- [23] E. Skrzypczak-Jankun, O. Y. Borbulevych, J. Jankun, Soybean lipoxygenase-3 in complex with 4-nitrocatechol., *Acta Crystallogr., Sect. D: Biol. Crystallogr.* 60 (2004) 613–615.
- [24] A. Vahedi-Faridi, P.-A. Brault, P. Shah, Y.-W. Kim, W. R. Dunham, M. O. Funk, Interaction between non-heme iron of lipoxygenases and cumene hydroperoxide: basis for enzyme activation, inactivation, and inhibition., *J. Am. Chem. Soc.* 126 (2004) 2006–2015.
- [25] E. Skrzypczak-Jankun, O. Y. Borbulevych, M. I. Zavodszky, M. R. Baranski, K. Padmanabhan, V. Petricek, J. Jankun, Effect of crystal freezing and small-molecule binding on internal cavity size in a large protein: X-ray and docking studies of lipoxygenase

- at ambient and low temperature at 2.0 Å resolution, *Acta Crystallogr., Sect. D: Biol. Crystallogr.* 62 (2006) 766–775.
- [26] B. Youn, G. E. Sellhorn, R. J. Mirchel, B. J. Gaffney, H. D. Grimes, C. Kang, Crystal structures of vegetative soybean lipoxygenase VLX-B and VLX-D, and comparisons with seed isoforms LOX-1 and LOX-3, *Proteins* 65 (2006) 1008–1020.
- [27] J. Newie, A. Andreou, P. Neumann, O. Einsle, I. Feussner, R. Ficner, Crystal structure of a lipoxygenase from *Cyanothece* sp. may reveal novel features for substrate acquisition., *J. Lipid Res.* 57 (2016) 276–287.
- [28] J. Newie, P. Neumann, M. Werner, R. A. Mata, R. Ficner, I. Feussner, Lipoxygenase 2 from *Cyanothece* sp. controls dioxygen insertion by steric shielding and substrate fixation., *Sci. Rep.* 7 (2017) 2069.
- [29] A. Garreta, S. P. Val-Moraes, Q. García-Fernández, M. Busquets, C. Juan, A. Oliver, A. Ortiz, B. J. Gaffney, I. Fita, À. Manresa, X. Carpena, Structure and interaction with phospholipids of a prokaryotic lipoxygenase from *Pseudomonas aeruginosa*., *FASEB J.* 27 (2013) 4811–4821.
- [30] S. Banthiya, J. Kalms, E. Galemou Yoga, I. Ivanov, X. Carpena, M. Hamberg, H. Kühn, P. Scheerer, Structural and functional basis of phospholipid oxygenase activity of bacterial lipoxygenase from *Pseudomonas aeruginosa*., *Biochim. Biophys. Acta* 1861 (2016) 1681–1692.
- [31] Y. Chen, A. Wennman, S. Karkehabadi, Å. Engström, E. H. Oliw, Crystal structure of linoleate 13R-manganese lipoxygenase in complex with an adhesion protein., *J. Lipid Res.* 57 (2016) 1574–1588.
- [32] A. Wennman, E. H. Oliw, S. Karkehabadi, Y. Chen, Crystal structure of manganese lipoxygenase of the rice blast fungus *Magnaporthe oryzae*., *J. Biol. Chem.* 291 (2016) 8130–8139.
- [33] I. Ivanov, D. Heydeck, K. Hofheinz, J. Roffeis, V. B. O'Donnell, H. Kühn, M. Walther, Molecular enzymology of lipoxygenases., *Arch. Biochem. Biophys.* 503 (2010) 161–174.
- [34] M. Jisaka, R. B. Kim, W. E. Boeglin, A. R. Brash, Identification of amino acid determinants of the positional specificity of mouse 8S-lipoxygenase and human 15S-lipoxygenase-2., *J. Biol. Chem.* 275 (2000) 1287–1293.
- [35] I. Ivanov, H. Kühn, D. Heydeck, Structural and functional biology of arachidonic acid 15-lipoxygenase-1 (ALOX15)., *Gene* 573 (2015) 1–32.
- [36] J. Z. Haeggström, C. D. Funk, Lipoxygenase and leukotriene pathways: biochemistry, biology, and roles in disease., *Chem. Rev.* 111 (2011) 5866–5898.
- [37] J. A. Ackermann, K. Hofheinz, M. M. Zaiss, G. Krönke, The double-edged role of 12/15-lipoxygenase during inflammation and immunity., *Biochim. Biophys. Acta* 1862 (2017) 371–381.

REFERENCES

- [38] A. Mosblech, I. Feussner, I. Heilmann, Oxylipins: structurally diverse metabolites from fatty acid oxidation., *Plant Physiol. Biochem.* 47 (2009) 511–517.
- [39] A. Andreou, F. Brodhun, I. Feussner, Biosynthesis of oxylipins in non-mammals, *Prog. Lipid Res.* 48 (2009) 148–170.
- [40] C. Wasternack, S. Song, Jasmonates: biosynthesis, metabolism, and signaling by proteins activating and repressing transcription., *J. Exp. Bot.* 68 (2017) 1303–1321.
- [41] H. Löhelaid, T. Teder, K. Töldsepp, M. Ekins, N. Samel, Up-regulated expression of AOS-LOXa and increased eicosanoid synthesis in response to coral wounding., *PLoS One* 9 (2014) e89215.
- [42] H. Löhelaid, T. Teder, N. Samel, Lipoxygenase-allene oxide synthase pathway in octocoral thermal stress response., *Coral Reefs* 34 (2015) 143–154.
- [43] S. Banthiya, M. Pekárová, H. Kühn, D. Heydeck, Secreted lipoxygenase from *Pseudomonas aeruginosa* exhibits biomembrane oxygenase activity and induces hemolysis in human red blood cells., *Arch. Biochem. Biophys.* 584 (2015) 116–124.
- [44] J. D. Deschamps, A. F. Ogunsola, J. B. Jameson, A. Yasgar, B. A. Flitter, C. J. Freedman, J. A. Melvin, J. V. M. H. Nguyen, D. J. Maloney, A. Jadhav, A. Simeonov, J. M. Bomberger, T. R. Holman, Biochemical and cellular characterization and inhibitor discovery of *Pseudomonas aeruginosa* 15-lipoxygenase., *Biochemistry* 55 (2016) 3329–3340.
- [45] A. Di Meco, E. Lauretti, A. N. Vagnozzi, D. Praticò, Zileuton restores memory impairments and reverses amyloid and tau pathology in aged Alzheimer’s disease mice., *Neurobiol. Aging* 35 (2014) 2458–2464.
- [46] Y. B. Joshi, P. F. Giannopoulos, D. Praticò, The 12/15-lipoxygenase as an emerging therapeutic target for Alzheimer’s disease., *Trends Pharmacol. Sci.* 36 (2015) 181–186.
- [47] Y. Zheng, H. Yin, W. E. Boeglin, P. M. Elias, D. Crumrine, D. R. Beier, A. R. Brash, Lipoxygenases mediate the effect of essential fatty acid in skin barrier formation: a proposed role in releasing omega-hydroxyceramide for construction of the corneocyte lipid envelope., *J. Biol. Chem.* 286 (2011) 24046–24056.
- [48] O. Rådmark, O. Werz, D. Steinhilber, B. Samuelsson, 5-Lipoxygenase, a key enzyme for leukotriene biosynthesis in health and disease., *Biochim. Biophys. Acta* 1851 (2015) 331–339.
- [49] J. Jankun, T. Doerks, A. M. Aleem, W. Lysiak-Szydlowska, E. Skrzypczak-Jankun, Do human lipoxygenases have a PDZ regulatory domain?, *Curr. Mol. Med.* 8 (2008) 768–773.
- [50] A. Bateman, R. Sandford, The PLAT domain: a new piece in the PKD1 puzzle., *Curr. Biol.* 9 (1999) R588–90.

- [51] T. Hammarberg, P. Provost, B. Persson, O. Rådmark, The N-terminal domain of 5-lipoxygenase binds calcium and mediates calcium stimulation of enzyme activity., *J. Biol. Chem.* 275 (2000) 38787–38793.
- [52] S. Kulkarni, S. Das, C. D. Funk, D. Murray, W. Cho, Molecular basis of the specific subcellular localization of the C2-like domain of 5-lipoxygenase., *J. Biol. Chem.* 277 (2002) 13167–13174.
- [53] R. Brinckmann, K. Schnurr, D. Heydeck, T. Rosenbach, G. Kolde, H. Kühn, Membrane translocation of 15-lipoxygenase in hematopoietic cells is calcium-dependent and activates the oxygenase activity of the enzyme., *Blood* 91 (1998) 64–74.
- [54] M. Walther, R. Wiesner, H. Kühn, Investigations into calcium-dependent membrane association of 15-lipoxygenase-1. Mechanistic roles of surface-exposed hydrophobic amino acids and calcium., *J. Biol. Chem.* 279 (2004) 3717–3725.
- [55] I. Kilty, A. Logan, P. J. Vickers, Differential characteristics of human 15-lipoxygenase isozymes and a novel splice variant of 15S-lipoxygenase., *Eur. J. Biochem.* 266 (1999) 83–93.
- [56] C. E. Naylor, M. Jepson, D. T. Crane, R. W. Titball, J. Miller, A. K. Basak, B. Bolgiano, Characterisation of the calcium-binding C-terminal domain of *Clostridium perfringens* alpha-toxin., *J. Mol. Biol.* 294 (1999) 757–770.
- [57] G. Bender, E. E. Schexnaydre, R. C. Murphy, C. Uhlson, M. E. Newcomer, Membrane-dependent activities of human 15-LOX-2 and its murine counterpart: implications for murine models of atherosclerosis., *J. Biol. Chem.* 291 (2016) 19413–19424.
- [58] J. Kalms, S. Banthiya, E. G. Yoga, M. Hamberg, H.-G. Holzhütter, H. Kühn, P. Scheerer, The crystal structure of *Pseudomonas aeruginosa* lipoxygenase Ala420Gly mutant explains the improved oxygen affinity and the altered reaction specificity., *Biochim. Biophys. Acta* 1862 (2017) 463–473.
- [59] A. M. Aleem, J. Jankun, J. D. Dignam, M. Walther, H. Kühn, D. I. Svergun, E. Skrzypczak-Jankun, Human platelet 12-lipoxygenase, new findings about its activity, membrane binding and low-resolution structure., *J. Mol. Biol.* 376 (2008) 193–209.
- [60] C. Nourry, S. G. N. Grant, J.-P. Borg, PDZ domain proteins: plug and play!, *Sci. STKE* 2003 (2003) RE7.
- [61] Y. Ivarsson, Plasticity of PDZ domains in ligand recognition and signaling., *FEBS Lett.* 586 (2012) 2638–2647.
- [62] C. Schneider, D. A. Pratt, N. A. Porter, A. R. Brash, Control of oxygenation in lipoxygenase and cyclooxygenase catalysis., *Chem. Biol.* 14 (2007) 473–488.
- [63] N. Lehnert, E. I. Solomon, Density-functional investigation on the mechanism of H-atom abstraction by lipoxygenase., *J. Biol. Inorg. Chem.* 8 (2003) 294–305.

REFERENCES

- [64] E. Hatcher, A. V. Soudackov, S. Hammes-Schiffer, Proton-coupled electron transfer in soybean lipoxygenase: dynamical behavior and temperature dependence of kinetic isotope effects., *J. Am. Chem. Soc.* 129 (2007) 187–196.
- [65] G. Coffa, A. R. Brash, A single active site residue directs oxygenation stereospecificity in lipoxygenases: Stereocontrol is linked to the position of oxygenation., *Proc. Natl. Acad. Sci. U.S.A.* 101 (2004) 15579–15584.
- [66] G. Coffa, A. N. Imber, B. C. Maguire, G. Laxmikanthan, C. Schneider, B. J. Gaffney, A. R. Brash, On the relationships of substrate orientation, hydrogen abstraction, and product stereochemistry in single and double dioxygenations by soybean lipoxygenase-1 and its Ala542Gly mutant., *J. Biol. Chem.* 280 (2005) 38756–38766.
- [67] G. Coffa, C. Schneider, A. R. Brash, A comprehensive model of positional and stereo control in lipoxygenases., *Biochem. Biophys. Res. Commun.* 338 (2005) 87–92.
- [68] D. L. Sloane, R. Leung, C. S. Craik, E. Sigal, A primary determinant for lipoxygenase positional specificity., *Nature* 354 (1991) 149–152.
- [69] S. Borngräber, R. J. Kuban, M. Anton, H. Kühn, Phenylalanine 353 is a primary determinant for the positional specificity of mammalian 15-lipoxygenases., *J. Mol. Biol.* 264 (1996) 1145–1153.
- [70] S. Borngräber, M. Browner, S. A. Gillmor, C. Gerth, M. Anton, R. Fletterick, H. Kühn, Shape and specificity in mammalian 15-lipoxygenase active site. The functional interplay of sequence determinants for the reaction specificity., *J. Biol. Chem.* 274 (1999) 37345–37350.
- [71] R. Vogel, C. Jansen, J. Roffeis, P. Reddanna, P. Forsell, H.-E. Claesson, H. Kühn, M. Walther, Applicability of the triad concept for the positional specificity of mammalian lipoxygenases., *J. Biol. Chem.* 285 (2010) 5369–5376.
- [72] P. Saura, I. Kaganer, D. Heydeck, J. M. Lluch, H. Kühn, A. González-Lafont, Mutagenesis of sequence determinants of truncated porcine ALOX15 induces changes in the reaction specificity by altering the catalytic mechanism of initial hydrogen abstraction., *Chemistry* 24 (2018) 962–973.
- [73] Q. F. Gan, M. F. Browner, D. L. Sloane, E. Sigal, Defining the arachidonic acid binding site of human 15-lipoxygenase. Molecular modeling and mutagenesis., *J. Biol. Chem.* 271 (1996) 25412–25418.
- [74] M. R. Egmond, J. F. Vliegenthart, J. Boldingh, Stereospecificity of the hydrogen abstraction at carbon atom n-8 in the oxygenation of linoleic acid by lipoxygenases from corn germs and soya beans., *Biochem. Biophys. Res. Commun.* 48 (1972) 1055–1060.
- [75] S. Mitra, S. G. Bartlett, M. E. Newcomer, Identification of the substrate access portal of 5-lipoxygenase., *Biochemistry* 54 (2015) 6333–6342.

- [76] E. Hornung, S. Kunze, A. Liavonchanka, G. Zimmermann, D. Kühn, K. Fritsche, A. Renz, H. Kühn, I. Feussner, Identification of an amino acid determinant of pH regioselectivity in a seed lipoxygenase from *Momordica charantia*., *Phytochemistry* 69 (2008) 2774–2780.
- [77] M. Walther, J. Roffeis, C. Jansen, M. Anton, I. Ivanov, H. Kühn, Structural basis for pH-dependent alterations of reaction specificity of vertebrate lipoxygenase isoforms., *Biochim. Biophys. Acta* 1791 (2009) 827–835.
- [78] C. P. Van Os, G. P. Rijke-Schilder, H. Van Halbeek, J. Verhagen, J. F. Vliegthart, Double dioxygenation of arachidonic acid by soybean lipoxygenase-1. Kinetics and regio-stereo specificities of the reaction steps., *Biochim. Biophys. Acta* 663 (1981) 177–193.
- [79] M. Jisaka, C. Iwanaga, N. Takahashi, T. Goto, T. Kawada, T. Yamamoto, I. Ikeda, K. Nishimura, T. Nagaya, T. Fushiki, K. Yokota, Double dioxygenation by mouse 8S-lipoxygenase: specific formation of a potent peroxisome proliferator-activated receptor α agonist., *Biochem. Biophys. Res. Commun.* 338 (2005) 136–143.
- [80] A. Di Venere, T. Horn, S. Stehling, G. Mei, L. Masgrau, A. González-Lafont, H. Kühn, I. Ivanov, Role of Arg403 for thermostability and catalytic activity of rabbit 12/15-lipoxygenase., *Biochim. Biophys. Acta* 1831 (2013) 1079–1088.
- [81] M. J. Knapp, F. P. Seebeck, J. P. Klinman, Steric control of oxygenation regiochemistry in soybean lipoxygenase-1., *J. Am. Chem. Soc.* 123 (2001) 2931–2932.
- [82] M. J. Knapp, J. P. Klinman, Kinetic studies of oxygen reactivity in soybean lipoxygenase-1., *Biochemistry* 42 (2003) 11466–11475.
- [83] J. Saam, I. Ivanov, M. Walther, H.-G. Holzhütter, H. Kühn, Molecular dioxygen enters the active site of 12/15-lipoxygenase via dynamic oxygen access channels., *Proc. Natl. Acad. Sci. U.S.A.* 104 (2007) 13319–13324.
- [84] L. Collazo, J. P. Klinman, Control of the Position of Oxygen Delivery in Soybean Lipoxygenase-1 by Amino Acid Side Chains within a Gas Migration Channel., *J. Biol. Chem.* 291 (2016) 9052–9059.
- [85] C. Jansen, K. Hofheinz, R. Vogel, J. Roffeis, M. Anton, P. Reddanna, H. Kühn, M. Walther, Stereocontrol of arachidonic acid oxygenation by vertebrate lipoxygenases: Newly cloned zebrafish lipoxygenase 1 does not follow the Ala-versus-Gly concept., *J. Biol. Chem.* 286 (2011) 37804–37812.
- [86] U. Haas, E. Raschperger, M. Hamberg, B. Samuelsson, K. Tryggvason, J. Z. Haegström, Targeted knock-down of a structurally atypical zebrafish 12S-lipoxygenase leads to severe impairment of embryonic development., *Proc. Natl. Acad. Sci. U.S.A.* 108 (2011) 20479–20484.
- [87] R. Järving, A. Löökene, R. Kurg, L. Siimon, I. Järving, N. Samel, Activation of 11R-lipoxygenase is fully Ca^{2+} -dependent and controlled by the phospholipid composition of the target membrane., *Biochemistry* 51 (2012) 3310–3320.

REFERENCES

- [88] M. Mittal, M. Hasan, N. Balagunaseelan, A. Fauland, C. Wheelock, O. Rådmark, J. Z. Haeggström, A. Rinaldo-Matthis, Investigation of calcium-dependent activity and conformational dynamics of zebra fish 12-lipoxygenase., *Biochim. Biophys. Acta* 1861 (2017) 2099–2111.
- [89] S. A. Tatulian, J. Steczko, W. Minor, Uncovering a calcium-regulated membrane-binding mechanism for soybean lipoxygenase-1., *Biochemistry* 37 (1998) 15481–15490.
- [90] K. Cho, J. Han, R. Rakwal, O. Han, Calcium modulates membrane association, positional specificity, and product distribution in dual positional specific maize lipoxygenase-1., *Bioorg. Chem.* 60 (2015) 13–18.
- [91] M. Walther, M. Anton, M. Wiedmann, R. Fletterick, H. Kühn, The N-terminal domain of the reticulocyte-type 15-lipoxygenase is not essential for enzymatic activity but contains determinants for membrane binding., *J. Biol. Chem.* 277 (2002) 27360–27366.
- [92] M. Walther, K. Hofheinz, R. Vogel, J. Roffeis, H. Kühn, The N-terminal β -barrel domain of mammalian lipoxygenases including mouse 5-lipoxygenase is not essential for catalytic activity and membrane binding but exhibits regulatory functions., *Arch. Biochem. Biophys.* 516 (2011) 1–9.
- [93] M. Hammel, M. Walther, R. Prassl, H. Kühn, Structural flexibility of the N-terminal beta-barrel domain of 15-lipoxygenase-1 probed by small angle X-ray scattering. Functional consequences for activity regulation and membrane binding., *J. Mol. Biol.* 343 (2004) 917–929.
- [94] W. Shang, I. Ivanov, D. I. Svergun, O. Y. Borbulevych, A. M. Aleem, S. Stehling, J. Jankun, H. Kühn, E. Skrzypczak-Jankun, Probing dimerization and structural flexibility of mammalian lipoxygenases by small-angle X-ray scattering., *J. Mol. Biol.* 409 (2011) 654–668.
- [95] E. Dainese, A. Sabatucci, G. van Zadelhoff, C. B. Angelucci, P. Vachette, G. A. Veldink, A. F. Agrò, M. Maccarrone, Structural stability of soybean lipoxygenase-1 in solution as probed by small angle X-ray scattering., *J. Mol. Biol.* 349 (2005) 143–152.
- [96] G. Mei, A. Di Venere, E. Nicolai, C. B. Angelucci, I. Ivanov, A. Sabatucci, E. Dainese, H. Kühn, M. Maccarrone, Structural properties of plant and mammalian lipoxygenases. Temperature-dependent conformational alterations and membrane binding ability., *Biochemistry* 47 (2008) 9234–9242.
- [97] O. Rådmark, O. Werz, D. Steinhilber, B. Samuelsson, 5-Lipoxygenase: regulation of expression and enzyme activity., *Trends Biochem. Sci.* 32 (2007) 332–341.
- [98] O. Rådmark, B. Samuelsson, Regulation of the activity of 5-lipoxygenase, a key enzyme in leukotriene biosynthesis., *Biochem. Biophys. Res. Commun.* 396 (2010) 105–110.

- [99] T. Hammarberg, O. Rådmark, 5-lipoxygenase binds calcium., *Biochemistry* 38 (1999) 4441–4447.
- [100] A. H. Pande, D. Moe, K. N. Nemeč, S. Qin, S. Tan, S. A. Tatulian, Modulation of human 5-lipoxygenase activity by membrane lipids., *Biochemistry* 43 (2004) 14653–14666.
- [101] A. H. Pande, S. Qin, S. A. Tatulian, Membrane fluidity is a key modulator of membrane binding, insertion, and activity of 5-lipoxygenase., *Biophys. J.* 88 (2005) 4084–4094.
- [102] C. Hörnig, D. Albert, L. Fischer, M. Hörnig, O. Rådmark, D. Steinhilber, O. Werz, 1-Oleoyl-2-acetyl-glycerol stimulates 5-lipoxygenase activity via a putative (phospho)lipid binding site within the N-terminal C2-like domain., *J. Biol. Chem.* 280 (2005) 26913–26921.
- [103] Y. Y. Zhang, T. Hammarberg, O. Rådmark, B. Samuelsson, C. F. Ng, C. D. Funk, J. Loscalzo, Analysis of a nucleotide-binding site of 5-lipoxygenase by affinity labelling: binding characteristics and amino acid sequences., *Biochem. J.* 351 Pt 3 (2000) 697–707.
- [104] N. C. Gilbert, Z. Rui, D. B. Neau, M. T. Waight, S. G. Bartlett, W. E. Boeglin, A. R. Brash, M. E. Newcomer, Conversion of human 5-lipoxygenase to a 15-lipoxygenase by a point mutation to mimic phosphorylation at Serine-663., *FASEB J.* 26 (2012) 3222–3229.
- [105] S. Adel, K. Hofheinz, D. Heydeck, H. Kühn, A.-K. Häfner, Phosphorylation mimicking mutations of ALOX5 orthologs of different vertebrates do not alter reaction specificities of the enzymes., *Biochim. Biophys. Acta* 1842 (2014) 1460–1466.
- [106] M. Peters-Golden, T. G. Brock, 5-lipoxygenase and FLAP., *Prostaglandins Leukot. Essent. Fatty Acids* 69 (2003) 99–109.
- [107] J. F. Evans, A. D. Ferguson, R. T. Mosley, J. H. Hutchinson, What's all the FLAP about?: 5-lipoxygenase-activating protein inhibitors for inflammatory diseases., *Trends Pharmacol. Sci.* 29 (2008) 72–78.
- [108] M. E. Newcomer, N. C. Gilbert, Location, location, location: compartmentalization of early events in leukotriene biosynthesis., *J. Biol. Chem.* 285 (2010) 25109–25114.
- [109] M. Rakonjac, L. Fischer, P. Provost, O. Werz, D. Steinhilber, B. Samuelsson, O. Rådmark, Coactosin-like protein supports 5-lipoxygenase enzyme activity and up-regulates leukotriene A4 production., *Proc. Natl. Acad. Sci. U.S.A.* 103 (2006) 13150–13155.
- [110] J. Esser, M. Rakonjac, B. Hofmann, L. Fischer, P. Provost, G. Schneider, D. Steinhilber, B. Samuelsson, O. Rådmark, Coactosin-like protein functions as a stabilizing chaperone for 5-lipoxygenase: role of tryptophan 102., *Biochem. J.* 425 (2010) 265–274.

REFERENCES

- [111] V. Dincbas-Renqvist, G. Pépin, M. Rakonjac, I. Plante, D. L. Ouellet, A. Hermansson, I. Goulet, J. Doucet, B. Samuelsson, O. Rådmark, P. Provost, Human Dicer C-terminus functions as a 5-lipoxygenase binding domain., *Biochim. Biophys. Acta* 1789 (2009) 99–108.
- [112] M. Schröder, A.-K. Häfner, B. Hofmann, O. Rådmark, F. Tumulka, R. Abele, V. Dötsch, D. Steinhilber, Stabilisation and characterisation of the isolated regulatory domain of human 5-lipoxygenase., *Biochim. Biophys. Acta* 1842 (2014) 1538–1547.
- [113] C. Palmieri-Thiers, J.-C. Alberti, S. Canaan, V. Brunini, C. Gambotti, F. Tomi, E. H. Oliw, L. Berti, J. Maury, Identification of putative residues involved in the accessibility of the substrate-binding site of lipoxygenase by site-directed mutagenesis studies., *Arch. Biochem. Biophys.* 509 (2011) 82–89.
- [114] M. Rakonjac Ryge, M. Tanabe, P. Provost, B. Persson, X. Chen, C. D. Funk, A. Rinaldo-Matthis, B. Hofmann, D. Steinhilber, T. Watanabe, B. Samuelsson, O. Rådmark, A mutation interfering with 5-lipoxygenase domain interaction leads to increased enzyme activity., *Arch. Biochem. Biophys.* 545 (2014) 179–185.
- [115] J.-C. Alberti, M. Mariani, V. Brunini-Bronzini de Caraffa, C. Gambotti, E. H. Oliw, L. Berti, J. Maury, A functional role identified for conserved charged residues at the active site entrance of lipoxygenase with double specificity., *J. Mol. Catal. B-Enzym.* 123 (2016) 167–173.
- [116] R. Mogul, E. Johansen, T. R. Holman, Oleyl sulfate reveals allosteric inhibition of soybean lipoxygenase-1 and human 15-lipoxygenase., *Biochemistry* 39 (2000) 4801–4807.
- [117] A. T. Wecksler, V. Kenyon, J. D. Deschamps, T. R. Holman, Substrate specificity changes for human reticulocyte and epithelial 15-lipoxygenases reveal allosteric product regulation., *Biochemistry* 47 (2008) 7364–7375.
- [118] A. T. Wecksler, C. Jacquot, W. A. van der Donk, T. R. Holman, Mechanistic investigations of human reticulocyte 15- and platelet 12-lipoxygenases with arachidonic acid., *Biochemistry* 48 (2009) 6259–6267.
- [119] A. T. Wecksler, V. Kenyon, N. K. Garcia, J. D. Deschamps, W. A. van der Donk, T. R. Holman, Kinetic and structural investigations of the allosteric site in human epithelial 15-lipoxygenase-2., *Biochemistry* 48 (2009) 8721–8730.
- [120] N. Joshi, E. K. Hoobler, S. Perry, G. Diaz, B. Fox, T. R. Holman, Kinetic and structural investigations into the allosteric and pH effect on the substrate specificity of human epithelial 15-lipoxygenase-2., *Biochemistry* 52 (2013) 8026–8035.
- [121] H. Meng, C. L. McClendon, Z. Dai, K. Li, X. Zhang, S. He, E. Shang, Y. Liu, L. Lai, Discovery of novel 15-lipoxygenase activators to shift the human arachidonic acid metabolic network toward inflammation resolution., *J. Med. Chem.* 59 (2016) 4202–4209.

- [122] A.-K. Häfner, M. Cernescu, B. Hofmann, M. Ermisch, M. Hörnig, J. Metzner, G. Schneider, B. Brutschy, D. Steinhilber, Dimerization of human 5-lipoxygenase., *Biol. Chem.* 392 (2011) 1097–1111.
- [123] I. Ivanov, W. Shang, L. Toledo, L. Masgrau, D. I. Svergun, S. Stehling, H. Gómez, A. Di Venere, G. Mei, J. M. Lluch, E. Skrzypczak-Jankun, A. González-Lafont, H. Kühn, Ligand-induced formation of transient dimers of mammalian 12/15-lipoxygenase: a key to allosteric behavior of this class of enzymes?, *Proteins* 80 (2012) 703–712.
- [124] R. B. Kumar, L. Zhu, H. Idborg, O. Rådmark, P.-J. Jakobsson, A. Rinaldo-Matthis, H. Hebert, C. Jegerschöld, Structural and functional analysis of calcium ion mediated binding of 5-lipoxygenase to nanodiscs., *PLoS One* 11 (2016) e0152116.
- [125] A.-K. Häfner, K. Beilstein, P. Graab, A.-K. Ball, M. J. Saul, B. Hofmann, D. Steinhilber, Identification and characterization of a new protein isoform of human 5-lipoxygenase., *PLoS One* 11 (2016) e0166591.
- [126] K. Varvas, I. Järving, R. Koljak, A. Vahemets, T. Pehk, A.-M. Müürisepp, Ü. Lille, N. Samel, *In vitro* biosynthesis of prostaglandins in the White Sea soft coral *Gersemia fruticosa*: Formation of optically active PGD₂, PGE₂, PGF_{2α} and 15-keto-PGF_{2α} from arachidonic acid., *Tetrahedron Lett.* 34 (1993) 3643–3646.
- [127] M. Mortimer, R. Järving, A. R. Brash, N. Samel, I. Järving, Identification and characterization of an arachidonate 11R-lipoxygenase., *Arch. Biochem. Biophys.* 445 (2006) 147–155.
- [128] L. Toledo, L. Masgrau, J.-D. Maréchal, J. M. Lluch, A. González-Lafont, Insights into the mechanism of binding of arachidonic acid to mammalian 15-lipoxygenases., *J. Phys. Chem. B* 114 (2010) 7037–7046.
- [129] L. Toledo, L. Masgrau, J. M. Lluch, A. González-Lafont, Substrate binding to mammalian 15-lipoxygenase., *J. Comput. Aided Mol. Des.* 25 (2011) 825–835.
- [130] M. C. Reed, A. Lieb, H. F. Nijhout, The biological significance of substrate inhibition: A mechanism with diverse functions., *Bioessays* 32 (2010) 422–429.
- [131] A. Di Venere, E. Nicolai, I. Ivanov, E. Dainese, S. Adel, C. B. Angelucci, H. Kühn, M. Maccarrone, G. Mei, Probing conformational changes in lipoxygenases upon membrane binding: fine-tuning by the active site inhibitor ETYA., *Biochim. Biophys. Acta* 1841 (2014) 1–10.
- [132] A. R. Offenbacher, A. T. Iavarone, J. P. Klinman, Hydrogen-deuterium exchange reveals long-range dynamical allostery in soybean lipoxygenase., *J. Biol. Chem.* 293 (2018) 1138–1148.
- [133] A. M. Aleem, L. Wells, J. Jankun, M. Walther, H. Kühn, J. Reinartz, E. Skrzypczak-Jankun, Human platelet 12-lipoxygenase: naturally occurring Q261/R261 variants and N544L mutant show altered activity but unaffected substrate binding and membrane association behavior., *Int. J. Mol. Med.* 24 (2009) 759–764.

ACKNOWLEDGMENTS

So long, and thanks for all the fish!,***

— Douglas Adams, *The Hitchhiker's Guide to the Galaxy*

I am most grateful to my supervisor, Prof. Nigulas Samel, who welcomed me as an undergraduate to his lab, and under whose supervision this thesis has become a reality. I owe great thanks to my first supervisor, Reet Järving, and also Ivar Järving, who both trained me in labwork and, most of all, taught me the art of noticing the little things. Warm thanks go to Kaia, Helike, Külliki, Tarvi, Mart, Aivar, Ly, Sandra, and other good colleagues for inspiration, help, and great company. Additionally, I really appreciate the contribution of my students Kaspar, Marianna, Janet, Helian, and Mari-Ann.

This work could not have been done without collaborators. I had a great time working in Prof. Marcia Newcomer's lab in Louisiana State University, and I want to extend my thanks to Nathan Gilbert for teaching me the tricks of protein crystallization. I value the input of collaborators Arvi Freiberg, Margus Rätsep, and also Sergo Kasvandik, whom I can appreciate as one of my dearest friends.

I am truly grateful to my family for supporting me all these years and also for sparking interest towards science already in my childhood. My dear sister Krista is in for an especially big thank you, since she corrected the language in the thesis. And my beloved Liina, who has stood by me since the beginning of my doctoral years; I thank her for forcing me to have a life outside the lab now and again—this has kept me going.

I acknowledge the funding bodies mentioned in the publications, and also the support from Archimedes Foundation through DoRa T8 and DoRa Plus 1.1 programs during the doctoral studies.

*This was the farewell message left for Earth-bound humans by dolphins, who decided to leave the planet just before its inevitable destruction. Contrary to the dolphins and Earth's demise, I am certain that TTÜ will not be destroyed after my graduation. I wish all the best to my *alma mater*, and for its research to stay strong.

**By fish I mean having coffee by the beautiful aquarium, of course. Thanks for that!

ABSTRACT

LIPPOXYGENASES (LOXs) are a diverse family of peripheral membrane proteins. Although they all catalyze the peroxidation of polyunsaturated fatty acids, homologs can vary not only in terms of substrate selectivity or catalytic specificity, but also in regulatory aspects. While many LOXs are stimulated by Ca^{2+} -induced membrane association, the arachidonate 11R-LOX from the Arctic coral *Gersemia fruticosa* is characterized by strict requirement for Ca^{2+} and lipid membranes for any catalytic activity. The thesis investigates the structure and regulation of 11R-LOX to unravel the mechanisms underlying its unique properties, and to ascertain common features with human LOXs.

Recombinant 11R-LOX was crystallized and the crystal structure was solved to a 2.47-Å resolution. The overall structure matches the canonical framework of animal LOXs with an N-terminal β -sandwich called the PLAT domain, and a larger, mostly α -helical C-terminal catalytic domain. The crystals were obtained in the absence of Ca^{2+} , so the PLAT domain loops that compose the putative Ca^{2+} -binding sites are not aligned as in known PLAT: Ca^{2+} complexes, indicating notable conformational changes upon Ca^{2+} binding. Regarding the catalytic domain, mutations in the substrate-binding channel suggested that arachidonic acid slides into the active site aliphatic tail-first, leaving its carboxylate head by the entrance. However, in the crystal structure model the active site is completely enclosed as the putative portal is blocked by a short $\alpha 2$ helix and the adjoining portion of the chain, meaning that here, too, conformational changes are necessary. The secondary structure of this region is fragmented, and folded in a serpentine shape unlike most other known LOX structures with open active sites, which feature long continuous $\alpha 2$ helices. Conserved interactions were found between the PLAT domain in the vicinity of Ca^{2+} -binding sites and the N-terminal side of the $\alpha 2$ region in the catalytic domain. Mutational studies revealed that two interdomain bridges, Trp¹⁰⁷-Lys¹⁷² and Arg¹⁰⁶-Asp¹⁷³, are crucial for proper enzymatic activity and also for structural stability, as demonstrated by thermal stability assays. Since 11R-LOX is a dimer in solution, the quaternary structure of the protein was investigated by small-angle X-ray scattering, chemical cross-linking, and mutagenesis experiments. In the determined dimer assembly, the catalytic domains associate by their PDZ-like subdomains and the C-terminal sides of the $\alpha 2$ regions. In sum, the results suggest that the closed, serpentine-like conformation of the $\alpha 2$ region may be imposed by stabilizing interactions from both interdomain connections on one side, and protein dimerization on the other.

Human ALOX5 is a key enzyme in the production of leukotrienes—potent inflammatory mediators—making ALOX5 a prominent biological target. Like 11R-LOX, it is a Ca^{2+} -induced enzyme featuring a similar fragmented $\alpha 2$ helix. As ALOX5 bears the greatest similarity to 11R-LOX among mammalian LOXs, the regulatory mechanisms of the two enzymes are likely comparable. ALOX12 and ALOX15 also participate in inflammatory processes in humans. Strikingly, both can dimerize, and the interfaces of their assemblies have been narrowed down to the same region of the protein surface as in 11R-LOX. While human LOXs

ABSTRACT

tend to be relatively unstable and difficult to handle, 11R-LOX is a remarkably stable enzyme facilitating extensive structural studies. As a result, 11R-LOX makes an exceptional source of information regarding the dynamic structure of LOXs. The knowledge obtained in the present thesis can be used to further our understanding about the regulation of these pharmacologically relevant enzymes.

KOKKUVÕTE

LIPOKSÜGENAASID (LOXid) moodustavad mitmekesise perifeersetes membraanvalkude perekonna. Kuigi kõik LOXid katalüüsivad polüküllastumata rasvhapete peroksüdatsiooni, võivad homoloogid erineda nii substraadi eelistuse, katalüütilise spetsiifilisuse, aga ka regulaatorsete aspektide poolest. Ca^{2+} tõstab paljude LOXide aktiivsust, kuna soodustab valgu seondumist lipiidmembraanile. Arktilisest korallist *Gersemia fruticosa* pärit arahhidoonhappe 11R-LOX on aga eriline seetõttu, et ilma Ca^{2+} ja lipiidmembraanita puudub sel ensüümil aktiivsus täielikult. Käesolev doktoritöö uurib 11R-LOXi struktuuri ja regulatsiooni, et mõista selle unikaalsete omaduste tagamaid ning määrata ühisosa inimese LOXidega.

Rekombinantne 11R-LOX kristalliti ning kristallstruktuur lahendati resolutsioonini 2,47 Å. Selle üldine struktuur vastab tüüpilisele loomsele LOXile, koosnedes N-terminaalsest β -struktuurist, mida nimetatakse PLAT domeeniks, ja suuremast valdavalt α -helikaalsest C-terminaalsest katalüütilisest domeenist. Kuivõrd valgukristallid saadi Ca^{2+} -vabades tingimustes, siis on PLAT domeeni lingud, mille vahel Ca^{2+} sidumiskohad peaks moodustuma, oluliselt erinevas konformatsioonis kui teistes teadaoleva struktuuriga PLAT: Ca^{2+} kompleksides. See viitab, et Ca^{2+} seondumisel leiavad aset märkimisväärsed konformatsiooni muutused. Katalüütilises domeenis asuva substraadi sidumiskanali muteerimine näitas, et arahhidoonhape siseneb aktiivtsentrisse alifaatne saba ees ja selle karboksüülrühm jääb kanali suudme juurde. Samas on kristallstruktuuri mudelis aktiivtsenter täielikult suletud, sest eeldatavat suuet blokeerib lühike $\alpha 2$ heeliks ja heeliksit vahetult ümbritsev ahelaosa. Sekundaarstruktuur on selles piirkonnas katkendlik ning peptiidahel kulgeb ebakorrapäraselt. Avatud aktiivtsentriga LOXide mudelites on $\alpha 2$ heeliks aga pikk ja pidev. PLAT ja katalüütilise domeeni vahel tuvastati konserveerunud interaktsioonid, mis seovad Ca^{2+} sidumiskohad $\alpha 2$ piirkonna N-terminaalse osaga. Mutatsioonanalüüsil selgus, et kaks domeenidevahelist silda, Trp¹⁰⁷-Lys¹⁷² ja Arg¹⁰⁶-Asp¹⁷³, on olulised 11R-LOXi aktiivsuse jaoks. Termilise denaturatsiooni katsed näitasid, et need sillad ka stabiliseerivad ensüümi struktuuri. Lisaks uuriti valgu kvaternaarstruktuuri väikese nurga röntgenhajumise, keemilise ristsidumise ja mutatsioonanalüüsi abil, kuna avastati, et 11R-LOX esineb lahuses dimeerina. Ilmnes, et dimeeris puutuvad omavahel kokku katalüütilised domeenid oma PDZ-sarnaste alamdomeenide ja $\alpha 2$ piirkondade C-terminaalsete osade kaudu. Kokkuvõtlikult viitavad tulemused sellele, et domeenidevahelised ühendused ja dimerisatsiooni liides võivad vastastikku fikseerida $\alpha 2$ piirkonna ebaregulaarsesse asendisse, mis omakorda tõkestab aktiivtsentri suudme.

Inimese ALOX5 on leukotrieenide signaaliraja võtmeensüüm. Kuna leukotrieenid on tugevatoimelised põletikuvahendajad, on ALOX5 äärmiselt huvipakkuvaks ravimsihtmärgiks. Sarnaselt 11R-LOXiga on tegemist Ca^{2+} -sõltuva ensüümiga, millel on lisaks samasugune katkendliku sekundaarstruktuuriga $\alpha 2$ piirkond. Kuivõrd ALOX5 on imetaja LOXidest primaarjärjestuse poolest 11R-LOXile lähedasim, siis võib eeldada, et nende kahe ensüümi reguleerivad mehhanismid on sarnased. Inimorganismi põletikuprotsessides osalevad ka ALOX12 ja ALOX15. Mõlemad ensüümid on võimelised dimeriseeruma ning uuringud

KOKKUVÕTE

viitavad, et nende dimeeride liidesed moodustuvad samade valguga pinna piirkondade kaudu nagu 11R-LOXil. Inimese LOXid on suhteliselt ebastabiilsed valgud ja tülikad käsitleda, 11R-LOX on aga märkimisväärselt stabiilsem ensüüm. Tänu sellele saab 11R-LOX-i kasutada põhjalikes struktuuriuuringutes, et hankida uut informatsiooni LOXide dünaamilise ehituse kohta. Käesoleva doktoritöö raames tehtud avastusi on võimalik kanda üle teistele, farmakoloogiliselt olulistele LOXidele, et mõista paremini ka nende regulatsiooni.

PUBLICATION I

P. Eek, R. Järving, I. Järving, N.C. Gilbert, M.E. Newcomer, N. Samel

**Structure of a calcium-dependent 11R-lipoxygenase suggests
a mechanism for Ca²⁺ regulation**

Journal of Biological Chemistry 287 (2012) 22377–22386

Structure of a Calcium-dependent 11*R*-Lipoxygenase Suggests a Mechanism for Ca²⁺ Regulation^{*[5]}

Received for publication, January 16, 2012, and in revised form, May 7, 2012. Published, JBC Papers in Press, May 9, 2012, DOI 10.1074/jbc.M112.343285

Priit Eek[‡], Reet Järving[‡], Ivar Järving[‡], Nathaniel C. Gilbert[§], Marcia E. Newcomer[§], and Nigulas Samel^{†1}

From the [‡]Department of Chemistry, Tallinn University of Technology, Akadeemia tee 15, 12618 Tallinn, Estonia and the [§]Department of Biological Sciences, Louisiana State University, Baton Rouge, Louisiana 70803

Background: Lipoxygenases vary in their catalytic specificity and regulation.

Results: 11*R*-LOX, strictly Ca²⁺-dependent, displays novel structural features in the membrane-binding domain.

Conclusion: A model for how access to an enclosed active site is linked to Ca²⁺-dependent membrane binding is proposed.

Significance: The 11*R*-LOX model provides structural insights into the allosteric regulation of lipoxygenases.

Lipoxygenases (LOXs) are a key part of several signaling pathways that lead to inflammation and cancer. Yet, the mechanisms of substrate binding and allosteric regulation by the various LOX isoforms remain speculative. Here we report the 2.47-Å resolution crystal structure of the arachidonate 11*R*-LOX from *Gersemia fruticosa*, which sheds new light on the mechanism of LOX catalysis. Our crystallographic and mutational studies suggest that the aliphatic tail of the fatty acid is bound in a hydrophobic pocket with two potential entrances. We speculate that LOXs share a common T-shaped substrate channel architecture that gives rise to the varying positional specificities. A general allosteric mechanism is proposed for transmitting the activity-inducing effect of calcium binding from the membrane-targeting PLAT (polycystin-1/lipoxygenase/ α -toxin) domain to the active site via a conserved π -cation bridge.

Lipoxygenases (LOXs)² are non-heme iron dioxygenases that catalyze the stereo- and regiospecific hydroperoxidation of polyunsaturated fatty acids (1). LOX catalysis products of arachidonic acid (AA), which is the main substrate in animals, are hydroperoxyeicosatetraenoic acids (HpETEs), these lipid mediators and their metabolites have been implicated in cancer (2), atherosclerosis (3), and allergic inflammation (4). Consequently, LOXs are targets for drug design. A complicating factor in the development of LOX inhibitors is that there are several LOX isoforms in an organism, all with equivalent catalytic machinery and chemical mechanism (5). Thus, differences in regiospecificity or regulation must be exploited to design iso-

form-specific inhibitors. Given the limited amount of structural information of arachidonate-metabolizing LOXs, each new structure provides crucial details related to LOX catalysis mechanism.

LOX catalysis begins with a stereoselective hydrogen abstraction by the catalytic non-heme iron from the methylene carbon (CH₂) of the selected 1,4-*cis,cis*-pentadiene unit on the fatty acid substrate, and is followed by regioselective dioxygen addition on the opposite face of the substrate either at -2 or +2 carbon (Fig. 1) (6). For such specific reactions to take place, a very distinct substrate channel that goes past the non-heme iron must position the fatty acid. This binding site must also vary among LOX isoforms to facilitate the different catalytic properties. The substrate-binding cavity has been described as "boot-shaped"; it is directly accessible from the surface of the protein and ends with a hydrophobic pocket (7). The pocket residues of several 12/15-LOXs have been mutated to demonstrate that bulkier side chains favor 15-lipoxygenation, whereas less space-filling residues, which would allow the fatty acid tail to penetrate deeper into the cavity, confer 12-LOX activity. These results are consistent with aliphatic tail-first entry (8–12). Also, a cationic arginine near the entrance of the cavity has been shown to stabilize the carboxylate head of the fatty acid (13). Computational docking studies based on x-ray crystallography data further support the boot-shaped substrate channel (14, 15). For some LOXs, carboxylate head-first binding has been suggested to explain differing specificity or double dioxygenation of AA (16, 17). In the light of the coral 8*R*-LOX crystal structure, however, a novel binding model was proposed with an alternative U-shaped channel that neglects the hydrophobic pocket (18). According to this hypothesis, the substrate is bound in a culvert that runs under a conserved arched helix; distinct lipoxygenases allow access to the catalytic iron from one of two possible directions. Although several lipoxygenase crystal structure models have been published, including rabbit 12/15-LOX (19, 20), coral 8*R*-LOX (18, 21), and recently a modified human 5-LOX (22) representing *Animalia*, the lack of experimental evidence on substrate binding, such as a crystalized enzyme-substrate complex, has precluded the emergence of a uniform theory.

The activity of various LOXs depends more or less on the presence of Ca²⁺ that promotes interactions with the lipid

* This work was supported by National Science Foundation Grant MCB 0818387 (to M. E. N.), Estonian Science Foundation Grants 8276 (to I. J.) and 9410 (to N. S.), the Estonian Ministry of Education and Research Grant SF140010508 (to N. S.), and the European Union Seventh Framework Programme Project VFP414 (to Prof. Mihkel Kaljurand and Dr. Mihkel Koel).

[5] This article contains supplemental Figs. S1–S4.

The atomic coordinates and structure factors (code 3yf1) have been deposited in the Protein Data Bank, Research Collaboratory for Structural Bioinformatics, Rutgers University, New Brunswick, NJ (<http://www.rcsb.org/>).

¹ To whom correspondence should be addressed. Tel.: 372-620-4376; Fax: 372-620-2828; E-mail: nigulas.samel@ttu.ee.

² The abbreviations used are: LOX, lipoxygenase; PLAT, polycystin-1/lipoxygenase/ α -toxin; AA, arachidonic acid; HpETE, hydroperoxyeicosatetraenoic acid; HETE, hydroxyeicosatetraenoic acid; bis-Tris, 2-[bis(2-hydroxyethyl)amino]-2-(hydroxymethyl)propane-1,3-diol.

Regulation of 11*R*-Lipoxygenase Catalysis

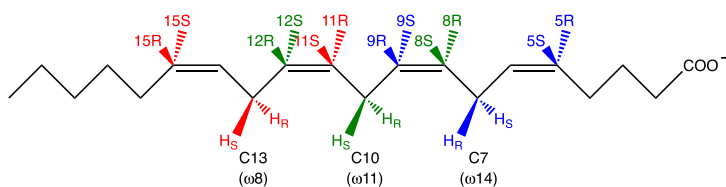


FIGURE 1. All 12 possible lipoxygenation positions in AA. The catalysis begins with stereoselective hydrogen abstraction from C7, C10, or C13 (labeled *proS/R*), followed by antarafacial dioxygen addition either at -2 or $+2$ carbon (grouped by colors). Based on data from Ref. 6.

membrane, from where the enzyme obtains its fatty acid substrate (21, 23). The human 5-LOX is effectively translocated to the nuclear envelope upon Ca^{2+} release, the C2-like PLAT domain being the selective membrane-targeting module (24). The calcium-binding sites of the PLAT domain appear to be conserved among human 5-LOX, coral 8*R*-LOX, gangrene α -toxin, as well as coral 11*R*-LOX, which are all induced by Ca^{2+} , but not in rabbit 12/15-LOX, which is only mildly affected (21, 25). The molecular mechanism of Ca^{2+} - and membrane-induced allosteric regulation is not clear. Although many mammalian lipoxygenases retain their reaction specificity after PLAT domain truncation, this is accompanied by reduced turnover rates (26). Moreover, tight association of PLAT and catalytic domains has been shown to be important for protein stability and catalytic activity (27). A possible structural element that may be under allosteric control is the $\alpha 2$ region that forms a "lid" over the putative substrate channel entrance, which can adopt different conformations, thereby either opening or closing the orifice (20, 28, 29). Another plausible allosteric mechanism could involve oligomerization, which has been noticed in case of human platelet 12-LOX and rabbit 12/15-LOX (30, 31), but no definite assembly has been described to date.

The arachidonate 11*R*-LOX from the white sea coral *Gersemia fruticosa* is the first described lipoxygenase with 11*R*-specificity (25). Based on primary structure comparison it is most closely related to the 8*R*-LOX from the allene oxide synthase-lipoxygenase fusion protein of the Caribbean sea whip coral *Plexaura homomalla* (42% identity) (32) and the analogous enzyme from *G. fruticosa* (43%) (33). The closest mammalian counterparts are 5-LOXs (about 33%). Experiments with alternative substrates suggest that the fatty acid enters the active site tail-first, as the catalysis specificity depends on the distance of the bisallylic methylene from the methyl end of the aliphatic tail (25). The conserved Gly/Ala sequence determinant, which acts like a switch that directs oxygen to either -2 or $+2$ carbon (*R*- or *S*-stereospecificity, respectively) (34), has been identified as Gly⁴¹⁶ (25), which agrees with previous findings linking glycine to *R*-stereoconfiguration. An important feature of the 11*R*-LOX is its complete dependence on both Ca^{2+} and lipid membranes, the presence of both components is necessary for catalytic activity (25). This, together with the remarkable stability and relative similarity of the enzyme to human 5-LOX, makes it an exceptional subject to study the mechanism of lipoxygenase catalysis specificity and regulation.

Hereby we report the 2.47-Å crystal structure model of the coral 11*R*-LOX that suggests a potential allosteric mechanism involving the PLAT domain and the $\alpha 2$ lid region. A highly

conserved π -cation bridge was found that could mediate the regulatory effect of the PLAT domain to the active site. Additionally, a mutation analysis of the hydrophobic pocket in the boot-shaped cavity was conducted to address questions regarding substrate binding. A general hypothesis of possible substrate orientations in the active site is described.

EXPERIMENTAL PROCEDURES

Expression and Purification—Recombinant *G. fruticosa* 11*R*-LOX with an N-terminal His₄ tag in pET-11a vector was transformed into *Escherichia coli* BL21(DE3) cells (Novagen). Colonies were grown overnight in 25 ml of LB containing 100 $\mu\text{g}/\text{ml}$ of ampicillin at 37 °C. A 500-ml volume of autoinducing medium ZYM-5052 (35) (with 100 $\mu\text{g}/\text{ml}$ ampicillin) was inoculated with 5 ml of overnight culture. The culture was incubated at 37 °C for 3–4 h, followed by growth to saturation at 20 °C. Cells were harvested by centrifugation and frozen at -80 °C when the absorbance at 600 nm had remained stable for 4 h (usually 27–30 h after the inoculation).

Cell pellets were resuspended in Bugbuster (Novagen) with added DNase I, pepstatin, and PMSF. The suspension was stirred and incubated on ice for 30 min, lysed in a French pressure cell, and centrifuged at 39,000 $\times g$ for 40 min at 4 °C. The supernatant was applied onto a HisTrap Ni-Sepharose column (GE Healthcare) and washed with binding buffer (50 mM Tris-HCl, 500 mM NaCl, 20 mM imidazole, pH 8.0) on an ÄKTA FPLC system (GE Healthcare). The protein was eluted with an imidazole gradient from 20 to 200 mM. Protein fractions were dialyzed overnight against 20 mM Tris-HCl, pH 8.0, or desalted in a Sephadex G-25 Fine column (Amersham Biosciences). The sample was then applied onto a Mono Q anion exchanger (GE Healthcare), washed with 20 mM Tris-HCl, pH 8.0, and eluted with a NaCl gradient from 0 to 500 mM. Concentrated protein fractions were run on a Superdex 200 size exclusion column (GE Healthcare) with 20 mM Tris-HCl, pH 8.0, and 150 mM NaCl. For long term storage, the protein was concentrated to ~ 15 mg/ml, flash frozen in liquid nitrogen, and stored at -80 °C.

Protein Crystallization—Showers of plate-like crystals formed in 1–2-day-old hanging-drop vapor diffusion experiments that contained a 1:1 mixture of 5 mg/ml of protein solution and reservoir solution (0.1 M bis-Tris, pH 7.2, 11–12% (w/v) PEG 3350, 15% (w/v) sucrose) at 22 °C. To obtain fewer and bigger crystals a microseed stock was prepared using the Seed Bead (Hampton Research) in stabilizing solution with 0.1 M bis-Tris, pH 7.2, 9% (w/v) PEG 3350, and 15% (w/v) sucrose. Seeding experiments were conducted with drops containing 2:1:1 mixture of protein and reservoir solution as described

above and serial dilutions of seed stock as described in the Seed Bead user guide. Larger single crystals grew in 2–3 days. For cryoprotection, crystals were transferred into 0.1 M bis-Tris, pH 7.2, 12% (w/v) PEG 3350, 20–25% (w/v) sucrose in two consecutive steps and then frozen in liquid nitrogen or a 100 K cryostream.

Data Collection and Structure Determination—Preliminary screens for crystal diffraction were conducted at the Gulf Coast Protein Crystallography Consortium beamline at the Center for Advanced Microstructures and Devices (CAMD, Louisiana State University). A full dataset was collected at the NE-CAT beamline 24-ID-E at the Advanced Photon Source (Argonne, IL) using 0.98-Å radiation at 100 K. Data were processed to a resolution of 2.47 Å (Table 1) using xia2 (36). The structure was determined by molecular replacement with MrBUMP (37, 38) using 3.2-Å *P. homomalla* 8R-LOX model (PDB code 2fnq). The initial refinement cycles were performed with REFMAC5 (39). Both MrBUMP and REFMAC5 are part of the CCP4 suite (40). Manual model building was done with COOT (41) and further refinement in PHENIX (42) using the program phenix.refine with non-crystallographic symmetry and Ramachandran restraints, individual isotropic atomic displacement factors, and automatic water picking. For the final refinement, hydrogens were added to the model, Ramachandran restraints were released and both stereochemistry and atomic displacement weights were optimized. Illustrations were prepared with UCSF Chimera (43), surfaces were obtained with MS-MS (44). The dimerization interface was analyzed using PISA (Protein Interfaces, Surfaces and Assemblies) (European Bioinformatics Institute) (45). Sequences were aligned with ClustalW2 (46) and rendered with ESPript (47).

Site-directed Mutagenesis—The V430A, L431A, V609A, and V609W mutations were introduced using whole plasmid PCR primed with complementary primers that additionally contained silent mutations for restriction analysis. The M606A mutant was obtained by separately cloning the upstream and downstream fragments of the recombinant cDNA using mutation-containing primers with respective cDNA upstream or downstream primers. Purified fragments were merged using PCR and the cDNA was ligated back into pET-11a vector (Stratagene) into the BamHI site. The desired mutations were confirmed by sequencing. For whole plasmid PCR protocol, the following DNA primers were used with their complementary primers for mutagenesis: 5'-GGT GCG GCT GAC AAA GCG CTG AGC ATT GGT GGA GG-3' for V430A, 5'-GGT GCG GCT GAC AAG GTG GCT AGC ATT GGT GGA GG-3' for L431A, 5'-GTT ACA ATG GTT TCA GCT GTG AAT GCG C-3' for V609A, 5'-ACA ATG GTT TCT TGG GTT AAC GCG CTA ACC ACG A-3' for V609W, and the following primers for cloning fragments with M606A mutation: 5'-AA GGA TCC ATG CAT CAC CAT CAC ATG AAG TAC AAG-3' (11R-LOX cDNA upstream) and 5'-G CGC ATT CAC AAC AGA AAC AGC TGT AAC AGC TTG-3' (M606A downstream) for the upstream fragment, 5'-CAA GCT GTT ACA GCT GTT TCT GTT GTG AAT GCG C-3' (M606A upstream) and 5'-GAT GGA TCC TTA GAT GGC AAT ACT GTT CGG-3' (11R-LOX cDNA downstream) for the downstream fragment.

Enzyme Assay—Initial enzyme specificity experiments were conducted on crude bacterial lysates. BL21-CodonPlus(DE3)-RP cells (Stratagene) were transformed and grown in LB medium with 100 µg/ml of ampicillin at 37 °C. Following 500 µM isopropyl β-D-thiogalactoside induction at $A_{600\text{ nm}} = 0.6$, cells were grown for 16–18 h at 10 °C. Cells were harvested by centrifugation at 4 °C, washed with 50 mM Tris-HCl, pH 8.0, aliquoted, and frozen at –80 °C.

For product analysis, aliquots of 2.5 ml of culture were resuspended in 500 µl of 50 mM Tris-HCl, pH 8.0, with 1 mM PMSF and sonicated 3 × 5 s using a Torbéo 36810-Series cell disruptor (Cole Parmer) at a setting of 5. The suspension was centrifuged at 13,000 × g for 20 min at 4 °C and the supernatant was harvested. CaCl₂ was added to the enzyme solution in final concentration of 10 mM. Incubations of 1–20 ml were carried out in 50 mM Tris-HCl, 250 mM NaCl, pH 9.0 buffer with 50 µM arachidonic acid at room temperature for 5 min with constant stirring. [1-¹⁴C]-Labeled arachidonic acid (GE Healthcare) was used in 1-ml incubations. HpETEs were reduced to corresponding hydroxy acids (HETEs) with 10 mM SnCl₂, the mixture was acidified with KH₂PO₄/HCl (1:1) to pH 6 and the products were extracted using ethyl acetate. Incubation products (10–20 ml volumes) were purified prior to HPLC analysis using thin layer chromatography: the extract was applied on a silica gel plate, eluted with a hexane/ethyl acetate/acetic acid (3:4:0.05) mixture, and the product band was determined using UV light (254 nm) and extracted with methanol.

For kinetic studies, wild-type enzyme and selected mutants were purified on an ÄKTA FPLC system as described above. Conjugated diene formation was monitored on a UV-1601 spectrophotometer (Shimadzu) at 236 nm. Reactions of 1 ml (50 mM Tris-HCl, pH 8.0, 100 mM NaCl, 2 mM CaCl₂, ~60 µM liposome) were performed in a thermostatted (20 °C) cuvette with continuous stirring. The concentration of arachidonic acid (Cayman) was varied from 2 to 200 µM. The reaction was initiated by adding 6 nM wild-type enzyme, or up to 32 nM for the less active mutants. The reaction velocity was determined from the slope of the linear portion of the curve. K_m and k_{cat} values were obtained by nonlinear regression analysis with the Michaelis-Menten equation. As 11R-LOX exhibits very strong substrate inhibition and, thus far, no suitable kinetic model has been derived, only the ascending part of the curve (2–30 µM AA) was used for fitting.

HPLC-MS Analysis—Catalysis products were analyzed by reverse phase HPLC using an Agilent Eclipse 3.5 µm 150 × 2.1-mm ODS column thermostatted at 35 °C. The sample was eluted isocratically with methanol/water/acetic acid (75:25:0.01, v/v/v) at 0.25 ml/min on an Agilent 2200 Series HPLC system. Products were detected using a diode array detector monitoring wavelengths 210–280 nm, followed by an Agilent LC/MSD Trap XCT mass spectrometer. The MS/MS spectra of arachidonic acid derivatives were obtained in negative mode using an APCI interface.

[1-¹⁴C]-Labeled products were additionally analyzed using a Radiomatic 500TR Flow Scintillation Analyzer (Packard Bioscience) preceded by an Agilent Eclipse 5 µm 150 × 4.6-mm ODS column thermostatted at 35 °C and a diode array detector. The same eluent was used at a flow rate of 1 ml/min.

Regulation of 11R-Lipoxygenase Catalysis

TABLE 1
Data collection and refinement statistics

Data collection	
Space group	C2
Cell dimensions	
<i>a</i> , <i>b</i> , <i>c</i> (Å)	114.80 148.71 117.33
α , β , γ (°)	90.00 119.16 90.00
Resolution (Å)	36.48–2.47 (2.54–2.47) ^a
R_{sym}^b	0.072 (0.474)
<i>I</i> / σ <i>I</i>	10.1 (1.7)
Completeness (%)	97.1 (84.6)
Redundancy	3.0 (2.3)
Refinement	
Resolution (Å)	36.48–2.47
No. of reflections	57,423
$R_{\text{work}}/R_{\text{free}}^c$	0.2019/0.2281
No. of atoms	
Protein	10,880
Iron	2
Sucrose	46
Water	482
<i>B</i> -factor (Å ²)	
Protein	42.9
Iron	36.3
Sucrose	56.9
Water	39.0
Root mean square deviation	
Bond lengths (Å)	0.005
Bond angles (°)	0.6

^a Values in the parentheses represent the highest resolution shell.

^b $R_{\text{sym}} = \sum_i \sum_j |I_{ij} - \langle I_{ij} \rangle| / \sum_i \sum_j \langle I_{ij} \rangle$, where I_{ij} is the intensity of the *i*th observation and $\langle I_{ij} \rangle$ is the mean intensity of the reflection *h*.

^c $R = \sum |F_o| - |F_c| / \sum |F_o|$, where F_o and F_c are the observed and calculated structure factor amplitudes, respectively. R_{free} was calculated using 3.33% of the total reflections.

To analyze the chirality of HETEs, the products were purified in a normal phase HPLC system using a Phenomenex Luna 5 μm 250 \times 4.6-mm Silica column in isopropyl alcohol (1% H₂O)/hexane (7:93, v/v) at 1 ml/min. HETEs were methylated using diazomethane and analyzed using a Chiralcel OD-H 250 \times 4.6-mm column in 0.7% isopropyl alcohol (dry), 0.7% methanol, hexane (v/v/v) at 1 ml/min.

Liposome Preparation—Small unilamellar vesicles were prepared from L- α -phosphatidylcholine, L- α -phosphatidylethanolamine, and L- α -phosphatidylserine (Avanti Polar Lipids). A mixture of phosphatidylcholine/phosphatidylethanolamine/phosphatidylserine (40:30:30 mol %) in chloroform was dried in a round-bottom flask using a nitrogen stream to form a thin film and was incubated in vacuum for 1 h at room temperature. Buffer (50 mM Tris-HCl, 100 mM NaCl, pH 8.0) was added to the dried lipids and the film was soaked for 1 h. The suspension was shaken vigorously, sonicated 15 \times 5 s on a Torbéo 36810-Series cell disruptor (Cole Parmer) with 1-min intervals at the setting of 5 in a water bath at room temperature. The sonicate was centrifuged at 13,000 \times *g* for 20 min at 4 °C. The supernatant was saved and stored at 4 °C.

RESULTS

Overall Structure—The crystal structure of 11R-LOX in a calcium-free environment was refined at 2.47 Å with R_{work} and R_{free} values of 0.20 and 0.23, respectively (Table 1). The protein crystallized in space group C2 with two molecules in the asymmetric unit. Phasing was done with molecular replacement using *P. homomalla* 8R-LOX (PBD code 2fnq) as a template. A total of 96.1% of the residues are in the favored region of the Ramachandran plot and there are no outliers according to MolProbity validation (48).

Like the majority of lipoxygenases, 11R-LOX consists of two distinct domains: the N-terminal C2-like PLAT domain (residues 1–115) and a larger mainly α -helical catalytic domain (residues 129–679), which are connected by a small linker region (residues 116–128). The catalytic domain contains the non-heme iron, which is coordinated by three highly conserved histidines, His³⁷³, His³⁷⁸, and His⁵⁵⁶, and the carboxylate group of the C-terminal Ile⁶⁷⁹. In general, the structure is very similar to that of the 8R-LOX domain of *P. homomalla* allene oxide synthase-LOX fusion protein, a root mean square deviation of 644 C α pairs being 1.37 Å. The greatest differences are found in the putative entrance to the active site, which more closely resembles the recently published human Stable-5-LOX (22). Similarly to 5-LOX, the α 2 helix of 11R-LOX that covers the putative entrance is only about 2 turns long and is flanked by loops and small 3₁₀-helices. It should also be mentioned that the overall similarity between the 11R- and 5-LOX is very high (root mean square deviation of 641 C α pairs is 1.49 Å).

Another heterogeneous region includes the putative Ca²⁺-binding sites in the PLAT domain. The PLAT domain is a β -sandwich consisting of two antiparallel 4-strand β -sheets. At the sheets' ends proximal to the catalytic domain (opposite to the N terminus) there are four loops that connect the two sheets, three of the loops being rather extensive, this is the region that contains the Ca²⁺-binding sites. The electron density map is less clear in the region of the PLAT domain, which is characterized by higher mean *B*-factors, 37.3 Å² for the catalytic domain versus 70.5 Å² in the PLAT domain. The least well defined densities are found in the putative calcium-binding loops, especially residues His⁴³-Glu⁴⁷ and Gly⁷³-Lys⁷⁷; whereas main chain density is not ambiguous, several side chains were modeled primarily according to optimal geometry (side chains present at $\geq 0.5 \sigma$). For refinement, all occupancies were set to 1. The apparent mobility of these residues is described by their elevated *B*-factors.

Dimerization—Size exclusion chromatography indicated that 11R-LOX appears as a dimer in a calcium-free buffer. The purified enzyme eluted with aldolase (158 kDa), which is double the molecular mass of the recombinant protein (79 kDa) (supplemental Fig. S1). Based on ultrafiltration assays, it was previously concluded that 11R-LOX is in a monomeric state in solution: in calcium-free conditions the enzyme passed a filter with a 100-kDa cutoff without major losses (25). The findings presented here clearly dispute those claims. In the presence of 10 mM CaCl₂, however, size exclusion chromatography analysis indicated the formation of large aggregates, as the protein eluted with the void volume (data not shown). Similar results were obtained using ultrafiltration (25). Potential dimerization interfaces were searched among the crystal contacts using PISA (45), but according to the criteria established by the algorithm, no significant assemblies were found.

Substrate Channel and Its Entrances—There is an array of consecutive, mostly hydrophobic cavities concealed in the catalytic domain alongside the coordinated non-heme iron (Fig. 2). These cavities are covered by a conserved arched helix (α 10– α 11 in *G. fruticosa*), and the potential entrances on either side are blocked by short helices and loops. The arched helix harbors the *R/S*-stereospecificity determinant Gly⁴¹⁶ (34).

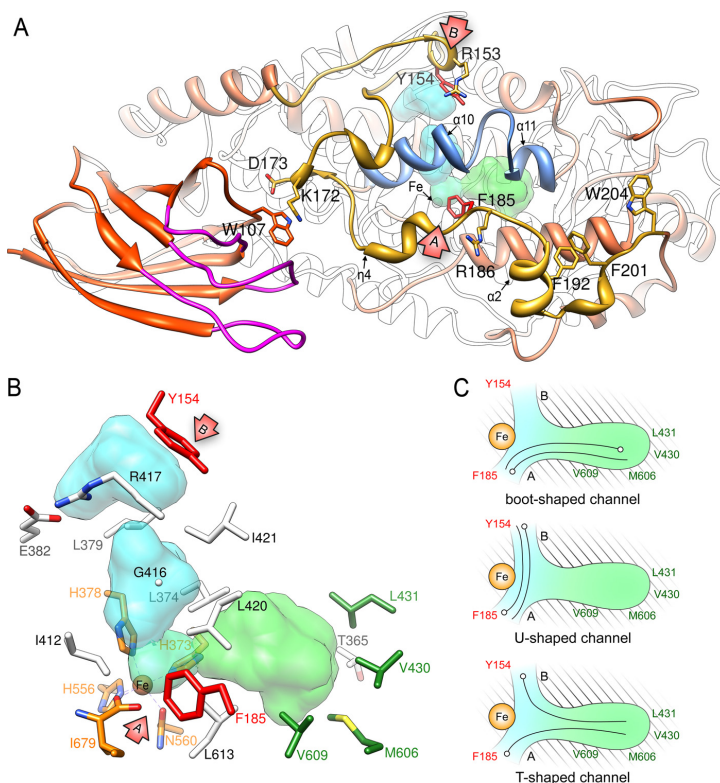


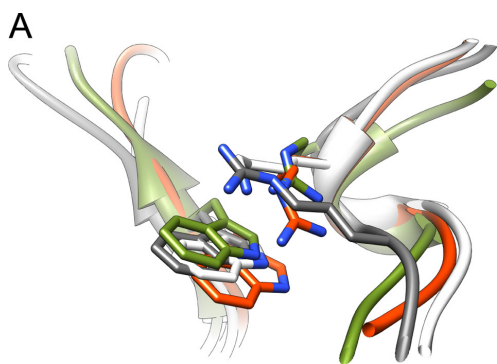
FIGURE 2. The active site and its accessibility. *A*, the active site with the non-heme iron (sphere) and substrate binding cavities (cyan and green surfaces) are covered by the conserved arches $\alpha 10$ – $\alpha 11$ (blue). Potential entrances A and B (arrows) are blocked by Phe¹⁸⁵ and Tyr¹⁵⁴ (red residues), respectively. Both have an arginine in the vicinity that could stabilize the carboxylate head of the fatty acid substrate. The entrances are covered by the lid segment (gold) that interacts with the PLAT domain (orange) near the loops, which contain the putative Ca²⁺-binding sites (magenta), via a π -cation bridge (Trp¹⁰⁷–Lys¹⁷²). Additionally, there are hydrophobic residues in the C-terminal part of the lid that could bind the lipid membrane. *B*, in the active site, the non-heme iron is coordinated by highly conserved residues (orange). The volume of the hydrophobic pocket (light green) has been found to be important in catalysis specificity (7, 12). Residues marked in green were mutated in this study to investigate that hypothesis. Another set of cavities (cyan) could give access to the active site via the alternative entrance C. *C*, schematic depictions of hypothesized substrate-binding channels and substrate orientations (viewing angle is analogous to panels A and B). The boot-shaped cavity is defined as a passage from entrance A to the bottom of the hydrophobic pocket (7, 12). The U-shaped channel would stretch between the two entrances (18). Yet another possibility is that the fatty acid tail is always bound into the hydrophobic pocket, but either one of the entrances is used depending on the enzyme isoform, this yields the T-shaped channel.

There is a small confined chamber (about 34 Å³) next to the catalytic iron that is surrounded by several conserved aliphatic residues, which have been thoroughly discussed in *P. homomalla* 8R-LOX by Neau *et al.* (18). Of those residues, Leu³⁷⁴, Leu⁴²⁰, and Leu⁶¹³ form an orifice that leads to the largest cavity (188 Å³), which is located under the arches toward the “rear” end of the enzyme (away from the PLAT domain). The bottom of this cavity is composed of residues Thr³⁶⁵, Val⁴³⁰, and Val⁶⁰⁹, which coincide with the regioselectivity determinants described for the boot-shaped channel in 12/15-LOX (7); Leu⁴³¹, also a regioselectivity determinant of some LOXs (8, 12); and Met⁶⁰⁶, a position claimed to be relevant in the binding orientation of the fatty acid substrate (49). On one side of the arches, the entrance to the active site chamber is blocked by Phe¹⁸⁵ that sits on a loop between helices $\eta 4$ (3₁₀-helix) and $\alpha 2$. On the other side, a gap between Leu³⁷⁴, Ile⁴¹², and Leu⁴²⁰ leads to a pair of cavities (95 and 113 Å³) that also reach toward the protein surface. These cavities are lined

perpendicularly to the largest one, and are separated from each other by a constriction formed by Leu³⁷⁹, Ile⁴²¹, and a conserved salt bridge Glu³⁸²–Arg⁴¹⁷, that participates in lodging the arches. Access on this side is obstructed by Tyr¹⁵⁴ and the loop where that residue is situated.

Let us call the orifices blocked by Phe¹⁸⁵ and Tyr¹⁵⁴ entrances A and B, respectively. Both of these entrances have a positively charged residue in the vicinity, which could neutralize the carboxylate group of a fatty acid, and therefore, aid to position the substrate for catalysis: these are Arg¹⁸⁶ for entrance A, and Arg¹⁵³ for B. It is interesting to note that the chain fragments that constitute the lids over both entrances interact with the PLAT domain, there is a π -cation interaction between Trp¹⁰⁷ and Lys¹⁷², as well as an H-bond connecting the main chain N–H of Trp¹⁰⁷ with Asp¹⁷³ (Fig. 2A). The lids of entrances A and B are on the C- and N-terminal sides of the interface, respectively. Therefore, either one of the entrances could be regulated via this bridge. The π -cation bond appears

Regulation of 11R-Lipoxygenase Catalysis



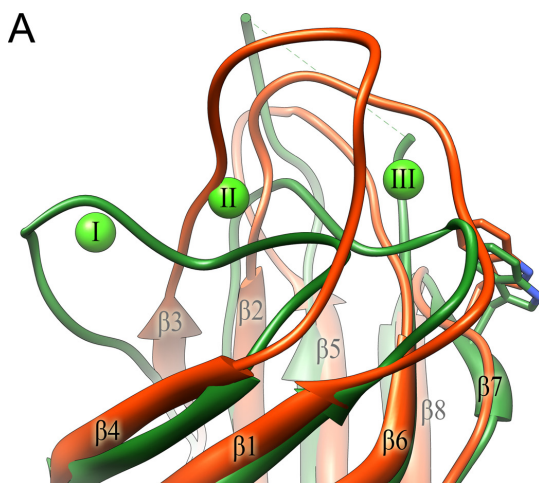
B

		β7		η3 α2
11R-LOX				
11R-LOX	97	SNKYI	FPCYRWV	170
AOSL_PLEHO	472	S...	FPCFRWV	537
LOX15_PONAB	89	GDEVRR	FPCYRWV	160
LOX15_HUMAN	89	GDEVRR	FPCYRWV	160
LOX12_PIG	90	GDEFRR	FPCYRWV	161
LOX12_BOVIN	90	GNEFRF	FPCYRWV	161
LOX12_RABBIT	90	EDKYWF	FPCYRWV	161
LOX15_RABBIT	90	EDKYWF	FPCYRWV	161
LX12L_MOUSE	90	GSEYTF	FPCYRWV	161
LX12L_RAT	90	GSEYTF	FPCYRWV	161
LOX12_MOUSE	89	QGEAF	FPCYSWV	160
LOX12_HUMAN	89	CAEVA	FPCYRWV	160
LOX12_MOUSE	89	SAEAV	FPCYRWV	160
LX15B_MOUSE	101	.AALR	FPCYOWL	171
LX15B_RAT	101	.AALR	FPCYOWL	171
LX15B_HUMAN	100	.GHLL	FPCYOWL	170
LX12B_MOUSE	95	.RVYH	FPAYOWM	196
LX12B_RAT	95	.RVYH	FPAYOWM	196
LX12B_HUMAN	95	.RYYH	FPAYOWM	196
LOXE3_HUMAN	95	.SVSH	FPCYOWI	206
LOXE3_MOUSE	95	.SAVH	FPCYOWI	206
LOX5_RAT	93	.DYIE	FPCYRWI	163
LOX5_MOUSE	94	.DYIE	FPCYRWI	164
LOX5_MESAU	93	.DYIE	FPCYRWI	163
LOX5_HUMAN	93	.DYIE	FPCYRWI	163
LOX2_SOYBN	150	QGTRIR	FVCNSWV	269
LOX1_SOYBN	120	QGTRIR	FVCNSWV	240
LOXX_SOYBN	146	HGTIEF	FVCNSWV	263
LOX4_SOYBN	134	HGTIEH	FVCNSWV	253
LOX3_SOYBN	138	HGSIVH	FVCNSWI	258
LOXA_SOLLC	134	HGKVVH	FVCNSWI	259
LOX1_ARATH	136	HGRVHV	FVCNSWI	258
LOX2_ARATH	175	.GSTIT	FPCESWV	297

FIGURE 3. The conserved π -cation bridge binds the regulatory PLAT and the catalytic domains. *A*, superposition of 11R-LOX (white), rabbit 12/15-LOX (gray), human 5-LOX (orange), and soybean LOX-1 (green) reveals the common interface. *B*, partial sequence alignments of the PLAT domain and the lid that establish the π -cation bridge. The PLAT domain Trp¹⁰⁷ is invariant, the cationic residue can be found in either of the two positions (blue arrows).

to be conserved as it is present in all published lipoxygenase crystal structures (18, 20, 22, 50–53) (Fig. 3A). The PLAT domain Trp¹⁰⁷ is invariant among studied LOXs and is a part of the conserved sequence FPCYRW on the β 7 strand of animal LOX (28). The cationic residue of the catalytic domain (Lys¹⁷² in 11R-LOX) is more variable, but can still be found in either of the two positions shown on the alignment (Fig. 3B).

Ca²⁺-binding Sites—The 11R-LOX crystals were obtained in calcium-free conditions, but for catalytic activity, the presence of Ca²⁺ is a must. When compared with available structures of Ca²⁺-PLAT complexes, the Ca²⁺-binding loops of the apo-domain in 11R-LOX differ significantly. The PLAT domains of coral 8R-LOX (21) and gangrene α -toxin (54) both contain



B

		β1		β2	TT
11R-LOX					
11R-LOX	1	MKYK	ITVE	TGDLRG	AGTDA
8R-LOX	2	AIYN	VEVE	TGDRFH	AGTDA
5-LOX	1	PSYT	VTVA	TGSGWF	AGTDD
α -toxin	256	KELV	AVLS	TSGEKD	AGTDD

		β3		β4
11R-LOX				
11R-LOX	32	EITSA	FSLDK	KYFHN
8R-LOX	33	.TDYL	LKDK	WFHND
5-LOX	32	.SEKHL	LDK	PFYND
α -toxin	287	.TQEW	EMDN	.PGNDF

		β5		β6
11R-LOX				
11R-LOX	61	.VGEI	AMIT	LKENG
8R-LOX	61	.VGD	IQLE	LHSD
5-LOX	62	G...E	IQLV	IEKRK
α -toxin	316	LKIDD	IQNM	WIRKR

		β7		β8
11R-LOX				
11R-LOX	87	TEIK	IIDEAT	GFSNKY
8R-LOX	90	IIIS	STQ...	DRVYS
5-LOX	87	LKT	PHG...	DYIE
α -toxin	345	VIA	ANGK...	VVVDK

FIGURE 4. The PLAT domain and putative Ca²⁺-binding sites. *A*, superposition of the coral 8R-LOX Ca²⁺-PLAT complex (green) and the 11R-LOX apo-PLAT (orange). The invariant Trp is situated on the β 7-strand right next to site III. *B*, conservation of binding sites, conserved residues are in red. 11R-LOX, 8R-LOX, and gangrene α -toxin are aligned according to a structural superposition; human 5-LOX is aligned according to sequence. Residues that constitute sites I (blue), II (red), and III (green) in 8R-LOX and α -toxin are denoted by circles (empty if participates by main chain, filled if by side chain atom). The invariant Trp is indicated by a star.

three occupied binding sites, these are formed by three adjacent loops and are well conserved both in sequence and structure (21). All three sites are also preserved in the 11R-LOX sequence, yet are absent in the tertiary structure (Fig. 4). The first Ca²⁺ complex is formed by a turn in the β 3– β 4 loop; in the apo-PLAT domain the turn is missing, and instead, there is an extra β -strand-like segment. The second site is situated between another turn in the β 3– β 4 loop and β 1– β 2 loop; again, the loops in 11R-LOX are arranged differently making a

TABLE 2

Positional specificity of 11R-LOX (%)

Arachidonic acid was incubated with the bacterial crude lysate, reaction products were analyzed by RP-HPLC-MS. Chromatograms and MS/MS spectra are provided in supplemental Fig. S3 and S4.

Enzyme	15-HpETE	11-HpETE	8/(12)-HpETE	5-HpETE
WT	2	98	ND ^a	ND
V430A	1	99	ND	ND
V609A	8	91	1	ND
L431A	3	87	10	ND
M606A	2	89	9	ND
V609W	23	69	3 ^b	5

^a ND, not detected.

^b 8- and 12-HETE did not separate in the HPLC system, but both derivatives were detected by MS for V609W.

smoother curve and reaching further away from the β -sandwich core. The same goes for the third site that lies between a turn in the β 1– β 2 loop and the β 5– β 6 loop. Site III is also the hardest to detect by sequence comparison as it is mostly defined by main chain atoms. Fig. 4 illustrates that the Ca^{2+} -binding sites are intertwined; therefore, a cascade of conformational changes could occur upon metal chelation. The aforementioned Trp¹⁰⁷ is right next to site III and makes contacts with residues that define the site in both apo- and holo-PLAT domains. This suggests it could be communicating the allosteric effect that occurs upon calcium and membrane binding in the PLAT domain to the lid segment.

Site-directed Mutagenesis of Substrate Channel—Several residues were mutated in the largest of the internal cavities to study its intrinsic role in the specificity of catalysis. Bulky, hydrophobic Val⁴³⁰, Leu⁴³¹, Met⁶⁰⁶, and Val⁶⁰⁹ were substituted with a compact alanine to deepen the boot-shaped channel, and potentially alter the regiospecificity of the enzyme, as has been previously shown by Kühn *et al.* (7). In the case of 11R-LOX, the additional space was expected to cause a frame-shift of substrate binding, resulting in a novel 8-LOX activity, unseen in the wild-type. The V430A and V609A substitutions failed to alter the position of hydrogen abstraction, although the corresponding residues have been described as regiospecificity determinants for rabbit 12/15-LOX (11) and many others (12) (full sequence alignment is provided in supplemental Fig. S2). Rather, the V609A mutant suffered from general loss of positional control, exhibiting increased 15-HpETE production (Table 2). On the other hand, modest 8-LOX activity was observed with L431A and M606A mutants, reaching up to 10% of 8-HpETE production. Further kinetic studies of those enzymes showed that there was no remarkable change in substrate affinity (K_m) (Table 3). However, the catalysis efficiency (k_{cat}/K_m) of the L431A mutant was only one-fourth of the wild-type as the turnover rate (k_{cat}) had dropped. One possible interpretation of this data is that the substrate cannot align in an orientation appropriate for hydrogen abstraction as the hydrophobic pocket has a role in substrate positioning. Granted, the data do not rule out an effect on the catalytic machinery itself, but the fact that enzyme retains catalytic activity might suggest that the iron coordination sphere remains intact. Moreover, the residue at this position varies significantly among LOX isoforms so it is in all likelihood not an essential element of the core LOX fold.

TABLE 3

Kinetic properties of wild-type 11R-LOX and selected mutants

All enzymes were readily purified and analyzed as described under "Experimental Procedures."

Enzyme	k_{cat} s^{-1}	K_m μM	k_{cat}/K_m
WT	310.7 \pm 24.6	12.3 \pm 2.2	25.2
L431A	50.6 \pm 3.3	7.8 \pm 1.4	6.5
M606A	398.0 \pm 20.8	13.7 \pm 1.5	29.0
V609W	5.8 \pm 0.6	12.4 \pm 3.0	0.5

Although the data display a trend, these studies do not rule out the use of the alternative U-shaped channel (Fig. 2C). To find more substantial evidence to differentiate between the channels, Val⁶⁰⁹, which lies near the proximal side of the hydrophobic pocket, was substituted with a large tryptophan to block the distal end of the cavity, and propagate the usage of the U-shaped channel. As a consequence, the catalytic efficiency of the enzyme plunged 50-fold, but surprisingly, the K_m remained unaffected despite the dramatic reduction in binding space that such a mutation should have caused. Apparently, the loss of activity was entirely due to the diminished turnover rate (Table 3). Reaction specificity suffered greatly, as well, as the share of 11-HpETE dropped down to 69% and a multitude of by-products (15/5/8/12-HpETE in descending order by proportion) was formed (Table 2). The chirality of the three major products of V609W mutant, 11/15/5-HpETE, was determined using chiral phase HPLC, to confirm the substrate orientation in the active site. Practically pure 11R and 5S products were detected, oxygenation at C15 created an *R/S* (35:65) mixture (data not shown). The formation of 5S-HpETE intimates a head-first binding if entrance A is considered as the point of entry, whereas for 11R-HpETE, tail-first orientation has been suggested (25).

The interpretation of these data is not straightforward. If one invokes the use of the boot-shaped cavity, the residual activity of the V609W mutant may be a result of incomplete closure of the cavity and a motional flexibility to allow room for substrate entry despite the bulky tryptophan (Fig. 2C). On the other hand, if the fatty acid binds into the U-shaped channel, the role of the hydrophobic pocket may be to provide the flexibility necessary for the substrate to product transition. This would easily explain the unchanged K_m . Nevertheless, the various regiospecificities of distinct LOXs must somehow be reflected by their binding sites (*e.g.* different cavity volumes). The U-shaped channel is highly conserved, as emphasized by Neau *et al.* (18), but the invariant amino acids alone cannot explain the distinct products among lipoxygenases. Those side chains that impart specificity would be expected to lie outside the cluster of conserved amino acids. The hydrophobic pocket fulfills that criterion, and binding of AA in that cavity is supported by product shifts in L431A and M606A mutants.

DISCUSSION

Allosteric Lid Segment—The substrate channel entrance A of 11R-LOX is blocked by Phe¹⁸⁵. Interestingly, a similar element, a Phe-Tyr "cork," has been described in human 5-LOX (22). This cork is situated where the other LOX crystal structure models are open to allow access to the catalytic site. In these

Regulation of 11R-Lipoxygenase Catalysis

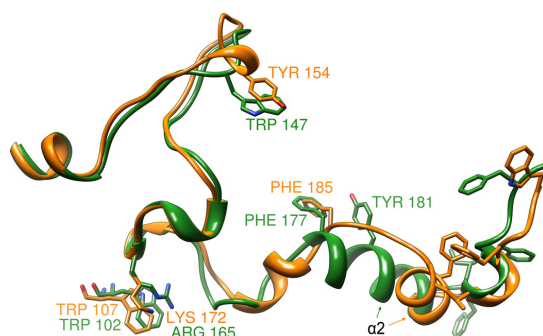


FIGURE 5. Superposed 11R-LOX (orange) and human 5-LOX (green) lid segments. In 5-LOX, entrance A is blocked by a Phe¹⁷⁷–Tyr¹⁸¹ cork (22), the 11R-LOX counterpart of which is Phe¹⁸⁵. For entrance B, the corks are Trp¹⁴⁷ and Tyr¹⁵⁴, respectively. Both structures include the conserved π -cation bridge and several hydrophobic residues in the C-terminal part, which could anchor into the lipid membrane.

two structures, however, the $\alpha 2$ helix is considerably shorter and is flanked by loops and 3_{10} -helices forming a lid that covers entrance A (Fig. 5). In the N-terminal end of this motif is the conserved π -cation bridge (Trp¹⁰⁷–Lys¹⁷²) that connects the PLAT and the catalytic domain. The π -cation bridge is preceded in turn by the lid of entrance B, with Tyr¹⁵⁴ blocking the access. The corresponding cork in human 5-LOX is Trp¹⁴⁷, and again, the similarity between the coral and human enzyme lids is remarkable. Notably, this is the entrance Gilbert *et al.* (22) have suggested to be utilized in 5-LOX, as opening it requires only a rotamer flip, and this way the substrate can enter the channel “tail first.” The stereochemistry of the products of 5- and 11R-LOX suggests that AA is bound in inverse orientations in these enzymes: may it be a result of the substrate entering the active site in inverse orientation using the same orifice or the utilization of different entrances. In either case, access to the catalytic site in both enzymes requires a conformational change, an opening of the lid. The structure of 11R-LOX can provide a stable framework for understanding the relationship between Ca²⁺-dependent membrane binding and lid opening.

It has been speculated that the interface of PLAT and catalytic domains, including the conserved FPCYRW fragment on the $\beta 7$ strand, might be involved in an allosteric regulatory mechanism, transmitting a conformational change in the PLAT domain induced by calcium and membrane binding to the lid component in the catalytic domain (28). We propose, that the conserved π -cation bond could be mediating this interaction, as it stands right between the Ca²⁺-binding sites and the allosteric lid. The different regulatory properties of various lipoxygenases (*e.g.* the necessity of calcium and membranes for 11R-LOX catalysis) can be explained by differing conditions that are needed to set off the cascade of conformational changes, which among other contributors depend strongly on the structure of the Ca²⁺-binding loops (55). The activity that is present without any inducing factors in most LOXs can be attributed to a semi-open orifice, or possibly allosteric binding of the substrate itself. Additionally, in human 5-LOX the FPCYRW fragment has been shown to be involved in the binding of the coactosin-like protein, which promotes leukotriene formation (56).

Although the exact mechanism of the latter is unknown, it further substantiates the regulatory role of the bridge.

In 11R-LOX, entrance A seems the more plausible access route for several reasons. First, the same orifice is used in rabbit 15S-LOX according to docking studies (14). For 11R- and 15S-specificity, the same hydrogen must be abstracted in the initial step of catalysis; thus, substrate binding should also be identical. Second, coral 8R-LOX, the binding of which should differ from 11R- and 15S-LOX only by “frameshift,” has been suggested to employ entrance A as well (18). Another detail in favor of entrance A is that there are several bulky, hydrophobic residues like Phe¹⁹², Phe²⁰¹, and Trp²⁰⁴ on the C-terminal end of its lid fragment, distal to the PLAT domain interface (Fig. 5). With slight conformational changes, these residues could readily anchor the catalytic domain to the lipid membrane, and facilitate an additional mechanism of lid removal. Analogous residues are present in other lipoxygenases, too, including human 5-LOX. Furthermore, the entrance A lid is followed by the putative PDZ domain, which might also contribute to allosteric regulation, making this opening the more likely candidate not only for 11R-LOX, but for other LOXs as well.

Additional experimental data are essential to elucidate the possible access portals in this family of enzymes. In a recent experiment, removing the entrance A cork of olive LOX1 by site-directed mutagenesis augmented the activity of the enzyme remarkably (57). A similar approach could be used in further study to determine the true substrate entrance of 11R-LOX, but also of other LOXs.

T-shaped Substrate Channel—In general, the 11R-LOX model contains a closed, roughly T-shaped system of cavities, wherein the active site iron is located at the junction of perpendicular channels, and the potential entrances for the substrate are situated at both ends of the “T-bar” (Fig. 2C). Although the channel system seems to be segmented in the model, minimal side chain movements are necessary to connect the neighboring pockets. In this system of cavities, the so called boot-shaped channel described by Kühn *et al.* (7, 12) would constitute the passage from entrance A to the bottom of the hydrophobic pocket. The alternative U-shaped channel proposed by Neau *et al.* (18), on the other hand, would consist of a culvert stretching below the arched helix and connecting both entrances, and thus, disregarding the pocket altogether.

The results obtained by site-directed mutagenesis of 11R-LOX suggest that the integrity of the T-shaped channel is required for proper positioning of the substrate. The fact that L431A and M606A substitutions resulted in an 8/11-LOX, albeit with modest amounts of the 8-product, suggests that AA enters the hydrophobic pocket tail-first. This model is also supported by the dramatic reduction of catalytic activity and specificity when the pocket was blocked by the V609W substitution, even though the kinetic parameters for that mutant have left room for alternative interpretations. It is likely that in regard to substrate binding, 11R-LOX is analogous to the enzymes described to have a boot-shaped channel (*e.g.* rabbit 12/15-LOX).

The presence of cavities that connect the hypothetical entrance B with the active site still makes one question their potential role. The U-shaped channel is lined with highly con-

served Leu and Ile residues that imply a structure-functional importance. However, the highly conserved amino acids alone cannot define the different catalytic properties of lipoxygenases. And whereas the cavity that forms the B side of the T-site may provide an entry way for molecular oxygen access as suggested for soybean LOX-1 (58, 59), it is not clear whether leucines, as opposed to any hydrophobic amino acids, are necessary for an O₂ channel. It just might be that distinct lipoxygenases each utilize the central core of the binding site, but regioselectivity is defined by the access to that core. One could imagine a theory that merges the boot- and U-shaped passages, yielding a T-shaped substrate channel. Depending on the catalytic specificity of a particular LOX, the substrate could enter tail-first utilizing either one T-bar entrances. Additional mechanisms like positively charged residues could further induce and stabilize the substrate binding. Yet, for specificity, the aliphatic tail requires the internal hydrophobic pocket. Further studies, especially co-crystallization of the enzyme with the substrate could bring more definitive answers to these matters.

Acknowledgments—We thank Cory LaCrouts for expert assistance in protein expression and purification, and Dr. David Neau in data collection. Preliminary work was performed at the Center for Advanced Microstructures and Devices (Baton Rouge), funded in part by the Louisiana Governors' Biotechnology Initiative. X-ray data were collected at Beam Line 24-ID-E of NE-CAT at the Advanced Photon Source, supported by Award RR-15301 from the National Center for Research Resources at the National Institutes of Health. Use of the Advanced Photon Source, an Office of Science User Facility operated for the United States Department of Energy (DOE) Office of Science by Argonne National Laboratory, was supported by the United States DOE under Contract DE-AC02-06CH11357.

REFERENCES

- Brash, A. R. (1999) Lipoxygenases. Occurrence, functions, catalysis, and acquisition of substrate. *J. Biol. Chem.* **274**, 23679–23682
- Pidgeon, G. P., Lysaght, J., Krishnamoorthy, S., Reynolds, J. V., O'Byrne, K., Nie, D., and Honn, K. V. (2007) Lipoxygenase metabolism. Roles in tumor progression and survival. *Cancer Metastasis Rev.* **26**, 503–524
- Yoshida, H., and Kisugi, R. (2010) Mechanisms of LDL oxidation. *Clin. Chim. Acta* **411**, 1875–1882
- Duroudier, N. P., Tulah, A. S., and Sayers, I. (2009) Leukotriene pathway genetics and pharmacogenetics in allergy. *Allergy* **64**, 823–839
- Ivanov, I., Heydeck, D., Hofheinz, K., Roffeis, J., O'Donnell, V. B., Kuhn, H., and Walther, M. (2010) Molecular enzymology of lipoxygenases. *Arch. Biochem. Biophys.* **503**, 161–174
- Schneider, C., Pratt, D. A., Porter, N. A., and Brash, A. R. (2007) Control of oxygenation in lipoxygenase and cyclooxygenase catalysis. *Chem. Biol.* **14**, 473–488
- Kuhn, H., Saam, J., Eibach, S., Holzhütter, H. G., Ivanov, I., and Walther, M. (2005) Structural biology of mammalian lipoxygenases. Enzymatic consequences of targeted alterations of the protein structure. *Biochem. Biophys. Res. Commun.* **338**, 93–101
- Sloane, D. L., Leung, R., Craik, C. S., and Sigal, E. (1991) A primary determinant for lipoxygenase positional specificity. *Nature* **354**, 149–152
- Chen, X. S., and Funk, C. D. (1993) Structure-function properties of human platelet 12-lipoxygenase. Chimeric enzyme and *in vitro* mutagenesis studies. *FASEB J.* **7**, 694–701
- Borngräber, S., Kuban, R. J., Anton, M., and Kühn, H. (1996) Phenylalanine 353 is a primary determinant for the positional specificity of mammalian 15-lipoxygenases. *J. Mol. Biol.* **264**, 1145–1153
- Borngräber, S., Browner, M., Gillmor, S., Gerth, C., Anton, M., Fletterick, R., and Kühn, H. (1999) Shape and specificity in mammalian 15-lipoxygenase active site. The functional interplay of sequence determinants for the reaction specificity. *J. Biol. Chem.* **274**, 37345–37350
- Vogel, R., Jansen, C., Roffeis, J., Reddanna, P., Forsell, P., Claesson, H. E., Kuhn, H., and Walther, M. (2010) Applicability of the triad concept for the positional specificity of mammalian lipoxygenases. *J. Biol. Chem.* **285**, 5369–5376
- Gan, Q. F., Browner, M. F., Sloane, D. L., and Sigal, E. (1996) Defining the arachidonic acid binding site of human 15-lipoxygenase. Molecular modeling and mutagenesis. *J. Biol. Chem.* **271**, 25412–25418
- Toledo, L., Masgrau, L., Maréchal, J. D., Lluch, J. M., and González-Lafont, A. (2010) Insights into the mechanism of binding of arachidonic acid to mammalian 15-lipoxygenases. *J. Phys. Chem. B* **114**, 7037–7046
- Toledo, L., Masgrau, L., Lluch, J. M., and González-Lafont, A. (2011) Substrate binding to mammalian 15-lipoxygenase. *J. Comput. Aided Mol. Des.* **25**, 825–835
- Boeglin, W. E., Itoh, A., Zheng, Y., Coffa, G., Howe, G. A., and Brash, A. R. (2008) Investigation of substrate binding and product stereochemistry issues in two linoleate 9-lipoxygenases. *Lipids* **43**, 979–987
- Jisaka, M., Iwanaga, C., Takahashi, N., Goto, T., Kawada, T., Yamamoto, T., Ikeda, I., Nishimura, K., Nagaya, T., Fushiki, T., and Yokota, K. (2005) Double dioxygenation by mouse 8S-lipoxygenase. Specific formation of a potent peroxisome proliferator-activated receptor α agonist. *Biochem. Biophys. Res. Commun.* **338**, 136–143
- Neau, D. B., Gilbert, N. C., Bartlett, S. G., Boeglin, W., Brash, A. R., and Newcomer, M. E. (2009) The 1.85-Å structure of an 8R-lipoxygenase suggests a general model for lipoxygenase product specificity. *Biochemistry* **48**, 7906–7915
- Gillmor, S. A., Villaseñor, A., Fletterick, R., Sigal, E., and Browner, M. F. (1997) The structure of mammalian 15-lipoxygenase reveals similarity to the lipases and the determinants of substrate specificity. *Nat. Struct. Biol.* **4**, 1003–1009
- Choi, J., Chon, J. K., Kim, S., and Shin, W. (2008) Conformational flexibility in mammalian 15S-lipoxygenase. Reinterpretation of the crystallographic data. *Proteins* **70**, 1023–1032
- Oldham, M. L., Brash, A. R., and Newcomer, M. E. (2005) Insights from the X-ray crystal structure of coral 8R-lipoxygenase. Calcium activation via a C2-like domain and a structural basis of product chirality. *J. Biol. Chem.* **280**, 39545–39552
- Gilbert, N. C., Bartlett, S. G., Waight, M. T., Neau, D. B., Boeglin, W. E., Brash, A. R., and Newcomer, M. E. (2011) The structure of human 5-lipoxygenase. *Science* **331**, 217–219
- Walther, M., Wiesner, R., and Kuhn, H. (2004) Investigations into calcium-dependent membrane association of 15-lipoxygenase-1. Mechanistic roles of surface-exposed hydrophobic amino acids and calcium. *J. Biol. Chem.* **279**, 3717–3725
- Kulkarni, S., Das, S., Funk, C. D., Murray, D., and Cho, W. (2002) Molecular basis of the specific subcellular localization of the C2-like domain of 5-lipoxygenase. *J. Biol. Chem.* **277**, 13167–13174
- Mortimer, M., Järving, R., Brash, A. R., Samel, N., and Järving, I. (2006) Identification and characterization of an arachidonate 11R-lipoxygenase. *Arch. Biochem. Biophys.* **445**, 147–155
- Walther, M., Hofheinz, K., Vogel, R., Roffeis, J., and Kühn, H. (2011) The N-terminal β -barrel domain of mammalian lipoxygenases including mouse 5-lipoxygenase is not essential for catalytic activity and membrane binding but exhibits regulatory functions. *Arch. Biochem. Biophys.* **516**, 1–9
- Ivanov, I., Di Venere, A., Horn, T., Scheerer, P., Nicolai, E., Stehling, S., Richter, C., Skrzypczak-Jankun, E., Mei, G., Maccarrone, M., and Kühn, H. (2011) Tight association of N-terminal and catalytic subunits of rabbit 12/15-lipoxygenase is important for protein stability and catalytic activity. *Biochim. Biophys. Acta* **1811**, 1001–1010
- Allard, J. B., and Brock, T. G. (2005) Structural organization of the regulatory domain of human 5-lipoxygenase. *Curr. Protein Pept. Sci.* **6**, 125–131
- Jankun, J., Doerks, T., Aleem, A. M., Lysiak-Szydłowska, W., and Skrzypczak-Jankun, E. (2008) Do human lipoxygenases have a PDZ regulatory domain? *Curr. Mol. Med.* **8**, 768–773

Regulation of 11R-Lipoxygenase Catalysis

30. Aleem, A. M., Jankun, J., Dignam, J. D., Walther, M., Kühn, H., Svergun, D. I., and Skrzypczak-Jankun, E. (2008) Human platelet 12-lipoxygenase, new findings about its activity, membrane binding, and low-resolution structure. *J. Mol. Biol.* **376**, 193–209
31. Shang, W., Ivanov, I., Svergun, D. I., Borbulevych, O. Y., Aleem, A. M., Stehling, S., Jankun, J., Kühn, H., and Skrzypczak-Jankun, E. (2011) Probing dimerization and structural flexibility of mammalian lipoxygenases by small-angle x-ray scattering. *J. Mol. Biol.* **409**, 654–668
32. Koljak, R., Boutaud, O., Shieh, B. H., Samel, N., and Brash, A. R. (1997) Identification of a naturally occurring peroxidase-lipoxygenase fusion protein. *Science* **277**, 1994–1996
33. Löhelaid, H., Järving, R., Valmsen, K., Varvas, K., Kreen, M., Järving, I., and Samel, N. (2008) Identification of a functional allene oxide synthase-lipoxygenase fusion protein in the soft coral *Gersemia fruticosa* suggests the generality of this pathway in octocorals. *Biochim. Biophys. Acta* **1780**, 315–321
34. Coffa, G., Schneider, C., and Brash, A. R. (2005) A comprehensive model of positional and stereo control in lipoxygenases. *Biochem. Biophys. Res. Commun.* **338**, 87–92
35. Studier, F. W. (2005) Protein production by autoinduction in high density shaking cultures. *Protein Expr. Purif.* **41**, 207–234
36. Winter, G. (2010) Xia2. An expert system for macromolecular crystallography data reduction. *J. Appl. Crystallogr.* **43**, 186–190
37. Keegan, R. M., and Winn, M. D. (2007) Automated search-model discovery and preparation for structure solution by molecular replacement. *Acta Crystallogr. D Biol. Crystallogr.* **63**, 447–457
38. McCoy, A. J., Grosse-Kunstleve, R. W., Adams, P. D., Winn, M. D., Storoni, L. C., and Read, R. J. (2007) Phaser crystallographic software. *J. Appl. Crystallogr.* **40**, 658–674
39. Vagin, A. A., Steiner, R. A., Lebedev, A. A., Potterton, L., McNicholas, S., Long, F., and Murshudov, G. N. (2004) REFMAC5 dictionary. Organization of prior chemical knowledge and guidelines for its use. *Acta Crystallogr. D Biol. Crystallogr.* **60**, 2184–2195
40. Collaborative Computational Project, Number 4 (1994) The CCP4 suite. Programs for protein crystallography. *Acta Crystallogr. D Biol. Crystallogr.* **50**, 760–763
41. Emsley, P., Lohkamp, B., Scott, W. G., and Cowtan, K. (2010) Features and development of Coot. *Acta Crystallogr. D Biol. Crystallogr.* **66**, 486–501
42. Adams, P. D., Afonine, P. V., Bunkóczi, G., Chen, V. B., Davis, I. W., Echols, N., Headd, J. J., Hung, L. W., Kapral, G. J., Grosse-Kunstleve, R. W., McCoy, A. J., Moriarty, N. W., Oeffner, R., Read, R. J., Richardson, D. C., Richardson, J. S., Terwilliger, T. C., and Zwart, P. H. (2010) PHENIX. A comprehensive Python-based system for macromolecular structure solution. *Acta Crystallogr. D Biol. Crystallogr.* **66**, 213–221
43. Pettersen, E. F., Goddard, T. D., Huang, C. C., Couch, G. S., Greenblatt, D. M., Meng, E. C., and Ferrin, T. E. (2004) UCSF Chimera. A visualization system for exploratory research and analysis. *J. Comput. Chem.* **25**, 1605–1612
44. Sanner, M. F., Olson, A. J., and Spehner, J. C. (1996) Reduced surface. An efficient way to compute molecular surfaces. *Biopolymers* **38**, 305–320
45. Krissinel, E., and Henrick, K. (2007) Inference of macromolecular assemblies from crystalline state. *J. Mol. Biol.* **372**, 774–797
46. Chenna, R., Sugawara, H., Koike, T., Lopez, R., Gibson, T. J., Higgins, D. G., and Thompson, J. D. (2003) Multiple sequence alignment with the Clustal series of programs. *Nucleic Acids Res.* **31**, 3497–3500
47. Gouet, P., Courcelle, E., Stuart, D. I., and Métoz, F. (1999) ESPript. Analysis of multiple sequence alignments in PostScript. *Bioinformatics* **15**, 305–308
48. Chen, V. B., Arendall, W. B., 3rd, Headd, J. J., Keedy, D. A., Immormino, R. M., Kapral, G. J., Murray, L. W., Richardson, J. S., and Richardson, D. C. (2010) MolProbity. All-atom structure validation for macromolecular crystallography. *Acta Crystallogr. D Biol. Crystallogr.* **66**, 12–21
49. Jisaka, M., Kim, R. B., and Boeglin, W. E. (2000) Identification of amino acid determinants of the positional specificity of mouse 8S-lipoxygenase and human 15S-lipoxygenase-2. *J. Biol. Chem.* **275**, 1287–1293
50. Youn, B., Sellhorn, G. E., Mirchel, R. J., Gaffney, B. J., Grimes, H. D., and Kang, C. (2006) Crystal structures of vegetative soybean lipoxygenase VLX-B and VLX-D, and comparisons with seed isoforms LOX-1 and LOX-3. *Proteins* **65**, 1008–1020
51. Minor, W., Steczko, J., Stec, B., Otwinowski, Z., Bolin, J. T., Walter, R., and Axelrod, B. (1996) Crystal structure of soybean lipoxygenase L-1 at 1.4-Å resolution. *Biochemistry* **35**, 10687–10701
52. Chruszcz, M., Wlodawer, A., and Minor, W. (2008) Determination of protein structures. A series of fortunate events. *Biophys. J.* **95**, 1–9
53. Skrzypczak-Jankun, E., Borbulevych, O. Y., Zawadzky, M. L., Baranski, M. R., Padmanabhan, K., Petricek, V., and Jankun, J. (2006) Effect of crystal freezing and small-molecule binding on internal cavity size in a large protein. X-ray and docking studies of lipoxygenase at ambient and low temperature at 2.0-Å resolution. *Acta Crystallogr. D Biol. Crystallogr.* **62**, 766–775
54. Naylor, C. E., Jepson, M., Crane, D. T., Titball, R. W., Miller, J., Basak, A. K., and Bolgiano, B. (1999) Characterization of the calcium-binding C-terminal domain of *Clostridium perfringens* α -toxin. *J. Mol. Biol.* **294**, 757–770
55. Hammarberg, T., Provost, P., Persson, B., and Rådmark, O. (2000) The N-terminal domain of 5-lipoxygenase binds calcium and mediates calcium stimulation of enzyme activity. *J. Biol. Chem.* **275**, 38787–38793
56. Esser, J., Rakonjac, M., Hofmann, B., Fischer, L., Provost, P., Schneider, G., Steinhilber, D., Samuelsson, B., and Rådmark, O. (2010) Coactosin-like protein functions as a stabilizing chaperone for 5-lipoxygenase. Role of tryptophan 102. *Biochem. J.* **425**, 265–274
57. Palmieri-Thiers, C., Alberti, J. C., Canaan, S., Brunini, V., Gambotti, C., Tomi, F., Oliw, E. H., Berti, L., and Maury, J. (2011) Identification of putative residues involved in the accessibility of the substrate-binding site of lipoxygenase by site-directed mutagenesis studies. *Arch. Biochem. Biophys.* **509**, 82–89
58. Knapp, M. J., Seebeck, F. P., and Klinman, J. P. (2001) Steric control of oxygenation regiochemistry in soybean lipoxygenase-1. *J. Am. Chem. Soc.* **123**, 2931–2932
59. Knapp, M. J., and Klinman, J. P. (2003) Kinetic studies of oxygen reactivity in soybean lipoxygenase-1. *Biochemistry* **42**, 11466–11475

SUPPLEMENTAL FIGURE LEGENDS

FIGURE S1. The size-exclusion chromatogram of 11R-LOX (solid line) with a theoretical M_w of 79 kDa displaying its dimeric state if compared to calibration standards (dashed line). Superdex 200 10/300 GL, 20 mM Tris-HCl pH 8.0 + 150 mM NaCl, 0.5 ml/min, $A_{280\text{ nm}}$, ÄKTApurifier.

FIGURE S2. Sequence alignment of lipoxygenases with 11R-LOX secondary structure. Included sequences are *Gersemia fruticosa* 11R-LOX, 8R-LOX from *Plexaura homomalla* AOS-LOX, human 5-LOX (LOX5_HUMAN), rabbit reticulocyte 15S-LOX (LOX15_RABIT), mouse 8S-LOX (LOX8_MOUSE), human platelet 12S-LOX (LOX12_HUMAN), soybean LOX-1 (LOX1_SOYBN) and olive LOX1 (LOX1_OLIVE). 11R-LOX secondary structure elements are denoted by α , α -helix; β , β -strand; η , $^3_{10}$ -helix; π , π -helix; T, turn. Sequences were aligned with ClustalW2 (1) and rendered with ESPript (2).

FIGURE S3. RP-HPLC chromatograms of HETEs. Agilent Eclipse 3.5 μm 150 \times 2.1 mm ODS column, thermostat 35 $^\circ\text{C}$, solvent methanol/0.01% acetic acid (75:25, v/v), 0.25 ml/min. The smaller peak (11-HETE³) was identified as 11-HETE by MS/MS analysis and it was also present in the ^{14}C -radiochromatogram (data not shown); it is most probably a result of *cis/trans*-isomerization (3).

FIGURE S4. MS/MS spectra of HETEs. Agilent LC/MSD Trap XCT, APCI interface, fragmentation of m/z 319, negative mode.

REFERENCES

1. Chenna, R., Sugawara, H., Koike, T., Lopez, R., Gibson, T. J., Higgins, D. G., and Thompson, J. D. (2003) *Nucleic Acids Res.* **31**, 3497–3500
2. Gouet, P., Courcelle, E., Stuart, D. I., and Métoz, F. (1999) *Bioinformatics* **15**, 305–308
3. Schneider, C., Pratt, D. A., Porter, N. A., and Brash, A. R. (2007) *Chem. Biol.* **14**, 473–488

Figure S1

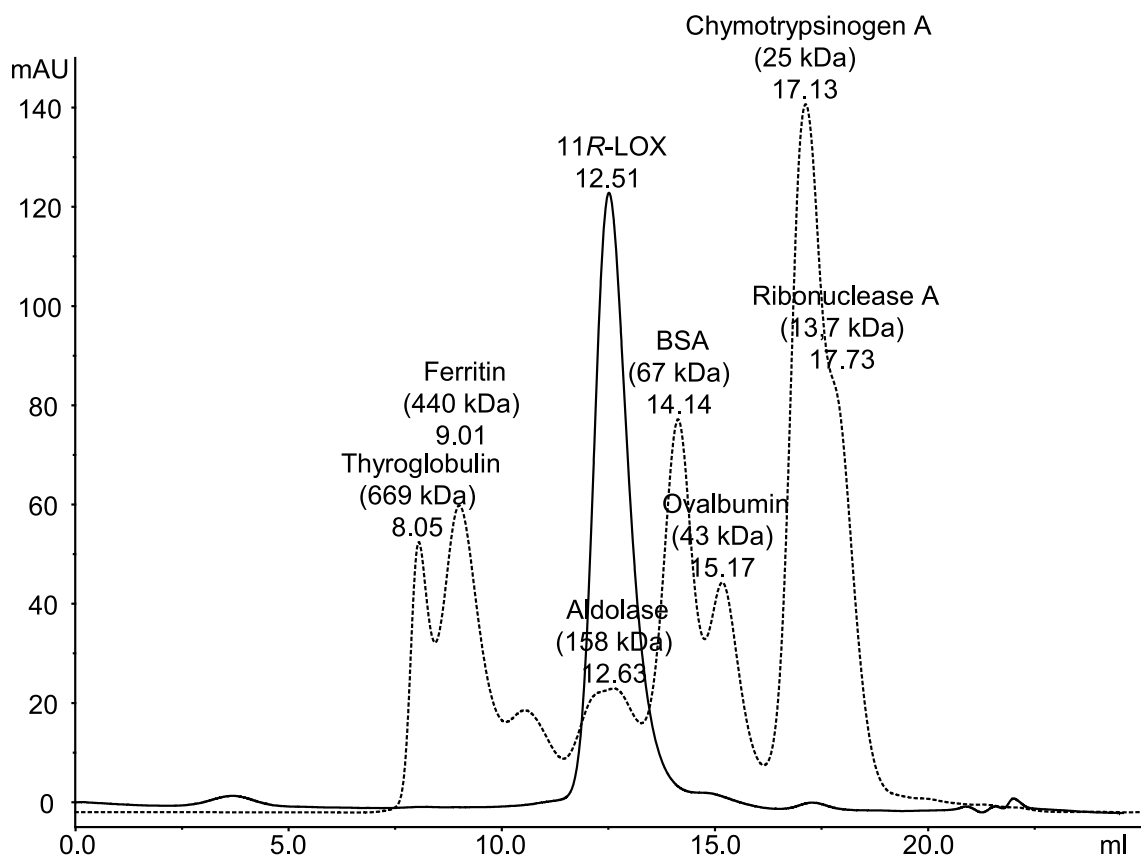


Figure S3

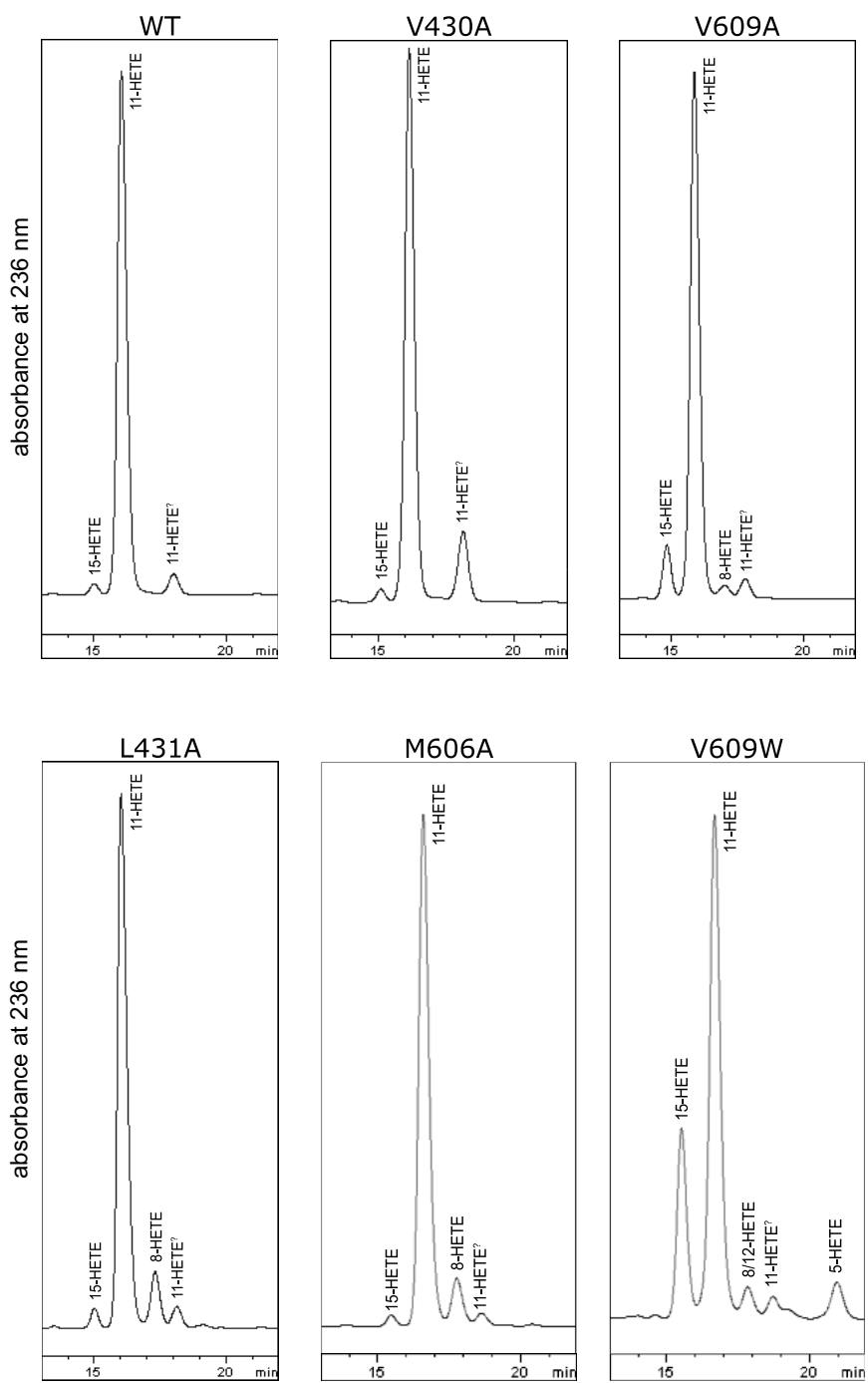
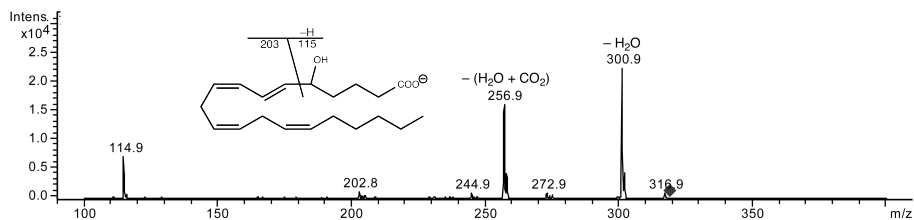
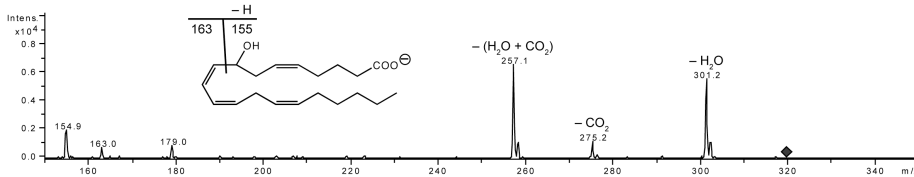


Figure S4

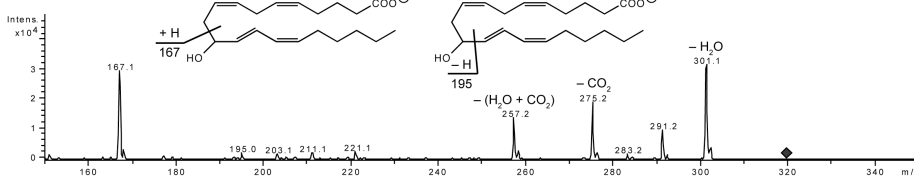
5-HETE



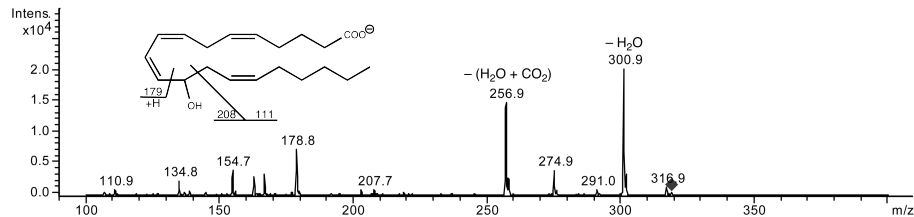
8-HETE



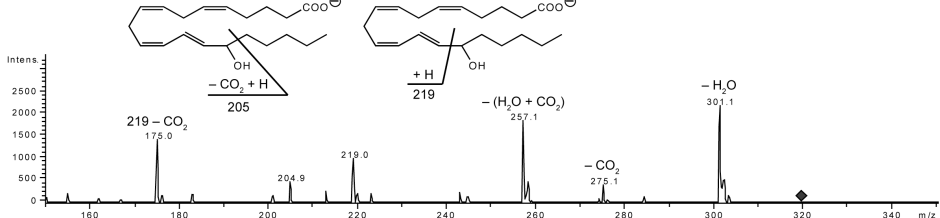
11-HETE



12-HETE



15-HETE

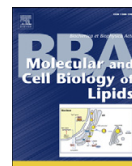


PUBLICATION II

P. Eek, M.-A. Piht, M. Rätsep, A. Freiberg, I. Järving, N. Samel

A conserved π -cation and an electrostatic bridge are essential for 11R-lipoxygenase catalysis and structural stability

Biochimica et Biophysica Acta 1851 (2015) 1377–1382



A conserved π -cation and an electrostatic bridge are essential for 11R-lipoxygenase catalysis and structural stability



Priit Eek^a, Mari-Ann Piht^a, Margus Rätsep^b, Arvi Freiberg^b, Ivar Järving^a, Nigulas Samel^{a,*}

^a Department of Chemistry, Tallinn University of Technology, Akadeemia tee 15, Tallinn 12618, Estonia

^b Institute of Physics, University of Tartu, Ravila 14c, Tartu 50411, Estonia

ARTICLE INFO

Article history:

Received 30 April 2015

Received in revised form 30 June 2015

Accepted 23 July 2015

Available online 26 July 2015

Keywords:

Lipoxygenase

Allosteric regulation

Domain interaction

PLAT domain

Arachidonic acid

Thermal denaturation

ABSTRACT

Lipoxygenases (LOXs) are lipid-peroxidizing enzymes that consist of a regulatory calcium- and membrane-binding PLAT (polycystin-1, lipoxygenase, α -toxin) domain and a catalytic domain. In a previous study, the crystal structure of an 11R-LOX revealed a conserved π -cation bridge connecting these two domains which could mediate the regulatory effect of the PLAT domain to the active site. Here we analyzed the role of residues Trp107 and Lys172 that constitute the π -cation bridge in 11R-LOX along with Arg106 and Asp173—a potential salt bridge, which could also contribute to the inter-domain communication. According to our kinetic assays and protein unfolding experiments conducted using differential scanning fluorimetry and circular dichroism spectroscopy, mutants with a disrupted link display diminished catalytic activity alongside reduced stability of the protein fold. The results demonstrate that both these bridges contribute to the two-domain interface, and are important for proper enzyme activation.

© 2015 Elsevier B.V. All rights reserved.

1. Introduction

Lipoxygenases (LOXs) are a superfamily of enzymes that peroxidize polyunsaturated fatty acids by highly stereo- and regiospecific addition of molecular oxygen [1,2]. LOX-initiated lipid mediator pathways play important regulatory roles in plants [3], mammals [4] and corals [5]. The catalytic activity of many LOXs is dependent on the presence of calcium [6], the most notable being human 5-LOX, which is a key enzyme in the inflammatory leukotriene pathway [7–9]. Another remarkable example is the coral 11R-LOX with calcium being an absolute prerequisite for catalysis [10,11]. LOXs share a common architecture consisting of an N-terminal C2-like PLAT domain, which can contain up to three calcium binding sites [12], and a C-terminal mainly α -helical catalytic domain [2,6]. In 5-LOX [13,14], 8R-LOX [12] and 11R-LOX [11] the act of calcium binding triggers association with the lipid membrane. This effect has been shown to be due to both electrostatic and hydrophobic interactions between the phospholipid layer and specific residues that become exposed in the course of calcium binding; therefore, PLAT domain serves as a true calcium-induced membrane-targeting module. Similar behavior has also been described in rabbit 15-LOX-1 (also known as 12/15-LOX) [15], although in this enzyme calcium *per se* is

not required neither for membrane association nor catalytic activity [16, 17].

Crystallographic studies have revealed a distinct feature that differentiates strongly calcium-dependent animal LOXs from the rest: the peptide segment that contains the α 2 helix and covers the putative substrate channel entrance. The coral 8R-LOX [12,20], rabbit 15-LOX-1 [21], and human 15-LOX-2 models [22] all have a long α 2 helix that leaves the orifice of the substrate channel open; these enzymes are also less stringent in regard to calcium requirement. However, in human 5-LOX [23] and coral 11R-LOX [18], which are both Ca^{2+} -induced enzymes, the α 2 is a much shorter helix flanked by several turns and helical fragments that restrict access to the active site. The entry point is “corked” by aromatic residues: in 5-LOX these are Phe177 and Tyr181, and in 11R-LOX Phe185. These aromatics are not exclusive to calcium-induced enzyme variants, but can be found in most LOXs from both animals and plants; thus, the corking effect is introduced by the broken structure of the α 2 helix, rather than the presence of aromatic residues [2]. Clearly a mechanism must exist in both 5-LOX and 11R-LOX that induces conformational changes in the α 2 region to allow effective substrate binding. Since this is a common feature of calcium-dependent LOXs, it has been hypothesized that the structural shift could be initiated by calcium binding in the PLAT domain and communicated allosterically to the active site *via* the interface between the regulatory PLAT and the catalytic domain [18,23,24]. Specifically, based on the crystal structure of 11R-LOX and other previously published LOX structures [20,21, 23,25–28], we described a conserved π -cation bridge (Trp107–Lys172 in 11R-LOX) that could be mediating this allosteric mechanism [18].

Abbreviations: LOX, lipoxygenase; PLAT, polycystin-1, lipoxygenase, α -toxin; SEC, size exclusion chromatography; AA, arachidonic acid; CD, circular dichroism; DSF, differential scanning fluorimetry; CLP, coactosin-like protein.

* Corresponding author.

E-mail address: nigulas.samel@ttu.ee (N. Samel).

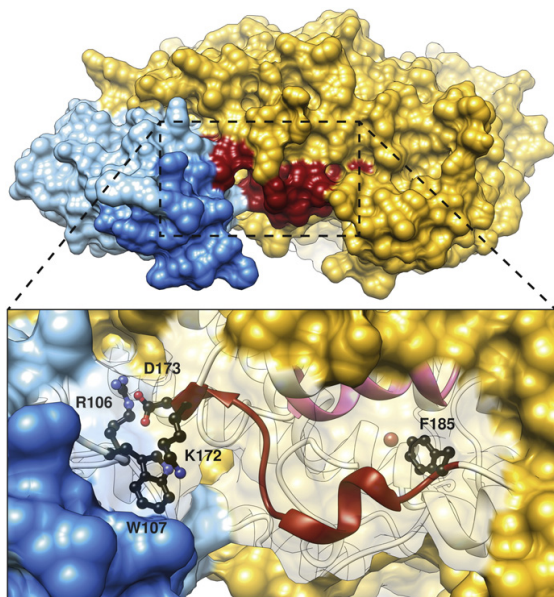


Fig. 1. Proposed allosteric regulation of 11R-LOX. The crystal structure of 11R-LOX revealed a conserved π -cation bridge (Trp107–Lys172) between the regulatory PLAT domain (blue; the Ca^{2+} -binding region is darker) and the catalytic domain (gold) [18]. Upon Ca^{2+} and membrane binding by the PLAT domain, conformational changes can transfer to the “lid” segment (red) in the catalytic domain, and expose the active site. The active site, including the non-heme iron (brown sphere), is enclosed beneath the conserved arched helix (pink), and the putative entrance is blocked by Phe185. Another potential allosteric link proposed in [19], Arg106–Asp173, is also shown.

Additionally, an adjacent salt bridge (Arg106–Asp173 in 11R-LOX) has been shown to participate in the two-domain interface of human 5-LOX [19]. These residues are outlined in Fig. 1.

In this study we introduced mutations to the aforementioned positions in order to assess their relevance to the catalytic and structural integrity of 11R-LOX. Our results indicate that the π -cation and the salt bridge are both prominent in the interaction between the PLAT and the catalytic domain, and this interaction is necessary for 11R-LOX activity.

2. Materials and methods

2.1. Materials

BL21–CodonPlus(DE3)–RP cells were from Stratagene. Tergitol NP-40, phenylmethylsulphonyl fluoride, lysozyme, SYPRO Orange were from Sigma. Benzoylase was from Santa Cruz Biotechnology. HisTrap HP, Mono Q, and Superdex 200 prep grade columns were from GE Healthcare. Sephadex G-25 Fine column was from Amersham Biosciences. Phospholipids were from Avanti Polar Lipids and arachidonic acid was from Cayman Chemical.

2.2. Site-directed mutagenesis

Mutations were introduced using whole plasmid PCR as reported previously [18]. Clones were screened by restriction mapping, small-scale expression using autoinduction [29], and confirmed by sequencing.

2.3. Expression and purification

A previously established production scheme [18] was used with slight modifications. In brief, recombinant *Gersemia fruticosa* 11R-LOX

with an N-terminal His₄-tag in pET-11a vector was transformed into *Escherichia coli* BL21–CodonPlus(DE3)–RP cells. Colonies were grown overnight in non-inducing MDG medium [29] with 100 $\mu\text{g}/\text{ml}$ ampicillin and 30 $\mu\text{g}/\text{ml}$ chloramphenicol. A 500-ml volume of autoinducing ZYM-5052 medium was inoculated with 500 μl of overnight culture. The culture was incubated at 37 $^{\circ}\text{C}$ for 4 h, and then grown to saturation at 15 $^{\circ}\text{C}$ (usually 2–3 days). Cells were harvested by centrifugation, and stored at -80°C . Subsequent expressions were performed by using glycerol stocks prepared as described in [29].

Cell pellets were resuspended in lysis buffer (20 mM Tris-HCl, pH 8.0, 0.2% Tergitol NP-40, 1 mM phenylmethylsulphonyl fluoride, 1 mg/ml lysozyme, 10 U/ml Benzoylase) by stirring on ice for 30 min. Cells were sonicated for 10×5 s on ice using a Bandelin Sonopuls HD 2200 ultrasonic homogenizer at about 40% power. The lysate was centrifuged at 39,000 $\times g$, 1 h, 4 $^{\circ}\text{C}$. The supernatant was applied onto a HisTrap HP Ni-affinity column, and washed with binding buffer (20 mM Tris-HCl, 500 mM NaCl, 20 mM imidazole, pH 8.0) on an ÄKTApurifier 10 FPLC system (GE Healthcare). The protein was eluted with an imidazole gradient from 20 to 200 mM. Protein fractions were pooled and desalted in a Sephadex G-25 Fine column into 20 mM Tris-HCl, pH 8.0. The sample was then applied onto a Mono Q anion exchanger, washed with 20 mM Tris-HCl, pH 8.0, and eluted with a NaCl gradient from 0 to 500 mM. Pooled protein fractions were concentrated using an Amicon Ultra-15 centrifugal filter (Millipore) with a 30 kDa cutoff, and subjected to a Superdex 200 prep grade size exclusion column in 20 mM Tris-HCl, 150 mM NaCl, pH 8.0 (SEC buffer). For long-term storage, the protein was concentrated to at least 1 mg/ml, aliquots were flash frozen in liquid nitrogen, and stored at -80°C .

The protein concentration was determined by absorbance at 280 nm using a BioSpec-nano spectrophotometer (Shimadzu) and extinction coefficients calculated with ExPASy ProtParam [30]. Up to 30 mg of electrophoretically pure protein was obtained from 1 l of autoinduction culture.

2.4. Activity assay

Kinetic studies were conducted as described in [18]. Briefly, the reaction was monitored on a UV-1601 spectrophotometer (Shimadzu) at 236 nm. A 1-ml continuously stirred and thermostatted (20 $^{\circ}\text{C}$) cuvette contained 50 mM Tris-HCl, 100 mM NaCl, 2 mM CaCl_2 , pH 8.0, and small unilamellar vesicles (liposomes) of phosphatidylcholine, phosphatidylethanolamine and phosphatidylserine (40:30:30 mol%) with a total phospholipid concentration of ~ 60 μM . The liposomes were prepared as described in [18]. The concentration of the substrate, arachidonic acid (AA), was varied between 2 and 100 μM . The reaction was started by adding purified enzyme in the range of 6–28 nM, depending on the activity of the enzyme variant. The reaction velocity was determined from the slope of the linear portion of the curve. K_m and k_{cat} values were obtained by nonlinear regression analysis with the Michaelis–Menten equation using Prism 5 (GraphPad). Due to substrate inhibition, only the ascending part of the curve was used for fitting, as described previously [18] (Fig. 2).

2.5. Differential scanning fluorimetry

Thermal denaturation of the protein was monitored on a Rotor-Gene Q 2-Plex HRM cyclor (Qiagen) using an adapted version of the method described in [31,32]. 0.1 mg/ml protein in SEC buffer was supplemented with the fluorophore SYPRO Orange in final concentration of $5 \times$ (a 1000-fold dilution of the supplied stock). Triplicate samples of 20 μl were heated from 35 to 95 $^{\circ}\text{C}$ with 0.5 $^{\circ}\text{C}$ increments at 10 s intervals. Fluorescence was measured at each increment with the High Resolution Melt (HRM) channel (excitation at 460 nm, emission at 510 nm) at a gain of 2. The melting point (T_m) was determined as the maximum of the first derivative plot of the denaturation curve (dF/dT) using the software package provided with the device.

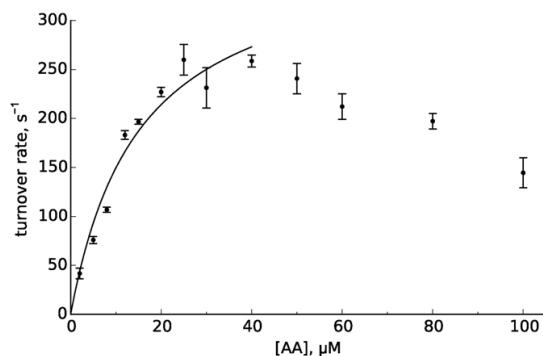


Fig. 2. Kinetic curve of wild-type 11R-LOX. The lipoygenation of AA suffers from substrate inhibition at substrate concentrations above 40 μM . In order to obtain comparable results, only the ascending part of the data was used for modeling Michaelis–Menten kinetics (solid line). Error bars denote SD ($n = 3$).

2.6. Circular dichroism

Circular dichroism (CD) spectra were measured on a Chirascan-plus spectrometer (Applied Photophysics) in a thermostatted 1 mm quartz cuvette. For thermal denaturation curves, CD signal was monitored at 220 nm while continuously ramping the temperature from 10 to 80 °C at a rate of 1 °C/min. Sample temperature in the cuvette was recorded by a thermocouple probe. In all experiments protein concentration was 0.1 mg/ml in SEC buffer. Unfolding models of a dimeric protein described by N. Greenfield [33] were modified to allow pre- and post-transition linear changes in ellipticity as a function of temperature. Models were fitted to data using SciPy [34] and plotted with Matplotlib [35]. For the equations used, see Appendix A. Supplementary materials.

3. Results

3.1. Conserved π -cation bridge

To elucidate whether the conserved Trp107–Lys172 π -cation bridge is involved in the regulation of 11R-LOX, we mutated these residues to

alter the properties of the bridge, and assayed the oxygenation of AA by the various mutants under constant conditions. The results given in Table 1 clearly indicate that the invariant Trp107 is structurally crucial for 11R-LOX, and an aromatic ring is essential in that position. While the conservative Trp107Phe mutation had only a minor effect on the turnover number k_{cat} (274 ± 13 vs $377 \pm 25 \text{ s}^{-1}$ for the wild-type), the Trp107Ala substitution reduced the rate 6-fold to $62 \pm 5 \text{ s}^{-1}$. The Trp107Lys single mutant, an intermediate variant of creating an enzyme with an inverted π -cation bridge, had an even stronger impact with k_{cat} of $24 \pm 2 \text{ s}^{-1}$. The influence of Lys172 is less pronounced. Mutations in which the positive charge was replaced with a hydrophobic group (Lys172Val) or a negative carboxylate (Lys172Glu) diminished the turnover numbers 2–3-fold (166 ± 13 and $137 \pm 12 \text{ s}^{-1}$, respectively). Interestingly, the other bridge swap single mutant, Lys172Trp, retained much of its turnover rate ($292 \pm 14 \text{ s}^{-1}$). Here the formation of alternative π - π interactions can be speculated. Finally, a double mutant (Trp107Lys/Lys172Trp) with an inverted bridge was constructed. The turnover rate of this enzyme variant was about 2-fold higher than of the Trp107Lys single mutant, further supporting the pro-catalysis role of the π -cation interaction.

It must be noted that while the substitutions affected the K_m value in the 2-fold range, the prominent effect was on k_{cat} . It is unlikely that mutations this far from the active site could drastically change the catalytic machinery of the enzyme, unless dealing with key residues in general structural stability or an allosteric mechanism. Resorting on the hypothesis that communication between the two domains is needed for catalysis, this phenomenon can be viewed as non-competitive inhibition in the sense that inhibition occurs when the two domains fail to interact. This could lead to either an unproductive active site conformation or a site that is closed-off altogether. In either case catalysis is obstructed resulting in a diminished k_{cat} , which is what has been observed.

Differential scanning fluorimetry (DSF) analysis showed that the conservative Trp107Phe, but also the Lys172Val substitution had a mild effect on protein stability, lowering the melting point (T_m) by less than 2 °C compared to the wild-type (Table 1). The melting curves featured a minor pre-phase at about 49 °C (Fig. 3), which could be caused by dimer dissociation or, alternatively, by separate melting of the two domains, as suggested by Schröder et al. [36]. In contrast, mutations that disrupted the π -cation bridge had a stronger impact: the first melting step of the biphasic process at 49 °C became more prominent and the higher T_m decreased further. This behavior was further confirmed

Table 1

The catalytic constants and melting points (T_m) of the Trp107–Lys172 π -cation bridge and the Arg106–Asp173 salt bridge mutants. The results are the best-fit values \pm SE for catalytic constants and T_m values determined by CD, and means \pm SD for T_m values determined by DSF.

	k_{cat} (s^{-1})	K_m (μM)	k_{cat}/K_m ($\mu\text{M}^{-1} \text{s}^{-1}$)	T_m ($^{\circ}\text{C}$) ^a	
				DSF	CD
Wild-type	377 ± 25	15 ± 2	25 ± 2	$49.6 \pm 0.1/54.8 \pm 0.1$	55.0 ± 0.0
π-cation bridge					
Conservative substitution					
Trp107Phe	274 ± 13	22 ± 2	13 ± 1	53.4 ± 0.1	
Interaction disruption					
Trp107Ala	62 ± 5	31 ± 5	2.0 ± 0.2	$49.2 \pm 0.1/51.9 \pm 0.1$	
Lys172Glu	137 ± 12	15 ± 3	9.2 ± 1.0	$49.1 \pm 0.1/51.9 \pm 0.2$	$47.9 \pm 0.2/61.2 \pm 0.1$
Lys172Val	166 ± 13	6.5 ± 1.6	26 ± 4	$49.6 \pm 0.0/53.9 \pm 0.6$	
Bridge swap					
Trp107Lys	24 ± 2	23 ± 4	1.1 ± 0.1	$49.4 \pm 0.1/52.7 \pm 0.1$	
Lys172Trp	292 ± 14	20 ± 2	15 ± 1	$49.3 \pm 0.1/52.4 \pm 0.3$	
Trp107Lys/Lys172Trp	57 ± 3	27 ± 3	2.1 ± 0.1	49.0 ± 0.1	
Salt bridge					
Charge removal					
Arg106Gln	238 ± 24	10 ± 2	23 ± 3	48.8 ± 0.1	
Asp173Asn	302 ± 19	12 ± 2	26 ± 2	$49.5 \pm 0.1/53.9 \pm 0.1$	
Charge swap					
Arg106Asp	15 ± 1	7.3 ± 1.1	2.1 ± 0.2	44.7 ± 0.3	
Asp173Arg	14 ± 2	14 ± 3	1.0 ± 0.1	45.8 ± 0.1	48.4 ± 0.1
Arg106Asp/Asp173Arg	140 ± 4	25 ± 2	5.7 ± 0.2	$49.2 \pm 0.1/52.5 \pm 0.3$	

^a The primary T_m value (the fastest change in fluorescence or the largest decrease in CD) is given in roman and the secondary in italic.

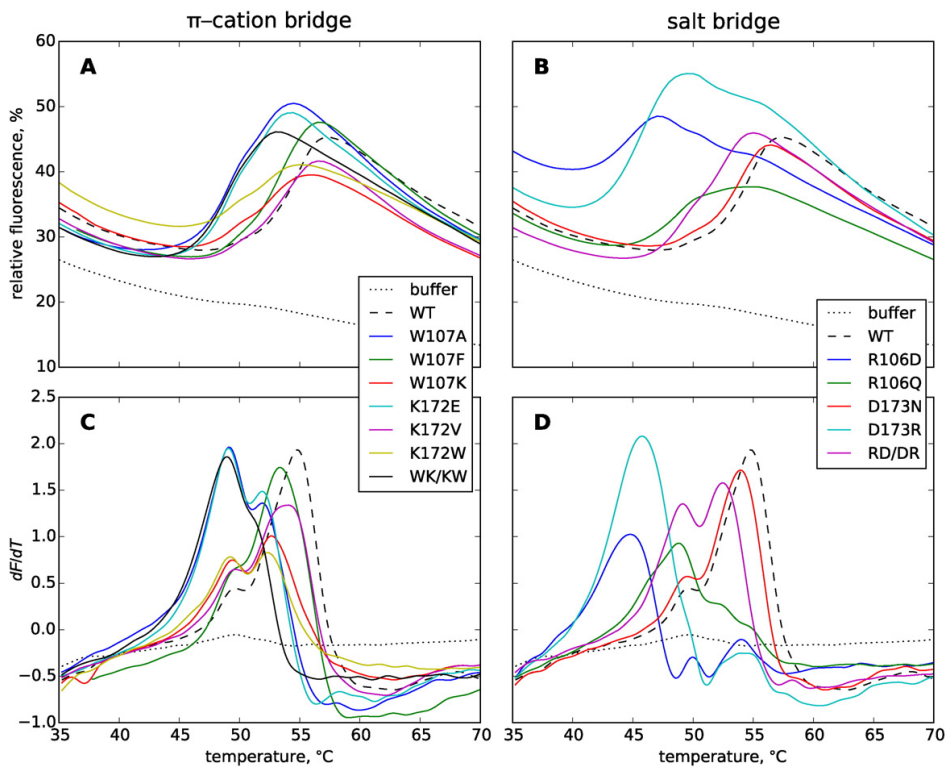


Fig. 3. Differential scanning fluorimetry analysis. (A, B) Thermal denaturation of 11R-LOX variants was monitored by the fluorescence of the hydrophobic dye SYPRO Orange, which fluoresces inside the hydrophobic core of a molten globule, but is quenched in an aqueous environment. (C, D) The melting point (T_m) was determined as the maximum of the first derivative of the melting curve (dF/dT).

by CD measurements of the Lys172Glu mutant for which a three-state melting curve was observed as opposed to the wild-type with a single resolvable transition (Fig. 4). The restoration of the π -cation bridge in an inverse orientation did not stabilize the enzyme compared to single mutants, despite the double mutant being more active. This result is not surprising in the light of the fact that the mutated regions are very

highly conserved among LOXs, and hence are most likely needed to maintain the structural integrity of the enzyme.

Although the T_m values for the wild-type measured by DSF and CD are in very good agreement at about 55 °C, the results for the mutants tend to differ on a larger scale (Table 1). This could be due to differences in temperature ramping as the ramification of melting induced by the

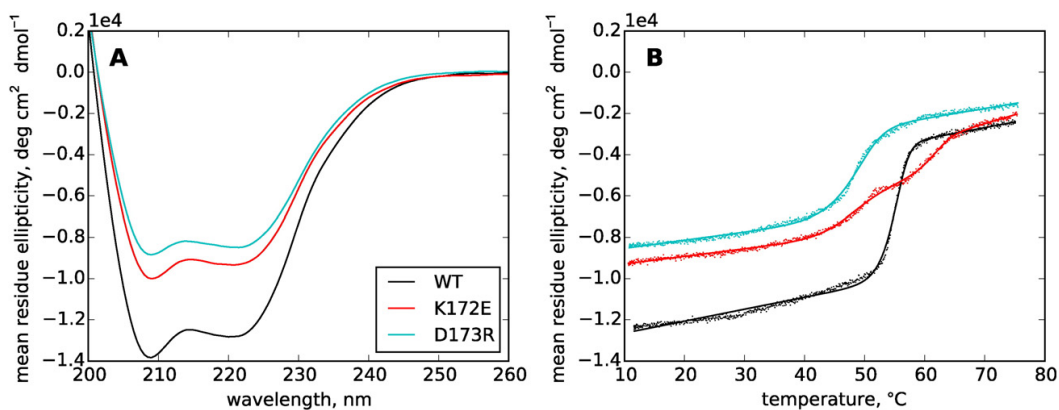


Fig. 4. Circular dichroism (CD) data. (A) CD spectra of 11R-LOX variants at the concentration of 0.1 mg/ml and 10 °C display similar overall characteristics. (B) CD signal at 220 nm was monitored as a function of temperature. Denaturation models (lines) were fitted to the data (dots) to determine the T_m values. A two-state model was used for the wild-type and the Asp173Arg mutant, whereas the Lys172Glu mutant displayed a clear three-state transition.

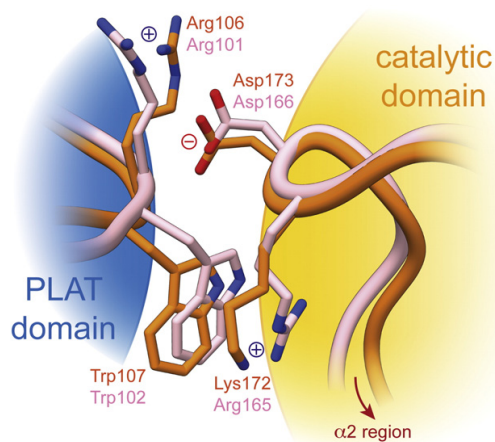


Fig. 5. LOX domains interface via the π -cation and the salt bridge. The alignment of coral 11R-LOX (orange) and human 5-LOX (pink) crystal structure models demonstrates the conservation of this feature. The bridges connect the regulatory PLAT domain to the $\alpha 2$ helix and its surroundings, which form a lid over the active site entrance in the catalytic domain. The models of 11R-LOX (PDB: 3VF1 chain A) and 5-LOX (PDB: 3O8Y chain A) were structurally superposed using UCSF Chimera [37].

mutations might lead to more time-dependent denaturation processes. Furthermore, as these methods employ different probes—DSF using a dye which fluoresces in the hydrophobic core of a molten globule, and CD determining the orderliness of peptide bonds due to secondary structure—the varying T_m values can mirror somewhat different stages of the denaturation process.

3.2. Arg106–Asp173 salt bridge

Next to the conserved π -cation bridge lies another possible link, the potential Arg106–Asp173 salt bridge. Although in the 11R-LOX model the two residues are not positioned optimally for an electrostatic interaction (Fig. 5), it is plausible that such a contact occurs in solution under modest conformational changes.

Conservative substitutions were firstly introduced to assess the significance of this link. The turnover rates of Arg106Gln and Asp173Asn mutants (238 ± 24 and 302 ± 19 s⁻¹, respectively) revealed that mere charge removal does not have a notable impact on enzymatic activity. However, creating electrostatic repulsion by swapping the charge caused k_{cat} to plummet, as demonstrated by Arg106Asp and Asp173Arg mutants (15 ± 1 and 14 ± 2 s⁻¹, respectively). The T_m value of the interaction-breaking Asp173Arg mutant was diminished by 6–10 °C, determined either by CD or DSF (Table 1). The importance of this structural feature is also supported by the fact that compared to wild-type, the observed melting curve is wider for the mutant, indicating greater structural heterogeneity (Fig. 4). As with the π -cation bridge swap, the enzymatic activity of the salt bridge mutants was partially restored by a double mutation that effectively inverts the salt bridge (Arg106Asp/Asp173Arg): the conversion rate was revived to 140 ± 4 s⁻¹. Furthermore, the T_m value improved, and the melting profile determined by DSF took the form of a biphasic transition, resembling those of the less detrimental π -cation bridge mutants (Fig. 3).

3.3. Calcium requirement

The mutants were also screened for changes in the requirement for calcium, as the presence of this ligand is an absolute necessity for wild-type 11R-LOX catalysis [11]. All reported enzyme variants retained

the need for Ca²⁺: no noticeable catalytic activity was detected in calcium-free assay conditions (data not shown).

4. Discussion

Recently, Neau et al. solved the crystal structure of a coral 8R-LOX in complex with its substrate, AA [38]. This milestone in the field of LOX research finally confirmed the actual substrate-binding cavity and, moreover, the entrance to the active site, at least in LOXs with analogous substrate orientation. The carboxylate-head of the fatty acid was found at the opening by the $\alpha 2$ helix, marking it the likely point of entry. Extensive experiments on soybean LOX-1 using electron paramagnetic resonance further substantiate this site as the substrate channel entrance for LOX enzymes [39]. The structural basis for lipooxygenation derived from the most current studies is thoroughly explained in the review by Newcomer and Brash [2].

Since the oxygenation in the 11R-position differs from 8R-specificity merely by the shift of hydrogen abstraction from C10 to C13, which could be achieved by employing a shallower substrate pocket, it is fair to assume that both enzymes bind the substrate in a similar manner using the same access route. For 11R-LOX this would mean that AA enters the active site hydrophobic tail-first via the entrance blocked by Phe185 (Fig. 1). In order to allow substrate binding, the $\alpha 2$ fragment with Phe185 needs to move away from the active site. Previously we hypothesized that this could occur due to allosteric changes induced by calcium-mediated membrane binding, and transferred to the catalytic domain via the two-domain interface [18]. Our results support this hypothesis: the disruption of either the π -cation or the salt bridge severely impeded the catalytic activity of the enzyme, inverse restoration of the interaction led to a partial recovery, and none of the substitutions abolished the requirement for calcium. Additionally, thermal denaturation studies indicated that bridge mutants are structurally less stable, and may also display more flexibility, advocating the role of these bridges in the interface assembly.

In human 5-LOX it was found that Trp102 is important for binding the coactosin-like protein (CLP)—a protein that prevents non-turnover inactivation of 5-LOX, and promotes leukotriene A₄ formation [40]. Computational docking suggested that although CLP is bound into the cleft between the PLAT and the catalytic domain, it does not interact with Trp102 directly, but rather with Arg165 in the catalytic domain, which in turn forms a bridge with the tryptophan. This is the same π -cation bridge that aids to stabilize the coral 11R-LOX (Fig. 5). In 5-LOX, however, the loss of an aromatic moiety did not affect catalytic activity; therefore, it seems that this interaction is more important in maintaining the structural integrity of the enzyme in general. The corresponding salt bridge in 5-LOX (Arg101–Asp166) was also shown to be essential for proper interaction of the two domains using the yeast two-hybrid system [19]. Surprisingly, the disruption of the link led to a 3-fold increase of the initial 5-LOX reaction velocity, instead of hindering it. The formation of alternative interactions can, of course, be speculated, and the placement of the PLAT β -sandwich seems to be rather flexible in relation to the catalytic domain in solution, as has been demonstrated by small-angle X-ray scattering experiments on human platelet 12-LOX and rabbit 15-LOX-1 [41,42]. Nevertheless, conclusions cannot be drawn based only on a single mutation. In general, truncation of the PLAT domain leads to impairment of mammalian LOXs [43]; 5-LOX is no exception in this matter and this was readily confirmed by the same authors [19]. Still, the question how a conserved motif can display such an obverse effect, remains to be answered.

The results presented in this paper demonstrate that interactions between the regulatory PLAT domain and the catalytic domain are vital for the regulation of 11R-LOX activity. Both Trp107–Lys172 π -cation and Arg106–Asp173 salt bridges participate in the mechanism that leads to pro-catalytic conformational changes. It is evident, along with the cited work, that these links play a regulatory and/or a structural role in other LOXs as well. High pressure fluorescence measurements with

12/15-LOX have indicated that the rigidity of the protein structure and the two-domain interface are affected by inhibitor and biomembrane binding [44]. Furthermore, the activity of the inflammatory 5-LOX is regulated by CLP, which is claimed to bind the very same interface region [9]. All this suggests that flexibility and interactions between the two domains are intrinsic to the allosteric regulation of many LOX isoforms, opening up a completely new prospect of inhibitor design.

Conflict of interest

The authors declare no potential conflict of interest.

Acknowledgments

We thank Kaspar Põldemaa for his assistance in conducting activity assays. This work was supported by Institutional Research Funding of the Estonian Ministry of Education and Research IUT 19-9 (to N.S.) and IUT 02-28 (to A.F.) and Estonian Science Foundation Grant 9410 (to N.S.).

Appendix A. Supplementary materials

Supplementary materials to this article can be found online at <http://dx.doi.org/10.1016/j.bbali.2015.07.007>.

References

- [1] A.R. Brash, Lipoxigenases: occurrence, functions, catalysis, and acquisition of substrate, *J. Biol. Chem.* 274 (1999) 23679–23682.
- [2] M.E. Newcomer, A.R. Brash, The structural basis for specificity in lipoxigenase catalysis, *Protein Sci.* 24 (2015) 298–309.
- [3] A. Liavonchanka, I. Feussner, Lipoxigenases: occurrence, functions and catalysis, *J. Plant Physiol.* 163 (2006) 348–357.
- [4] H. Kühn, S. Banthiya, K. van Leyen, Mammalian lipoxigenases and their biological relevance, *Biochim. Biophys. Acta Mol. Cell Biol. Lipids* 1851 (2015) 308–330.
- [5] H. Löhelaid, T. Teder, N. Samel, Lipoxigenase-allene oxide synthase pathway in octocoral thermal stress response, *Coral Reefs* 34 (2015) 143–154.
- [6] I. Ivanov, D. Heydeck, K. Hofheinz, J. Roffeis, V.B. O'Donnell, H. Kühn, M. Walther, Molecular enzymology of lipoxigenases, *Arch. Biochem. Biophys.* 503 (2010) 161–174.
- [7] O. Rådmark, B. Samuelsson, Regulation of the activity of 5-lipoxygenase, a key enzyme in leukotriene biosynthesis, *Biochem. Biophys. Res. Commun.* 396 (2010) 105–110.
- [8] J.Z. Haeggström, C.D. Funk, Lipoxigenase and leukotriene pathways: biochemistry, biology, and roles in disease, *Chem. Rev.* 111 (2011) 5866–5898.
- [9] O. Rådmark, O. Wertz, D. Steinhilber, B. Samuelsson, 5-Lipoxygenase, a key enzyme for leukotriene biosynthesis in health and disease, *Biochim. Biophys. Acta Mol. Cell Biol. Lipids* 1851 (2014) 331–339.
- [10] M. Mortimer, R. Järving, A.R. Brash, N. Samel, I. Järving, Identification and characterization of an arachidonate 11R-lipoxygenase, *Arch. Biochem. Biophys.* 445 (2006) 147–155.
- [11] R. Järving, A. Lökene, R. Kurg, L. Siimon, I. Järving, N. Samel, Activation of 11R-lipoxygenase is fully Ca²⁺-dependent and controlled by the phospholipid composition of the target membrane, *Biochemistry* 51 (2012) 3310–3320.
- [12] M.L. Oldham, A.R. Brash, M.E. Newcomer, Insights from the X-ray crystal structure of coral 8R-lipoxygenase: calcium activation via a C2-like domain and a structural basis of product chirality, *J. Biol. Chem.* 280 (2005) 39545–39552.
- [13] T. Hammarberg, P. Provost, B. Persson, O. Rådmark, The N-terminal domain of 5-lipoxygenase binds calcium and mediates calcium stimulation of enzyme activity, *J. Biol. Chem.* 275 (2000) 38787–38793.
- [14] S. Kulkarni, S. Das, C.D. Funk, D. Murray, W. Cho, Molecular basis of the specific subcellular localization of the C2-like domain of 5-lipoxygenase, *J. Biol. Chem.* 277 (2002) 13167–13174.
- [15] R. Brinckmann, K. Schnurr, D. Heydeck, T. Rosenbach, G. Kolde, H. Kühn, Membrane translocation of 15-lipoxygenase in hematopoietic cells is calcium-dependent and activates the oxygenase activity of the enzyme, *Blood* 91 (1998) 64–74.
- [16] M. Walther, M. Anton, M. Wiedmann, R. Fletterick, H. Kühn, The N-terminal domain of the reticulocyte-type 15-lipoxygenase is not essential for enzymatic activity but contains determinants for membrane binding, *J. Biol. Chem.* 277 (2002) 27360–27366.
- [17] M. Walther, R. Wiesner, H. Kühn, Investigations into calcium-dependent membrane association of 15-lipoxygenase-1. Mechanistic roles of surface-exposed hydrophobic amino acids and calcium, *J. Biol. Chem.* 279 (2004) 3717–3725.
- [18] P. Eek, R. Järving, I. Järving, N.C. Gilbert, M.E. Newcomer, N. Samel, Structure of a calcium-dependent 11R-lipoxygenase suggests a mechanism for Ca²⁺ regulation, *J. Biol. Chem.* 287 (2012) 22377–22386.
- [19] M. Rakonjac Ryge, M. Tanabe, P. Provost, B. Persson, X. Chen, C.D. Funk, A. Rinaldo-Matthis, B. Hofmann, D. Steinhilber, T. Watanabe, B. Samuelsson, O. Rådmark, A mutation interfering with 5-lipoxygenase domain interaction leads to increased enzyme activity, *Arch. Biochem. Biophys.* 545 (2014) 179–185.
- [20] D.B. Neau, N.C. Gilbert, S.G. Bartlett, W.E. Boeglin, A.R. Brash, M.E. Newcomer, The 1.85 Å structure of an 8R-lipoxygenase suggests a general model for lipoxygenase product specificity, *Biochemistry* 48 (2009) 7906–7915.
- [21] J. Choi, J.K. Chon, S. Kim, W. Shin, Conformational flexibility in mammalian 15S-lipoxygenase: reinterpretation of the crystallographic data, *Proteins Struct. Funct. Bioinforma.* 70 (2008) 1023–1032.
- [22] M.J. Kobe, D.B. Neau, C.E. Mitchell, S.G. Bartlett, M.E. Newcomer, The structure of human 15-lipoxygenase-2 with a substrate mimic, *J. Biol. Chem.* 289 (2014) 8562–8569.
- [23] N.C. Gilbert, S.G. Bartlett, M.T. Waight, D.B. Neau, W.E. Boeglin, A.R. Brash, M.E. Newcomer, The structure of human 5-lipoxygenase, *Science* 331 (2011) 217–219.
- [24] J.B. Allard, T.G. Brock, Structural organization of the regulatory domain of human 5-lipoxygenase, *Curr. Protein Pept. Sci.* 6 (2005) 125–131.
- [25] B. Youn, G.E. Sellhorn, R.J. Mirchel, B.J. Gaffney, H.D. Grimes, C. Kang, Crystal structures of vegetative soybean lipoxygenase VLX-B and VLX-D, and comparisons with seed isoforms LOX-1 and LOX-3, *Proteins Struct. Funct. Bioinforma.* 65 (2006) 1008–1020.
- [26] W. Minor, J. Steczko, B. Stec, Z. Otwinowski, J.T. Bolin, R. Walter, B. Axelrod, Crystal structure of soybean lipoxygenase L-1 at 1.4 Å resolution, *Biochemistry* 35 (1996) 10687–10701.
- [27] M. Chruszcz, A. Wlodawer, W. Minor, Determination of protein structures—a series of fortunate events, *Biophys. J.* 95 (2008) 1–9.
- [28] E. Skrzypczak-Jankun, O.Y. Borbulevych, M.I. Zavadzky, M.R. Baranski, K. Padmanabhan, V. Petricek, J. Jankun, Effect of crystal freezing and small-molecule binding on internal cavity size in a large protein: X-ray and docking studies of lipoxygenase at ambient and low temperature at 2.0 Å resolution, *Acta Crystallogr. Sect. D: Biol. Crystallogr.* 62 (2006) 766–775.
- [29] F.W. Studier, Protein production by auto-induction in high density shaking cultures, *Protein Expr. Purif.* 41 (2005) 207–234.
- [30] E. Gasteiger, C. Hoogland, A. Gattiker, S. Duvaud, M. Wilkins, R. Appel, A. Bairoch, Protein identification and analysis tools on the ExPASy server, in: J.M. Walker (Ed.), *The Proteomics Protocols Handbook*, Humana Press 2005, pp. 571–607.
- [31] F.H. Niesen, H. Berglund, M. Vedadi, The use of differential scanning fluorimetry to detect ligand interactions that promote protein stability, *Nat. Protoc.* 2 (2007) 2212–2221.
- [32] K. Malik, P. Matejtschuk, C. Thelwell, C.J. Burns, Differential scanning fluorimetry: rapid screening of formulations that promote the stability of reference preparations, *J. Pharm. Biomed. Anal.* 77 (2013) 163–166.
- [33] N.J. Greenfield, Using circular dichroism collected as a function of temperature to determine the thermodynamics of protein unfolding and binding interactions, *Nat. Protoc.* 1 (2006) 2527–2535.
- [34] T.E. Oliphant, Python for scientific computing, *Comput. Sci. Eng.* 9 (2007) 10–20.
- [35] J.D. Hunter, Matplotlib: A 2D graphic environment, *Comput. Sci. Eng.* 9 (2007) 90–95.
- [36] M. Schröder, A.-K. Häfner, B. Hofmann, O. Rådmark, F. Tumulka, R. Abele, V. Dötsch, D. Steinhilber, Stabilisation and characterisation of the isolated regulatory domain of human 5-lipoxygenase, *Biochim. Biophys. Acta Mol. Cell Biol. Lipids* 1842 (2014) 1538–1547.
- [37] E.F. Pettersen, T.D. Goddard, C.C. Huang, G.S. Couch, D.M. Greenblatt, E.C. Meng, T.E. Ferrin, UCSF Chimera — a visualization system for exploratory research and analysis, *J. Comput. Chem.* 25 (2004) 1605–1612.
- [38] D.B. Neau, G. Bender, W.E. Boeglin, S.G. Bartlett, A.R. Brash, M.E. Newcomer, Crystal structure of a lipoxygenase in complex with substrate: the arachidonic acid-binding site of 8R-lipoxygenase, *J. Biol. Chem.* 289 (2014) 31905–31913.
- [39] B.J. Gaffney, Connecting lipoxygenase function to structure by electron paramagnetic resonance, *Acc. Chem. Res.* 47 (2014) 3588–3595.
- [40] J. Esser, M. Rakonjac, B. Hofmann, L. Fischer, P. Provost, G. Schneider, D. Steinhilber, B. Samuelsson, O. Rådmark, Coactosin-like protein functions as a stabilizing chaperone for 5-lipoxygenase: role of tryptophan 102, *Biochem. J.* 425 (2010) 265–274.
- [41] A.M. Aleem, J. Jankun, J.D. Dignam, M. Walther, H. Kühn, D.I. Svergun, E. Skrzypczak-Jankun, Human platelet 12-lipoxygenase, new findings about its activity, membrane binding and low-resolution structure, *J. Mol. Biol.* 376 (2008) 193–209.
- [42] W. Shang, I. Ivanov, D.I. Svergun, O.Y. Borbulevych, A.M. Aleem, S. Stehling, J. Jankun, H. Kühn, E. Skrzypczak-Jankun, Probing dimerization and structural flexibility of mammalian lipoxygenases by small-angle X-ray scattering, *J. Mol. Biol.* 409 (2011) 654–668.
- [43] M. Walther, K. Hofheinz, R. Vogel, J. Roffeis, H. Kühn, The N-terminal β -barrel domain of mammalian lipoxygenases including mouse 5-lipoxygenase is not essential for catalytic activity and membrane binding but exhibits regulatory functions, *Arch. Biochem. Biophys.* 516 (2011) 1–9.
- [44] A. Di Venere, E. Nicolai, I. Ivanov, E. Dainese, S. Adel, B.C. Angelucci, H. Kühn, M. Maccarrone, G. Mei, Probing conformational changes in lipoxygenases upon membrane binding: fine-tuning by the active site inhibitor ETYA, *Biochim. Biophys. Acta Mol. Cell Biol. Lipids* 1841 (2014) 1–10.

Supplementary Materials

Models for denaturation curves obtained by CD

Equations for modeling a two-state transition between a folded dimer and an unfolded monomer, and a multiple transition model given in Ref. [1] Supplementary Equations IV and IX, respectively, were taken as starting points. These were modified according to Supplementary Equations II from the same source to account for pre- and post-transition linear changes in ellipticity as a function of temperature. Final equations for modeling the transitions are as follows.

The two-state transition of ellipticity, θ , is described as

$$\theta = \alpha [(\theta_F + c_F T) - (\theta_U + c_U T)] + (\theta_U + c_U T) \quad (1)$$

where θ_F and θ_U are the ellipticities of completely folded and unfolded protein, c_F and c_U the pre- and post-transition correction coefficients, respectively, T is the temperature in Kelvin, and α the fraction of folded protein. For a dimeric protein α is expressed as

$$\alpha = \frac{4CK + 1 - \sqrt{8CK + 1}}{4CK} \quad (2)$$

where C is the molar concentration of the dimer. Under the assumption that the change in heat capacity during unfolding is 0, the constant of folding, K , equals

$$K = \exp \left[\frac{\Delta H}{RT} \left(\frac{T}{T_m} - 1 \right) - \ln C \right] \quad (3)$$

where ΔH is the enthalpy of unfolding, R is the universal gas constant (1.987 cal mol⁻¹), and T_m is the protein melting temperature ($\alpha = 0.5$).

The three-state transition is modeled as

$$\theta = (u_1 \alpha_1 + u_2 \alpha_2) [(\theta_F + c_F T) - (\theta_U + c_U T)] + (\theta_U + c_U T) \quad (4)$$

where u_1 and u_2 are the fractional extinction coefficients, and α_1 and α_2 are the fractions of the folded protein in the sequential transition steps. The sum of coefficients $u_1 + u_2 = 1$.

$$\alpha_1 = \frac{K_1}{1 + K_1} \quad (5)$$

$$K_1 = \exp \left[\frac{\Delta H_1}{RT} \left(\frac{T}{T_{m,1}} - 1 \right) \right] \quad (6)$$

α_2 and K_2 take the same form as Equations 2 and 3.

References

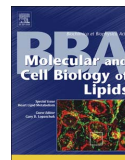
- [1] N. J. Greenfield, Using circular dichroism collected as a function of temperature to determine the thermodynamics of protein unfolding and binding interactions, *Nat. Protoc.* 1 (2006) 2527–2535.

PUBLICATION III

P. Eek, K. Põldmaa, S. Kasvandik, I. Järving, N. Samel

A PDZ-like domain mediates the dimerization of 11R-lipoxygenase

Biochimica et Biophysica Acta 1862 (2017) 1121–1128



A PDZ-like domain mediates the dimerization of 11R-lipoxygenase



Priit Eek^a, Kaspar Põldemaa^a, Sergo Kasvandik^b, Ivar Järving^a, Nigulas Samel^{a,*}

^a Department of Chemistry and Biotechnology, School of Science, Tallinn University of Technology, Akadeemia tee 15, 12618 Tallinn, Estonia

^b Institute of Technology, University of Tartu, Nooruse 1, 50411 Tartu, Estonia

ARTICLE INFO

Keywords:

Lipoxygenase
Dimerization
PDZ domain
Allosteric regulation
Small-angle X-ray scattering
Protein cross-linking

ABSTRACT

Lipoxygenases (LOXs), participating in inflammatory processes and cancer, are a family of enzymes with high potential as drug targets. Various allosteric effects have been observed with different LOX isozymes (e.g. lipid/ATP binding, phosphorylation), yet there is a lot of uncertainty concerning the regulation of these enzymes. It has been recently found that a number of LOXs form dimers, extending the list of possible allosteric mechanisms with oligomerization. Coral 11R-LOX is, unlike several mammalian counterparts, a stable dimer in solution facilitating quaternary structure studies that demand high sample homogeneity. By combining previous crystallographic data of 11R-LOX with small-angle X-ray scattering and chemical cross-linking, we were able to narrow down the possible dimerization interfaces, and subsequently determined the correct assembly by site-directed mutagenesis of potential contacting residues. The region of interest is located in the vicinity of an $\alpha + \beta$ formation in the catalytic domain, also coined the PDZ-like domain. Being situated just between the active site and the dimer interface, our results further implicate this putative subdomain in the regulation of LOXs.

1. Introduction

Lipoxygenases (LOX) are polyunsaturated fatty acid peroxidizing enzymes that catalyze the key reactions in the formation of several bioactive lipid mediators in mammals such as leukotrienes, hexoxilins, lipoxins and resolvins. In humans there are 6 functional LOX variants with distinctive and even contrary functions, varying from pro-inflammatory to pro-resolving effects, but also cell proliferation and skin water barrier formation [1,2]. These enzymes are widely spread and can also be found in bacteria, fungi, plants, and invertebrates like corals. Some coral LOXs are additionally incorporated into fusion proteins with catalase-like enzymes [3,4], and have been related to stress response [5,6]. Generally, LOXs consist of two domains: a regulatory β -sandwich called the PLAT domain, and a larger, mainly α -helical catalytic domain [7]. The former can act as a Ca^{2+} -mediated membrane-targeting module, lipid membrane being the source of the fatty acid substrate.

LOXs have been regarded as functional monomers, but in recent years this status quo has been questioned by several studies (reviewed in [1]). Both human leukocyte 5-LOX (ALOX5) [8] and platelet 12-LOX (ALOX12) [9] can aggregate into dimers or higher oligomers, respectively, by disulfide bridge formation. Small-angle X-ray scattering (SAXS) was employed to show that platelet 12-LOX is a stable dimer in

solution [9,10], and rabbit 12/15-LOX (ALOX15), although a monomer, can undergo dimerization that is induced by allosteric fatty acid binding [10,11].

The arachidonate 11R-LOX from the arctic coral *Gersemia fruticosa*, with a known crystal structure [12], displays peculiar regulatory aspects: while Ca^{2+} and lipid membranes augment the catalytic activity of most LOXs, for 11R-LOX the presence of both of these components is an absolute prerequisite for catalysis [13,14]. Calcium-binding by the PLAT domain induces translocation to a lipid surface, and only there can this enzyme acquire its fatty acid substrate. It has previously been hypothesized that allosteric communication between PLAT and catalytic domains is behind this regulatory mechanism [15]. Since the active site in the crystallographic model is enclosed and not accessible from the surface of the protein, it makes sense that conformational shifts are needed for productive substrate binding. Another potential allosteric mechanism emerges when quaternary structure is considered. Size exclusion chromatography (SEC) proved 11R-LOX to be a stable dimer in solution, however, none of the contacts in the crystal structure were deemed a substantial interface by *in silico* analysis [12].

In this study we analyzed the quaternary structure of 11R-LOX by SEC-SAXS and chemical cross-linking coupled with liquid chromatography–mass spectrometry (LC-MS). By combining the obtained results with previous crystallographic data, and introducing mutations that

Abbreviations: LOX, lipoxygenase; SAXS, small-angle X-ray scattering; SEC, size exclusion chromatography; LC-MS, liquid chromatography–mass spectrometry; DLS, dynamic light scattering; DST, disuccinimidyl tartrate

* Corresponding author.

E-mail address: nigulas.samel@ttu.ee (N. Samel).

<http://dx.doi.org/10.1016/j.bbalip.2017.07.012>

Received 9 March 2017; Received in revised form 4 July 2017; Accepted 26 July 2017

Available online 01 August 2017

1388-1981/© 2017 Elsevier B.V. All rights reserved.

would disrupt potential interactions between the subunits, we succeeded in singling out the actual dimer assembly. The interface is formed in the vicinity of a PDZ-like subdomain in the catalytic part of the enzyme, and includes two electrostatic clusters that glue the monomers together. The proposed quaternary structure can hopefully aid in understanding the potential allosteric role of the PDZ-like structural region and the dimerization of LOXs in general.

2. Experimental procedures

2.1. Materials

Chromatography equipment was from GE Healthcare. Reagents were from Sigma-Aldrich, if not stated otherwise. Recombinant HRV 3C protease with an N-terminal His₆-tag was produced in-house using the pET/3C construct and instructions kindly provided by Arie Geerlof (Helmholz Zentrum München).

2.2. Protein production

To obtain tagless native protein for structural studies, the encoding sequence of *G. fruticosa* 11R-LOX was ligated into pET-47b(+) vector (Novagen) at *Sma*I site. In this construct the target protein is expressed with an N-terminal His₆-tag separated by a HRV 3C protease site, so only two extra residues (Gly-Pro) are retained in the N-terminus after cleavage.

11R-LOX was expressed in BL21-CodonPlus(DE3)-RP cells (Startagene) using the autoinduction method as described in [15], except 100 µg/ml kanamycin was used for plasmid selection instead of ampicillin. The cells were lysed and centrifuged as reported previously [15]. The supernatant was supplied with 500 mM NaCl and 20 mM imidazole-HCl, pH 8.0, and applied to a HisTrap HP Ni-affinity column. The column was washed with 20 mM Tris-HCl, 500 mM NaCl, 20 mM imidazole-HCl, pH 8.0 and eluted step-wise with a raised imidazole concentration of 150 mM. Prior to proteolysis, the sample buffer was exchanged for 20 mM Tris-HCl, 150 mM NaCl, pH 8.0 (SEC buffer) in a Sephadex G-25 Fine desalting column. The sample was supplemented with HRV 3C protease in 1:5 (protease/11R-LOX) weight ratio, and incubated overnight at 4 °C. Cleaved protein was separated from the protease and uncleaved material in a second Ni-affinity run analogous to the first one, but was collected from the flow-through. The sample was then desalted into 20 mM Tris-HCl, pH 8.0, and applied to a Mono Q column. Elution was performed with a NaCl gradient from 0 to 500 mM. 11R-LOX fractions were pooled and concentrated in a 30,000 MWCO VivaSpin Turbo ultrafiltration device (Sartorius). For the final purification step, a Superdex 200 prep grade column in SEC buffer was used. Purified tag-free 11R-LOX was concentrated to > 10 mg/ml, flash frozen dropwise in liquid nitrogen, and stored at -80 °C.

The concentration of 11R-LOX was determined by absorption at 280 nm using a calculated ϵ_{280} of 129,720 M⁻¹ cm⁻¹. The polydispersity of SEC eluate was assessed by dynamic light scattering (DLS) on a Zetasizer µV instrument (Malvern) in a 12-µl quartz cuvette at 20 °C.

2.3. Size exclusion chromatography-coupled small-angle X-ray scattering

In-line SEC-SAXS experiments were conducted on the SWING beamline at synchrotron SOLEIL (Gif-sur-Yvette, France) using a wavelength of $\lambda = 1.03$ Å and a PCCD170170 (Aviex) detector at 1.8 m distance, resulting in q range of 0.01–0.62 Å⁻¹ ($q = 4\pi \sin \theta/\lambda$, where 2θ is the scattering angle). 100 µl of 14 mg/ml tagless 11R-LOX was applied to a Superdex 200 10/300 Increase column thermostatted at 15 °C and eluted with SEC buffer at 0.5 ml/min. Exposures of 1000 ms (with a dead time of 500 ms between frames) were collected in a 1.5 mm quartz capillary flow cell in a vacuum chamber. 120 frames were collected before column dead volume elution for buffer subtraction. Data were reduced and averaged using Foxtrot 3.3.0 software. Guinier approximation $I(q) = I_0 \exp(-q^2 R_g^2/3)$ for $qR_g < 1.3$

was used to determine the radius of gyration (R_g) and forward scattering intensity (I_0) of all sample curves. Peak frames were selected (40 in total) and averaged to obtain final data. Subsequent processing was done with the ATSAS suite [16]. R_g and I_0 were determined with PRIMUS, the pair-distance distribution function $P(r)$, the maximal dimension D_{max} , and Porod volume were calculated with GNOM.

2.4. Structure modelling

Ab initio bead models based on SAXS data were generated with DAMMIF [17] in slow mode. No constraints were used for initial shape determination. Subsequent calculations were carried out with P2 symmetry and prolate anisometry across the symmetry axis. To obtain a representative model, 20 models were generated with DAMMIF, averaged with DAMAVER [18] in automatic mode, and further refined with DAMMIN [19].

Contacts in the crystal structure of 11R-LOX (PDB ID: 3vf1)[12] were analyzed with PISA [20] and EPPIC [21] web services. ClusPro Dimer Classification service [22–25] was used to evaluate potential dimer structures. X-ray scattering curves for crystallographic dimers were calculated and fit to experimental data using CRY SOL [26] with constant subtraction enabled. Multicomponent mixtures of different oligomeric states were evaluated using OLIGOMER [27] with disabled non-negativity condition and an added constant component. Molecular graphics were produced with UCSF Chimera [28].

2.5. Chemical cross-linking

2.5.1. Sample preparation and cross-linking

Tagless 11R-LOX was dialyzed into 20 mM HEPES, 150 mM NaCl, pH 8.0, and diluted to 1 mg/ml. The cross-linking agent disuccinimidyl tartrate (DST; AppliChem) was freshly dissolved in dimethyl sulfoxide, and added to ~70 µg of enzyme in 50:1 molar excess. After a 30-min incubation at room temperature, the reaction was stopped by adding 1 M Tris-HCl, pH 8.0 buffer in final concentration of 50 mM, and incubated another 15 min. The sample was separated in a NuPAGE Novex Bis-Tris 4–12% gradient gel (Thermo Scientific) according to manufacturer's instructions.

2.5.2. In gel digestion and nano-LC/MS/MS analysis of cross-linked peptides

The gel bands that contained cross-linked 11R-LOX dimers were excised and destained in 1:1 acetonitrile / 100 mM ammonium bicarbonate with vortexing, reduced with 10 mM dithiothreitol at 56 °C and alkylated with 50 mM iodoacetamide. Overnight in-gel digestion was carried out with 10 ng/µl of dimethylated porcine trypsin (Sigma) at 37 °C. Peptides were extracted from the gel matrix using bath sonication, followed by 30 min vortexing in 2 volumes of 1:2 5% formic acid / acetonitrile. The organic phase was evaporated in a vacuum-centrifuge and the peptide mixture was desalted on an in-house made C18 (3M Empore) solid phase extraction tip.

Samples were injected to an Ultimate 3000 RSLCnano system (Dionex) using a C18 trap-column (Dionex) and an in-house packed (3 µm C18 particles, Dr. Maisch) analytical 50 cm × 75 µm emitter-column (New Objective). Peptides were eluted at 200 nl/min with a 8–40% B 120 min gradient (buffer A: 0.1% formic acid; buffer B: 80% acetonitrile + 0.1% formic acid) to a Q Exactive Plus (Thermo Fisher Scientific) mass spectrometer operating with a top-10 data-dependent acquisition strategy. Briefly, one 400–1600 m/z MS scan at a resolution setting of $R = 70,000$ at 200 m/z was followed by higher-energy collisional dissociation fragmentation (normalized collision energy of 27) of 10 most intense ions ($z: +3$ to $+7$) at $R = 35,000$. MS and MS/MS ion target values were 3e6 and 5e4 with 50 and 240 ms injection times, respectively. Dynamic exclusion was limited to 50 s.

2.5.3. Identification of cross-linked peptides from raw mass spectrometric data

Proteins contained in the sample were first identified with MaxQuant's Andromeda search engine [29] using UniProt's (www.uniprot.org) *Escherichia coli* K12 reference proteome database supplemented with 11R-LOX and human keratin sequences. Sequences of top 20 proteins with most identified peptides in the gel bands were included into the cross-linked peptide search along with their reversed sequence counterparts. Search was performed with the SIM-XL software 1.2.0.3 [30]. The detailed parameters are found in Supplementary File cx11lox.xml. Briefly, DST was defined as the cross-linking agent, carbamidomethylation of cysteine and oxidation of methionine was defined as the fixed and variable modification, respectively. Trypsin specificity was defined as the cleavage rule with maximum of three miscleavages. Precursor and fragment ion tolerances were set to 5 and 10 ppm, respectively. Search filter parameter thresholds (min 5 identified peaks per chain; inter- and intra-link scores of 3.3 and 2.0, respectively) were set such that no identifications were found from the reverse sequences. This resulted on average with 50 identified cross-linked peptide species per sample and thus an estimation of false discovery rate $\leq 1\%$. The cross-links were evaluated and visualized with XLink Analyzer [31] and UCSF Chimera [28].

2.6. Site-directed mutagenesis

Mutations were introduced using whole plasmid PCR of N-His₆-tagged wild-type 11R-LOX in pET-11a vector with mutagenic primers (Supplementary Table S1). Clones were screened using restriction mapping, small-scale expression, and sequencing. 0.5-l expression and purification of successful clones was done as in [15]. The oligomeric state of the mutants was determined on an in-house packed Superdex 200 prep grade column in SEC buffer.

Enzyme catalysis was assayed as described in [12,15]. Briefly, purified 11R-LOX was incubated in 50 mM Tris-HCl, 100 mM NaCl, 2 mM CaCl₂, pH 8.0 with 30 μ M arachidonic acid in the presence of small unilamellar vesicles. The formation of conjugated double bonds was monitored on a UV-1601 spectrophotometer (Shimadzu) at 236 nm.

3. Results

3.1. SAXS analysis

Crystallographic data of 11R-LOX left its dimer assembly ambiguous. To elucidate the matter, we subjected the enzyme to SAXS analysis which gives low-resolution structural data i.e. the size and shape of a particle in solution. Our personal experience has shown that LOXs are prone to aggregate, therefore we applied SAXS coupled with in-line SEC to avoid any distortions in data due to sample aggregation. Beforehand, the polydispersity of SEC eluate was evaluated by DLS and deemed monodisperse (Supplementary Fig. S1).

11R-LOX was expressed with a cleavable N-terminal His₆-tag to preclude artificial interactions and contributions to scattering. Purified protein was injected to a SEC column and the scattering profile of the eluate was continuously monitored on SWING beamline at synchrotron SOLEIL. The forward scattering intensity (I_0) chromatogram illustrates that the protein eluted in a single symmetrical peak with a constant radius of gyration (R_g) suggesting a monodisperse analyte (Fig. 1A). Guinier analysis of the averaged scattering curve yielded an R_g value of 41.61 Å, and the maximum dimension (D_{max}) was estimated at 148 Å according to the pair distance distribution function $P(r)$. SAXS data and corresponding plots are shown in Fig. 1B–D, and statistics given in Table 1.

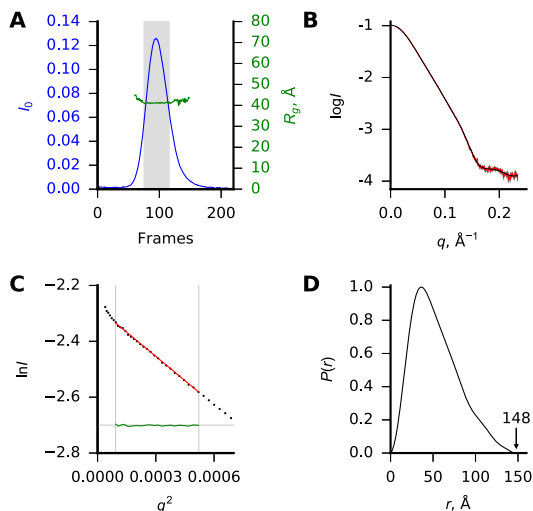


Fig. 1. SAXS analysis of 11R-LOX. (A) SEC-SAXS chromatogram with I_0 (blue) and R_g (green) values calculated by Guinier approximation for each recorded frame. The frame range used in averaging is highlighted in gray. (B) The averaged scattering profile of peak frames (red) and the profile calculated from the $P(r)$ function (black). (C) Guinier plot with experimental data (dots), fit (red) and residuals (green). Only a few data points were discarded from the low q region due to nonlinearity. (D) $P(r)$ distance distribution function and estimated D_{max} value.

Table 1
Statistics of SAXS analysis.

Structural parameters	
R_g [from Guinier]	41.61 ± 0.05 Å
R_g [from $P(r)$]	42.27 ± 0.02 Å
D_{max}	148 Å
V_{porod}	$214,722$ Å ³
M_w estimates (kDa)	
From sequence (dimer)	154.3
From DLS	134 ± 23.5
From V_{porod}	126.3^a
From excluded volume of ab initio model	128.9^a

^a M_w (Da) is approximately $V_{porod}/1.7$ or Excluded volume/2, if volumes are in Å³ [16].

3.2. Ab initio modelling

The averaged SAXS profile of the peak frames was used for ab initio modelling. Initial unconstrained trials using DAMMIF yielded prolate-shaped bead models with symmetrical features, therefore, prolate anisometry and 2-fold symmetry constraints were applied in further calculations. 17 out of 20 generated models were selected and averaged by DAMAVER, and further refined with DAMMIN to obtain the final model depicted in Fig. 2A. The particle is a slightly bent or dented prolate spheroid which could easily accommodate two 11R-LOX chains. The fit to experimental data is very good by visual inspection (Fig. 3, black and cyan lines), and the χ^2 value of 1.99, which denotes the discrepancy between data and the model, can also be considered satisfactory as the experimental errors were very low due to the large number of averaged data frames.

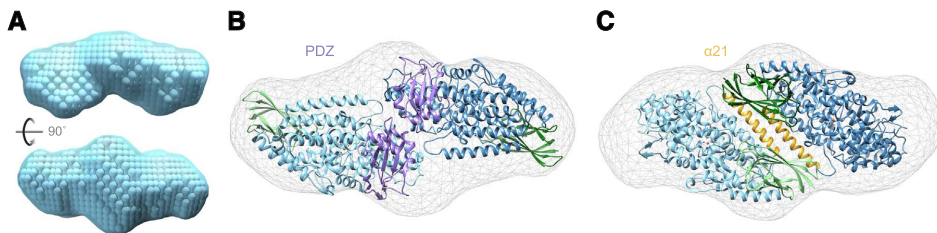


Fig. 2. SAXS modelling. (A) Ab initio space-filling bead model constructed by DAMMIF, DAMAVER and DAMMIN. The lower depiction is rotated by 90°. (B–C) Crystallographic dimers were superposed on the ab initio model using SUPCOMB. Catalytic and PLAT domains are colored in blue and green hues, respectively, and the surface of the ab initio model is shown in wireframe. The main interfacing regions of the models are the PDZ-like domain (B, purple) and helix $\alpha 21$ (C, gold). The view roughly coincides with the lower depiction in panel A.

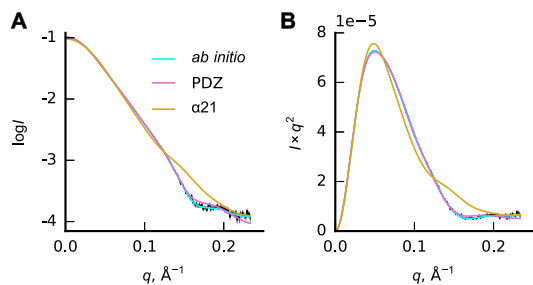


Fig. 3. Model fitting. Scattering profiles (A) and Kratky plots (B) of experimental data (black), and the ab initio (cyan) and crystallographic dimer models (PDZ, purple; $\alpha 21$, gold). The Kratky plot features a bell-shaped curve at low q values, which is characteristic to a well-folded globular protein.

Table 2
Comparison of crystallographic dimer interfaces.

	PDZ	$\alpha 21$
Symmetry	$x - 1/2, y - 1/2, z$	x, y, z
<i>PISA</i>		
Area (\AA^2)	1335.8	404.2
ΔG (kcal/mol) ^a	-1.5	-8.5
N of hydrogen bonds	8	0
N of salt bridges	13	0
CSS ^b	0.000	0.000
<i>EPPIC</i>		
Area (\AA^2)	1341.97	401.91
Consensus call	Crystal packing	Crystal packing
<i>ClusPro</i>		
Near-native count	45	3
Probability of biological dimer (%)	60	15
<i>CRY SOL</i>		
χ^2	16	881

^a Solvation free energy gain upon formation of the interface.

^b Complexation Significance Score, which indicates how significant the interface is for assembly formation on a scale of 0–1.

3.3. Revisiting the crystal structure

In a previous study we concluded that none of the contacts in 11R-LOX crystal structure model are strong enough to form a stable dimer in solution [12]. However, slight conformational changes could facilitate an increase in attraction that might be enough to stabilize an assembly. Therefore, we compared all possible crystallographic dimers with the obtained SAXS data to search for a starting point for further studies.

Out of 9 interfaces described by PISA and EPPIC web services, 2

candidates stood out as most resembling the ab initio bead model. One of them is formed by the tail of the catalytic domain opposite to the regulatory PLAT domain (Fig. 2B). This region has also been called a PDZ-like domain, and speculated to function as a second regulatory subdomain of LOXs [32]. The other interface connects mainly via helix $\alpha 21$, a 7-turn long helix that runs along the side of the catalytic domain (Fig. 2C). This assembly also happens to comprise the asymmetric unit of the crystal structure. The PDZ interface is larger with an area over 1300 \AA^2 versus 400 \AA^2 for the $\alpha 21$ version (Table 2). The latter relies purely on hydrophobic interactions, while several hydrogen bonds and salt bridges interweave the PDZ assembly. Nevertheless, neither of these contact regions was regarded sufficient for dimerization according to PISA and EPPIC analysis.

We also evaluated the interfaces using the Dimer Classification algorithm of the protein docking server ClusPro, which re-docks the subunits of a given dimer and checks how many solutions resemble the original assembly. 45 near-native structures were counted for the PDZ interface yielding a 60% probability of being a biological dimer. A much lower probability of 15% was suggested for the $\alpha 21$ interface.

The scattering profiles of the two models were evaluated and fitted to SAXS data using CRY SOL. The PDZ dimer model displayed a much better fit to data as illustrated by χ^2 values (Table 2) and the Kratky plot (Fig. 3B): the maxima of the peaks coincide, whereas for the $\alpha 21$ model it is shifted towards lower q values. Additionally, the $\alpha 21$ curve has a pronounced shoulder that strongly deviates from experimental data, suggesting a different particle shape.

Given that the M_w estimates by different methods were somewhat lower than the calculated weight of an 11R-LOX dimer (Table 1), we also considered the possibility that an equilibrium of different oligomeric states might exist in solution. Combinations of three models (PDZ dimer, $\alpha 21$ dimer, monomer) were evaluated with the program OLIGOMER. The best fit to data ($\chi^2 = 8.1$) was obtained with all three components included in the calculation. The corresponding volume fractions were 90.5%, 6.9% and 2.6% for PDZ dimer, monomer and $\alpha 21$ dimer, respectively. Therefore, the PDZ model was concluded to be the major contributor and the most likely assembly according to SAXS analysis.

3.4. Chemical cross-linking

For validation purposes, chemical cross-linking coupled with MS was carried out using the cross-linking agent DST, which reacts with primary amines and has a spacer arm of 6.4 \AA . Summed with the length of two lysine side chains (6–6.5 \AA each) and a model error of 1–1.5 \AA , this gives a maximum cross-linked C_{α} - C_{α} distance of 22.4 \AA [33]. Tagless 11R-LOX was incubated with DST in buffer solution, reaction products were separated in a gradient gel, and only the band that contained covalently bound dimers was excised for further treatment (Supplementary Fig. S2). The sample was subjected to trypsinolysis, and resulting cross-linked peptides were identified by high-resolution MS analysis.

Table 3

C_{α} – C_{α} distances between cross-linked residues (Å). The distances that satisfy the 22.4-Å limit of DST links are in bold.

Residues	Monomer	PDZ dimer	α 21 dimer
Intrapeptide			
Lys118–Lys125	12.7		
Lys125–Lys129	10.4		
Lys143–Lys144	3.8		
Lys144–Lys147	6.6		
Lys168–Lys172	7.9		
Lys256–Lys264	12.3		
Lys280–Lys283	5.1		
Lys503–Lys504	3.8		
Lys587–Lys591	10.8		
Lys591–Lys600	14.7		
Lys644–Lys652	12.4		
Interpeptide			
Lys84–Lys99	12.5	114.5	26.6
Lys99–Lys644	26.7	101.9	16.3
Lys99–Lys652	38.2	92.2	15.6
Lys99–Lys99	–	124.5	32.6
Lys110–Lys172	11.3	103.2	51.2
Lys222–Lys652	25.2	49.7	52.9
Lys222–Lys591	30.6	18.9	90.5
Lys256–Lys283	8.7	35.2	86.5
Lys264–Lys347	11.7	35.0	114.9
Lys504–Lys652	41.6	85.1	25.8

In all, 21 unique cross-links were detected including 11 intrapeptide links, which had formed between lysine residues of a same peptide, and 10 interpeptide links, which connected separate peptides (Table 3). The intrapeptide links carry no information with regard to oligomerization, they do however indicate that the participating residues are solvent-exposed. All of them are consistent with the crystallographic model as the distance threshold of 22.4 Å is satisfied in each case. The interpeptide bridges that do not exceed the limit should also be considered likely of monomeric origin. Although Lys222–Lys652 distance surpasses that value, it is possible for the link to form within a monomer in case of a slight conformational change (Fig. 4A). Both Lys99–Lys644 and Lys99–Lys652 links connect the PLAT domain with helix α 21, which suggests that the β -sandwich is shifted more towards the helix in solution than it is in the crystal structure, where these bridges are over 26 and 38 Å long, respectively. It has indeed been observed that the relative arrangement of PLAT and catalytic domains is flexible in mammalian LOXs [10,34–36]. Alternatively, these links could connect the subunits of a dimer that interact via α 21 helices (Fig. 4B). Lys99–Lys99, which is the only definite inter-subunit cross-link, can also support the α 21 assembly provided that PLAT domains shift closer together. However, such conformational changes would likely render this interface less solvent-accessible, making it harder for the reagent to reach these particular residues in the first place. The source of Lys504–Lys652 bridge is also ambiguous: the α 21 dimer could be considered, but alternative intramolecular lysines would be readily available and probably preferred. On a different note, the PDZ dimer configuration is clearly supported by the link of Lys222–Lys591,

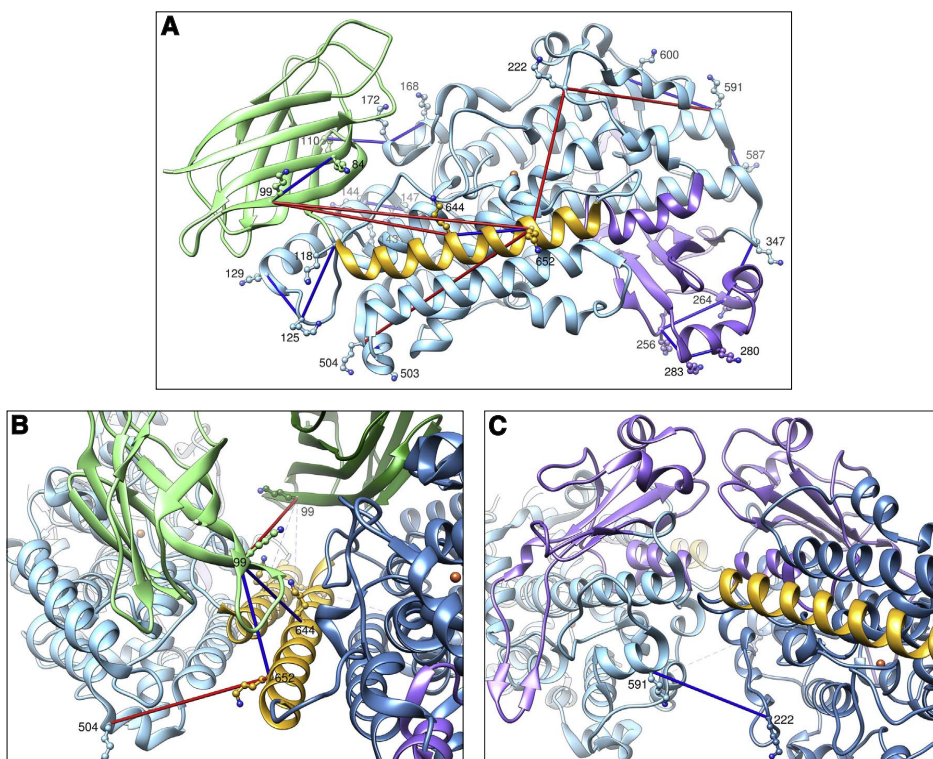


Fig. 4. Detected cross-links shown on 11R-LOX crystal structure (A) monomer, (B) α 21 interface and (C) PDZ interface model. The cross-links are rendered as sticks that connect the corresponding lysines by their C_{α} -s. Blue or red color denotes whether the length is below or above the 22.4-Å threshold, respectively. Regulatory PLAT domains are in shades of green, and catalytic cores in blue, helix α 21 is in gold, and PDZ subdomain in purple. In panels B and C, the mirroring cross-links are represented as dashed lines.

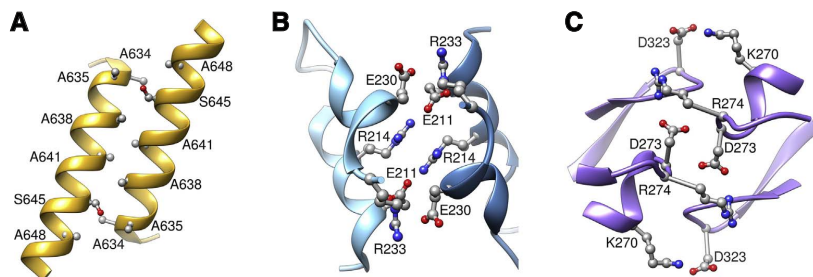


Fig. 5. Contacts between chains in 11R-LOX crystal structure. (A) Hydrophobic alanines of helices $\alpha 21$ interact in a zipper-like fashion. (B) Catalytic and (C) PDZ domains form two electrostatic clusters that constitute the PDZ assembly.

particularly as the residues stay well-exposed even in the assembly (Fig. 4C).

It should be mentioned that DST, an N-hydroxysuccinimide ester (as opposed to imidoesters), neutralizes the charge of lysine side chains. This could affect the interactions that drive dimerization, and consequently produce artifacts, hence cross-linking results leave room for alternative binding mode interpretations. Nevertheless, they do confirm the current view on 11R-LOX tertiary structure, and the feasibility of aforementioned quaternary structure hypotheses.

3.5. Interface disruption

In order to determine the actual interface region, we mutated residues that might participate in quaternary structure formation to disrupt potential interactions. Position of Ala641 was picked to impede dimerization via helix $\alpha 21$ as it interacts with its own counterpart from another chain in the crystal structure (Fig. 5A). Charged Glu or Arg residues were introduced to create steric and electrostatic repulsion. Yet neither of these mutations affected the oligomeric state of the enzyme as detected by SEC, and both variants retained catalytic activity similar to wild-type (data not shown). The same result was obtained with a quadruple mutant A634K/A635D/A638D/A641N that was constructed to mimic the corresponding helix of coral 8R-LOX, which is a stable monomer in solution (sequence alignment in Supplementary Fig. S3). Thus we conclude that helices $\alpha 21$ likely interact due to crystal packing, and this assembly is not relevant in dimerization.

The alternative PDZ interface contains two electrostatic clusters of 8 residues each — one in the catalytic part and the other in the PDZ subdomain — that bind the monomers together with several salt bridges and H-bonds (Fig. 5B–C). Again, repulsion-inducing charge swaps and substitutions based on monomeric LOXs were tested.

In the catalytic domain cluster, three single mutants were constructed with a positively charged arginine exchanged for a negative glutamate or vice versa: E211R, R214E and R233E. Despite the substitution of E211R having no apparent effect on quaternary structure as illustrated by the SEC chromatogram (Fig. 6), the alteration of the other side of the same electrostatic bridge, R214E, caused the enzyme to elute in an asymmetric peak with a tailing shoulder suggesting the presence of monomeric species. Even more, R233E mutant eluted in two peaks with a minor dimeric fraction and a major one at lower M_w , reckoned monomeric. As expected, the monomeric peak of R214E/R233E double mutant was delayed even further, although the ratio of the peaks was shifted in favor of dimers. The fact that the elution maxima of monomeric species are not constant suggests a dynamic monomer–dimer equilibrium in these mutants, which is likely dependent on both interaction strength and protein concentration.

A charged β -turn, Asp273–Arg274, establishes the two inner electrostatic bridges of the second cluster, which is formed by PDZ subdomains. These were neutralized by substituting the residues with Gly-Pro, a sequence that can be found in several mammalian LOXs (Supplementary Fig. S3). Another mutation based on sequence

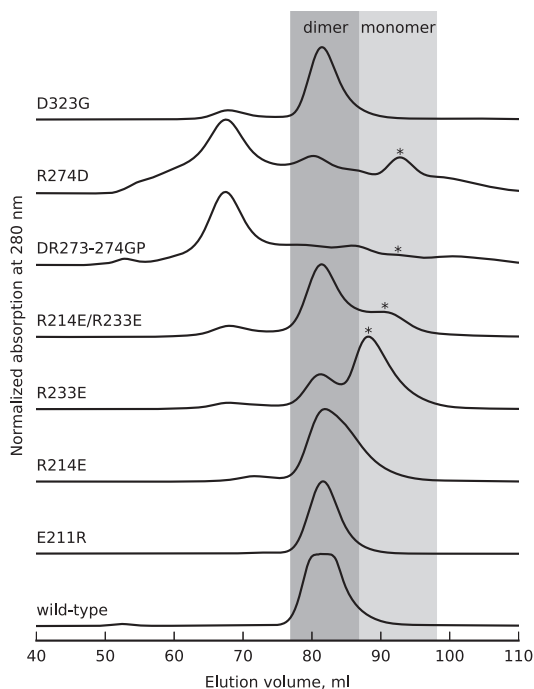


Fig. 6. Size exclusion chromatograms of PDZ interface mutants. Asterisk (*) denotes the most catalytically active peak in chromatograms with separated oligomeric states.

alignment was D323G as a Gly-residue is conserved in that position in most LOXs. The latter failed to significantly modify the elution profile of the enzyme, however, DR273–274GP replacement led to severe aggregation. Only trace amounts of 11R-LOX were salvaged from dimeric and monomeric elution regions of this variant. The most successful substitution was R274D charge swap that yielded dimeric and monomeric peaks in about 1:1 ratio, even though the mutant was prone to aggregate. Furthermore, we were able to isolate the monomeric species of R274D mutant, albeit in low amounts, which persisted as a monomer after storage at -80°C (data not shown).

These results clearly indicate that the quaternary structure of 11R-LOX in solution is analogous to the PDZ assembly in crystal structure. Interestingly we found that the catalytic activity of mutant enzymes tended to be higher in monomeric fractions even with protein concentrations being much lower (Fig. 6). This might suggest allosteric regulation between the two subunits in a dimer, which, when compromised, could lead to dysfunctional communication and inhibition. Nevertheless, the requirement for calcium and lipid membranes in the

reaction mixture was retained (data not shown). It should also be noted that the obtained monomeric fractions were generally not stable and tended to dimerize with handling (e.g. centrifugal concentration, long-term storage), so further molecular engineering would be necessary in order to obtain truly stable monomeric 11R-LOX.

4. Discussion

CATH database [37] classifies the subdomain found in the structural region responsible for 11R-LOX dimerization as an NTF2 (Nuclear Transport Factor 2) domain. Jankun et al., on the other hand, analyzed this feature in different mammalian and plant LOXs, and concluded that it carries greater resemblance to PDZ domains [32], which are known to bind peptide C-termini, other PDZ domains, and lipids, and mediate protein network formation [38–41]. Although both of these known folds comprise a β -sheet flanked by 2 to 3 helices, neither one actually matches the topology of the fragment found in LOXs. For instance, the antiparallel β -sheet of LOXs has a simple up-and-down topology, whereas a more entwined sheet is characteristic of NTF2 and PDZ domains. The location of helical segments in loops also varies greatly. Regardless, structural permutations are common among PDZ domains [41]. Additionally, PDZ domains contain a GLGF motif that is responsible for binding the C-terminus of a ligand peptide. In the subdomain of human platelet 12-LOX, a comparable GSLF(271–274) sequence is situated on the lip of a funnel-like crevice creating an analogous spatial feature [32]. In 11R-LOX the corresponding fragment, GLIF(285–288), matches the motif even better. Hence we agree that “PDZ-like domain” is currently the most suitable name for this structural element. Recently, Meng et al. identified an allosteric pocket in human 15-LOX-1, and were able to augment the enzymatic activity by up to 85% with specific ligands serving as activators [42]. The site they found is the very same crater between the PDZ-like domain and the active site, and directly involves residues from both parts of the enzyme structure. If this truly is a specific allosteric site in LOXs, it is reasonable to speculate that conformational changes related to oligomerization, which is mediated by the same structural region, could also affect the enzyme via a similar mechanism.

An extensive study revealed that about 30% of murine PDZ domains engage in PDZ–PDZ interactions, which is more common than previously thought [43]. The novel assemblies indicate that these interactions are more specific than canonical peptide binding by PDZ domains, and can provide a means to colocalize and form functional multiprotein complexes. Notably, both hetero- and homotypic complexes have been observed. PDZ domains can assemble by β -sheet merging, but also via loop interactions [44] as is the case with 11R-LOX. The same region has been suggested to participate in the dimerization of platelet 12-LOX based on SAXS experiments [9], although lack of crystallographic data hindered exact assembly determination in that particular study. The crystal structure of rabbit 12/15-LOX apoenzyme / inhibitor complex [45] gave rise to a slightly different dimer interface proposal, one that employs α 2 helices, which also line the entrance to the active site cavity. SAXS studies revealed that the formation of such dimers is induced by fatty acid ligand binding [11]. Although the assembly is different, the PDZ-like domain is still in the vicinity of this interface and could perform a regulatory function, perhaps even provide an allosteric fatty acid binding site. It has indeed been demonstrated that in addition to peptides PDZ domains can bind lipids, especially phosphoinositides, and lipid membranes [40,41].

Of human LOXs, 5-LOX bears the greatest resemblance to coral 11R-LOX, sharing 37% of its primary structure. The quaternary assembly described for 5-LOX is believed to involve two ATP-binding sites — one in PLAT and the other in the catalytic domain — and according to docking studies the dimer should form in a head-to-tail fashion [8]. Controversially, this makes it the least similar assembly compared to 11R-LOX dimer. One of the ATP-sites in 5-LOX (residues 193–209) partially overlaps the electrostatic cluster in the catalytic domain of

11R-LOX, but PDZ domain is left on the opposite side, away from the interface. However, this is not surprising since there are numerous examples of protein families where the oligomeric state might be conserved, yet the binding modes differ, especially if sequence identity falls below 50% [46,47]. The activity of 5-LOX is modulated also by phosphorylation (reviewed in [48]). Interestingly, one of the phosphorylation sites that stimulates the enzyme, Ser271, is located in PDZ domain on a helix just after the loop that 11R-LOX utilizes for dimerization. Even if human 5-LOX does not employ this region in quaternary structure formation, it evidently participates in allosteric regulation of the enzyme.

Members of another arachidonic acid-metabolizing enzyme family, prostaglandin endoperoxide H synthases or cyclooxygenases, function as conformational heterodimers [49,50]. Although both monomers of a dimer are identical by sequence, there are subtle conformational differences that facilitate different affinities of binding sites. These are enough to designate one monomer as allosteric and the other, catalytic. The allosteric subunit is able to bind non-substrate fatty acids, which in turn can stimulate cyclooxygenation by the catalytic monomer. A somewhat similar phenomenon was recently observed on human 5-LOX: Häfner et al. found that a catalytically inactive but structurally intact splice variant, 5-LOX Δ 4, stimulates the catalytic activity of the full-length isoform [51]. The deletion in 5-LOX Δ 4 did not hinder its ability to bind ATP, so it was reasoned that the two enzyme variants could form a complex in the same way as proposed for full-length 5-LOX. If the determined quaternary assembly of 11R-LOX stays intact upon membrane binding and catalysis, analogous regulatory mechanisms could be considered.

In humans there are 6 functional LOX variants with distinctive and even contrary functions, hence it is clear that pharmacological intervention must be very selective. To date, only one LOX-targeting drug is commercially available, the 5-LOX inhibitor Zileuton, which chelates the catalytic iron [52]. Zileuton, however, is not in the first line of asthma treatment due to its liver toxicity and suboptimal pharmacokinetic properties. As was demonstrated by Meng et al. [42], allosteric sites do exist in LOXs and can be manipulated with both inhibitory and activating compounds, so novel drug design should try and look beyond the active site. The results presented in this study provide insight into yet another potential dimension of LOX regulation, that is, dimerization. We have established the basis of 11R-LOX quaternary structure, which involves electrostatic clusters in the catalytic and PDZ-like domains (Figs. 2B, 4C and 5B–C). Further studies are to reveal whether these interactions participate in allosteric communication between the subunits of a complex, and if these structural features are more widespread among LOXs.

Conflict of interest

The authors declare that they have no conflicts of interest with the contents of this article.

Transparency document

The <http://dx.doi.org/10.1016/j.bbalip.2017.07.012> associated with this article can be found, in the online version.

Acknowledgments

We acknowledge SOLEIL for provision of synchrotron radiation facilities and we would like to thank Aurélien Thureau for assistance in using beamline SWING. We are grateful to Arie Geerlof (Helmholz Zentrum München, Germany) for providing the DNA construct and the protocol for protease production, and Helian Vunk, Janet Tamm and Merilin Saarma for their assistance in protein production and cross-linking studies.

Funding

This work was supported by Institutional Research Funding of the Estonian Ministry of Education and Research (IUT 19–9 to N.S.), and the European Community's Seventh Framework Programme (FP7/2007–2013) under BioStruct-X (grant agreement No. 283570).

Appendix A. Supplementary data

Supplementary data to this article can be found online at <http://dx.doi.org/10.1016/j.bbalip.2017.07.012>.

References

- H. Kühn, S. Banthiya, K. van Leyen, Mammalian lipoxygenases and their biological relevance, *Biochim. Biophys. Acta* 1851 (2015) 308–330.
- J.Z. Haeggström, C.D. Funk, Lipoxygenase and leukotriene pathways: biochemistry, biology, androisindisease, *Chem. Rev.* 111 (2011) 5866–5898.
- R. Koljak, O. Boutaud, B.H. Shieh, N. Samel, A.R. Brash, Identification of a naturally occurring peroxidase-lipoxygenase fusion protein, *Science* 277 (1997) 1994–1996.
- H. Löhelaid, R. Järving, K. Valmsen, K. Varvas, M. Kreen, I. Järving, N. Samel, Identification of a functional allene oxide synthase-lipoxygenase fusion protein in the soft coral *Gersemia fruticosa* suggests the generality of this pathway in octocorals, *Biochim. Biophys. Acta* 1780 (2008) 315–321.
- H. Löhelaid, T. Teder, K. Töldsepp, M. Ekins, N. Samel, Up-regulated expression of AOS-LOXa and increased eicosanoid synthesis in response to coral wounding, *PLoS One* 9 (2014) e89215.
- H. Löhelaid, T. Teder, N. Samel, Lipoxygenase-allene oxide synthase pathway in octocoral thermal stress response, *Coral Reefs* 34 (2015) 143–154.
- M.E. Newcomer, A.R. Brash, The structural basis for specificity in lipoxygenase catalysis, *Protein Sci.* 24 (2015) 298–309.
- A.-K. Häfner, M. Cernescu, B. Hofmann, M. Ermisch, M. Hörnig, J. Metzner, G. Schneider, B. Brutschy, D. Steinhilber, Dimerization of human 5-lipoxygenase, *Biol. Chem.* 392 (2011) 1097–1111.
- A.M. Aleem, J. Jankun, J.D. Dignam, M. Walther, H. Kühn, D.I. Svergun, E. Skrzypczak-Jankun, Human platelet 12-lipoxygenase, new findings about its activity, membrane binding and low-resolution structure, *J. Mol. Biol.* 376 (2008) 193–209.
- W. Shang, I. Ivanov, D.I. Svergun, O.Y. Borbulevych, A.M. Aleem, S. Stehling, J. Jankun, H. Kühn, E. Skrzypczak-Jankun, Probing dimerization and structural flexibility of mammalian lipoxygenases by small-angle X-ray scattering, *J. Mol. Biol.* 409 (2011) 654–668.
- I. Ivanov, W. Shang, L. Toledo, L. Masgrau, D.I. Svergun, S. Stehling, H. Gómez, A. DiVenere, G. Mei, J.M. Lluch, E. Skrzypczak-Jankun, A. González-Lafont, H. Kühn, Ligand-induced formation of transient dimers of mammalian 12/15-lipoxygenase: a key to allosteric behavior of this class of enzymes? *Proteins* 80 (2012) 703–712.
- P. Eek, R. Järving, I. Järving, N.C. Gilbert, M.E. Newcomer, N. Samel, Structure of a calcium-dependent 11R-lipoxygenase suggests a mechanism for Ca²⁺ regulation, *J. Biol. Chem.* 287 (2012) 22377–22386.
- R. Järving, A. Löökene, R. Kurg, L. Siimon, I. Järving, N. Samel, Activation of 11R-lipoxygenase is fully Ca(2+)-dependent and controlled by the phospholipid composition of the target membrane, *Biochemistry* 51 (2012) 3310–3320.
- M. Mortimer, R. Järving, A.R. Brash, N. Samel, I. Järving, Identification and characterization of an arachidonate 11R-lipoxygenase, *Arch. Biochem. Biophys.* 445 (2006) 147–155.
- P. Eek, M.-A. Piht, M. Rätsep, A. Freiberg, I. Järving, N. Samel, A conserved π -cation and an electrostatic bridge are essential for 11R-lipoxygenase catalysis and structural stability, *Biochim. Biophys. Acta* 1851 (2015) 1377–1382.
- M.V. Petoukhov, D. Franke, A.V. Shkumatov, G. Tria, A.G. Kikhney, M. Gajda, C. Gorba, H.D.T. Mertens, P.V. Konarev, D.I. Svergun, New developments in the ATSAS program package for small-angle scattering data analysis, *J. Appl. Crystallogr.* 45 (2012) 342–350.
- D. Franke, D.I. Svergun, DAMMIF, a program for rapid ab-initio shape determination in small-angle scattering, *J. Appl. Crystallogr.* 42 (2009) 342–346.
- V.V. Volkov, D.I. Svergun, Uniqueness of ab initio shape determination in small-angle scattering, *J. Appl. Crystallogr.* 36 (2003) 860–864.
- D.I. Svergun, Restoring low resolution structure of biological macromolecules from solution scattering using simulated annealing, *Biophys. J.* 76 (1999) 2879–2886.
- E. Krissinel, K. Henrick, Inference of macromolecular assemblies from crystalline state, *J. Mol. Biol.* 372 (2007) 774–797.
- J.M. Duarte, A. Srebnik, M.A. Schäfer, G. Capitani, Protein interface classification by evolutionary analysis, *BMC Bioinformatics* 13 (2012) 334.
- D. Kozakov, R. Brenke, S.R. Comeau, S. Vajda, PIPER: an FFT-based protein docking program with pairwise potentials, *Proteins* 65 (2006) 392–406.
- D. Kozakov, D. Beglov, T. Bohnuud, S.E. Mottarella, B. Xia, D.R. Hall, S. Vajda, How good is automated protein docking? *Proteins* 81 (2013) 2159–2166.
- S.R. Comeau, D.W. Gatchell, S. Vajda, C.J. Camacho, ClusPro: a fully automated algorithm for protein-protein docking, *Nucleic Acids Res.* 32 (2004) W96–W99.
- S.R. Comeau, D.W. Gatchell, S. Vajda, ClusPro: an automated docking and discrimination method for the prediction of protein complexes, *Bioinformatics* 20 (2004) 45–50.
- D. Svergun, C. Barberato, M. Koch, CRYSOLE – a program to evaluate X-ray solution scattering of biological macromolecules from atomic coordinates, *J. Appl. Crystallogr.* 28 (1995) 768–773.
- P.V. Konarev, V.V. Volkov, A.V. Sokolova, M.H.J. Koch, D.I. Svergun, PRIMUS: a Windows PC-based system for small-angle scattering data analysis, *J. Appl. Crystallogr.* 36 (2003) 1277–1282.
- E.F. Pettersen, T.D. Goddard, C.C. Huang, G.S. Couch, D.M. Greenblatt, E.C. Meng, T.E. Ferrin, UCSF Chimera – a visualization system for exploratory research and analysis, *J. Comput. Chem.* 25 (2004) 1605–1612.
- J. Cox, N. Neuhauser, A. Michalski, R.A. Scheltema, J.V. Olsen, M. Mann, Andromeda: a peptide search engine integrated into the MaxQuant environment, *J. Proteome Res.* 10 (2011) 1794–1805.
- D.B. Lima, T.B. de Lima, T.S. Balbuena, A.G.C. Neves-Ferreira, V.C. Barbosa, F.C. Gozzo, P.C. Carvalho, SIM-XL: a powerful and user-friendly tool for peptide cross-linking analysis, *J. Proteome* 129 (2015) 51–55.
- J. Kosinski, A. von Appen, A. Ori, K. Karius, C.W. Müller, M. Beck, Xlink Analyzer: software for analysis and visualization of cross-linking data in the context of three-dimensional structures, *J. Struct. Biol.* 189 (2015) 177–183.
- J. Jankun, T. Doerks, A.M. Aleem, W. Lysiak-Szydłowska, E. Skrzypczak-Jankun, Do human lipoxygenases have a PDZ regulatory domain? *Curr. Mol. Med.* 8 (2008) 768–773.
- J. Rappsilber, The beginning of a beautiful friendship: cross-linking/mass spectrometry and modelling of proteins and multi-protein complexes, *J. Struct. Biol.* 173 (2011) 530–540.
- I. Ivanov, A. Di Venere, T. Horn, P. Scheerer, E. Nicolai, S. Stehling, C. Richter, E. Skrzypczak-Jankun, G. Mei, M. Maccarrone, H. Kühn, Tight association of N-terminal and catalytic subunits of rabbit 12/15-lipoxygenase is important for protein stability and catalytic activity, *Biochim. Biophys. Acta* 1811 (2011) 1001–1010.
- S.T. Moin, T.S. Hofer, R. Sattar, Z. Ul-Haq, Molecular dynamics simulation of mammalian 15S-lipoxygenase with AMBER force field, *Eur. Biophys. J.* 40 (2011) 715–726.
- M. Hammel, M. Walther, R. Prassl, H. Kühn, Structural flexibility of the N-terminal beta-barrel domain of 15-lipoxygenase-1 probed by small angle X-ray scattering. Functional consequences for activity regulation and membrane binding, *J. Mol. Biol.* 343 (2004) 917–929.
- N.L. Dawson, T.E. Lewis, S. Das, J.G. Lees, D. Lee, P. Ashford, C.A. Orengo, I. Sillitoe, CATH: an expanded resource to predict protein function through structure and sequence, *Nucleic Acids Res.* 45 (2017) D289–D295.
- C. Nourry, S.G.N. Grant, J.-P. Borg, PDZ domain proteins: plug and play!, *Sci. STKE* 2003 (2003) RE7.
- C.N. Chi, A. Bach, K. Strömgaard, S. Gianni, P. Jemth, Ligand binding by PDZ domains, *Biofactors* 38 (2012) 338–348.
- R. Gallardo, Y. Ivarsson, J. Schymkowitz, F. Rousseau, P. Zimmermann, Structural diversity of PDZ-lipid interactions, *Chembiochem* 11 (2010) 456–467.
- Y. Ivarsson, Plasticity of PDZ domains in ligand recognition and signaling, *FEBS Lett.* 586 (2012) 2638–2647.
- H. Meng, C.L. McClendon, Z. Dai, K. Li, X. Zhang, S. He, E. Shang, Y. Liu, L. Lai, Discovery of novel 15-lipoxygenase activators to shift the human arachidonic acid metabolic network toward inflammation resolution, *J. Med. Chem.* 59 (2016) 4202–4209.
- B.H. Chang, T.S. Gujral, E.S. Karp, R. BuKhalid, V.P. Grantcharova, G. MacBeath, A systematic family-wide investigation reveals that ~30% of mammalian PDZ domains engage in PDZ-PDZ interactions, *Chem. Biol.* 18 (2011) 1143–1152.
- Y.J. Im, J.H. Lee, S.H. Park, S.J. Park, S.-H. Rho, G.B. Kang, E. Kim, S.H. Eom, Crystal structure of the Shank PDZ-ligand complex reveals a class I PDZ interaction and a novel PDZ-PDZ dimerization, *J. Biol. Chem.* 278 (2003) 48099–48104.
- J. Choi, J.K. Chon, S. Kim, W. Shin, Conformational flexibility in mammalian 15S-lipoxygenase: reinterpretation of the crystallographic data, *Proteins* 70 (2008) 1023–1032.
- K. Hashimoto, H. Nishi, S. Bryant, A.R. Panchenko, Caught in self-interaction: evolutionary and functional mechanisms of protein homooligomerization, *Phys. Biol.* 8 (2011) 035007.
- J.E. Dayhoff, B.A. Shoemaker, S.H. Bryant, A.R. Panchenko, Evolution of protein binding modes in homooligomers, *J. Mol. Biol.* 395 (2010) 860–870.
- O. Rådmark, O. Werz, D. Steinhilber, B. Samuelsson, 5-lipoxygenase, a key enzyme for leukotriene biosynthesis in health and disease, *Biochim. Biophys. Acta* 1851 (2014) 331–339.
- L. Dong, A.J. Vecchio, N.P. Sharma, B.J. Jurban, M.G. Malkowski, W.L. Smith, Human cyclooxygenase-2 is a sequence homodimer that functions as a conformational heterodimer, *J. Biol. Chem.* 286 (2011) 19035–19046.
- H. Zou, C. Yuan, L. Dong, R.S. Sidhu, Y.H. Hong, D.V. Kuklev, W.L. Smith, Human cyclooxygenase-1 activity and its responses to COX inhibitors are allosterically regulated by nonsubstrate fatty acids, *J. Lipid Res.* 53 (2012) 1336–1347.
- A.-K. Häfner, K. Beilstein, P. Graab, A.-K. Ball, M.J. Saul, B. Hofmann, D. Steinhilber, Identification and characterization of a new protein isoform of human 5-lipoxygenase, *PLoS One* 11 (2016) e0166591.
- D. Steinhilber, B. Hofmann, Recent advances in the search for novel 5-lipoxygenase inhibitors, *Basic Clin. Pharmacol. Toxicol.* 114 (2014) 70–77.

A PDZ-like domain mediates the dimerization of 11R-lipoxygenase

Priit Eek¹, Kaspar Pöldemaa¹, Sergio Kasvandik², Ivar Järving¹, and Nigulas Samel¹

¹Department of Chemistry and Biotechnology, School of Science, Tallinn University of Technology, Akadeemia tee 15, 12618 Tallinn, Estonia

²Institute of Technology, University of Tartu, Nooruse 1, 50411 Tartu, Estonia

Supplementary materials

SIM-XL search parameters for cross-linked peptide identification can be found in the supplementary file `cx11lox.xml`.

Table 1: Mutagenic primers. The up- and downstream primers for whole plasmid PCR are shown, respectively. Non-complementary nucleotides are underlined.

Mutation	Primers
E211R	5' GACTTTCGACAGCTGATCACTC 3' 5' <u>GCGCAAACAATCCCAATCATC</u> 3'
R214E	5' CTTTGAACAGCTGATCACTCCTGC 3' 5' GCTGTTCAAAGTCTTCCAAAC 3'
R233E	5' CTGGGAAGATGATGTGTGGTTTGG 3' 5' CATCTTCCAGTACTCTGCAGCATG 3'
DR273-274GP	5' CTTGGGCCCGGGATATACTTTGG 3' 5' GTATATCCCGGCCCAAGAGCTTTTC 3'
R274D	5' AAGCTTTGGATGACGGATATACTTTGG 3' 5' TTCCACCATTTCATTCTTAC 3'
D323G	5' AACGGTGACATTATTCCGATCGCCATTTC 3' 5' GTCACCGTTGTTCTTCCAGATAAAAC 3'
A641E	5' GCAGCCATGGAAAAGTTCAAGAG 3' 5' CTTTCCATGGCTGCATGAGCTGC 3'
A641R	5' CATGCGCAATGCGCAAGTTCAAGAGT 3' 5' GAACTTGCGCATTGCCGCATGGGCTGCA 3'
A634K/A635D/ A638D/A641N	5' AAAGATGCTCATGATGCAATGAATAAGTTCAAGAGTAATTTGGC 3' 5' <u>ATT</u> CATTGCATCATGAGCATCTTTATCACCAAACAAGTTATCCG 3'

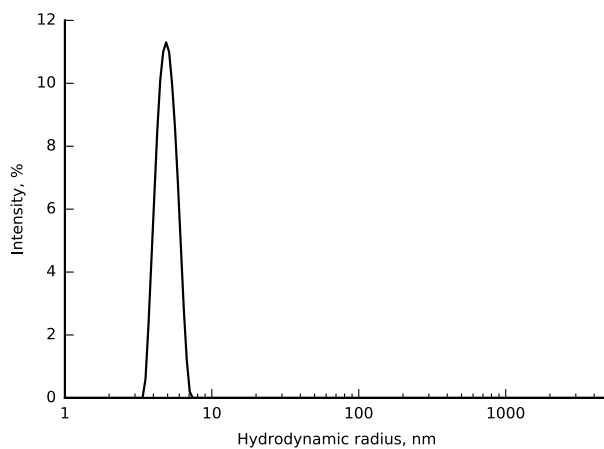


Figure 1: DLS pattern of 11R-LOX. The SEC eluate containing tagless 11R-LOX was analyzed with DLS and was found to be highly monodisperse with a polydispersity of 17.5% as determined by Zetasizer software (Malvern).

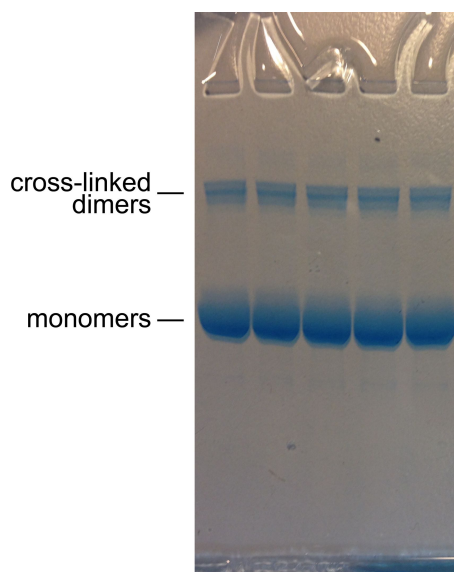


Figure 2: SDS-PAGE of cross-linked 11R-LOX. The reaction mixture was separated on a gradient gel and only covalently bound dimers (upper bands) were excised for further treatment and analysis.

	η7	α6	α21
11R-LOX_G.fruticosa	270	KLLDRGYTLEK	630
11R-LOX_G.fruticosa	270	KLLDRGYTLEK	630
AOS-LOX_P.homomalla	637	ASLDRGKNIIDE	1017
ALOx5_H.sapiens	265	CSLERQLSLEQ	625
Allox5_M.auratus	264	CSLERHLSLEQ	624
Allox5_M.musculus	265	CSLERQLSLEQ	625
Allox5_R.norvegicus	264	CSLERQLSLEQ	624
ALOx12_H.sapiens	260	...LQAQLEK	614
Allox12_M.musculus	260	...LQAQLEK	614
ALOx12B_H.sapiens	296	PFLGEGTCLQA	652
Allox12b_M.musculus	296	PFLGEGTCLQA	652
ALOx12b_R.norvegicus	296	PFLGEGTCLQA	652
ALOx3_H.sapiens	306	PLLGDQTCCLQT	662
Allox3_M.musculus	306	PLLGGTCLQT	662
Allox12e_M.musculus	260	...VQTQLEK	613
ALOx15_H.sapiens	260	...LQAQLEK	613
Allox15_B.taurus	261	...LQAQLEK	614
Allox15_M.musculus	261	...LQAQLEK	614
Allox15_O.cuniculus	261	...LQAQLEK	614
Allox15_P.abelii	260	...LQAQLEK	613
Allox15_R.norvegicus	261	...LQAQLEK	614
Allox15_S.scrofa	261	...LQAQLEK	614
ALOx15B_H.sapiens	270	SVLGGTSLQA	627
Allox15b_M.musculus	271	PVLGGTSLQA	628
Allox15b_R.norvegicus	271	PVLGGTSLQA	628
LOX1_1_G.max	390	L.DG.YTMD	772
LOX1_2_G.max	419	L.DG.YTVD	800
LOX1_3_G.max	408	PNLEGLTVDE	791
LOX1_4_G.max	414	INMGG.VTVE	798
LOX1_5_G.max	403	PNLGG.LTVE	787
LOXA_S.lycopersicum	411	GKLDG.LTIDE	794
LOX1_A.thaliana	410	HNLDDG.LTVE	793
LOX2_A.thaliana	444	REVKGNM.TVDE	830

Figure 3: Sequence alignment. Positions of 11R-LOX mutations DR273-274GP and A634K/A635DA638D/A641N are highlighted in yellow. Gene-based nomenclature is used where applicable and the following organisms are represented: soft corals (*Gersemia fruticosa* and *Plexaura homomalla*), human (*Homo sapiens*), golden hamster (*Mesocricetus auratus*), mouse (*Mus musculus*), rat (*Rattus norvegicus*), bovine (*Bos taurus*), rabbit (*Oryctolagus cuniculus*), orangutang (*Pongo abelii*), pig (*Sus scrofa*), soybean (*Glycine max*), tomato (*Solanum lycopersicum*) and mouse-ear cress (*Arabidopsis thaliana*). Sequences were aligned with ClustalW2 [1] and the alignment rendered with ESPript [2].

References

- Chenna, R., Sugawara, H., Koike, T., Lopez, R., Gibson, T. J., Higgins, D. G. & Thompson, J. D. Multiple sequence alignment with the Clustal series of programs. *Nucleic Acids Res.* **31**, 3497–3500 (2003).
- Robert, X. & Gouet, P. Deciphering key features in protein structures with the new ENDscript server. *Nucleic Acids Res.* **42**, W320–4 (2014).

CURRICULUM VITAE

PERSONAL INFORMATION

Name Priit Eek
Date of birth 24.04.1986
Place of birth Tallinn, Estonia
Citizenship Estonian
Address Department of Chemistry and Biotechnology
Tallinn University of Technology
Akadeemia tee 15, 12618 Tallinn, Estonia
Phone +372 620 4387
E-mail priit.eek@ttu.ee

EDUCATION

2011-... Tallinn University of Technology, chemistry and gene technology
(chemistry), PhD
2008-2011 Tallinn University of Technology, applied chemistry and biotechnology
(biochemistry), MSc (cum laude)
2005-2008 Tallinn University of Technology, applied chemistry and biotechnology,
BSc (cum laude)
2002-2005 Viimsi Secondary School (gold medal)

LANGUAGES

Estonian (native), English (proficient), Finnish (independent), Russian (good),
German (basic)

SPECIAL COURSES

2013 EMBO practical course "Small angle neutron and X-ray scattering from
proteins in solution"
2012 "RapiData 2012" Rapid data collection and structure solving at the NSLS:
A practical course in macromolecular X-ray diffraction measurement

PROFESSIONAL EMPLOYMENT

2017-... Tallinn University of Technology, Department of Chemistry and
Biotechnology, Early Stage Researcher
2015-2016 Tallinn University of Technology, Department of Chemistry,
Early Stage Researcher
2009-2010 Louisiana State University (Baton Rouge, LA, USA), Department of
Biological Sciences, Research Associate

CURRICULUM VITAE

OTHER AFFILIATIONS

- 2008–... Estonian Biochemical Society, member
- 2005–... Academic Male Choir of Tallinn University of Technology, member (senior since 2014)

HONORS AND AWARDS

- 2010 Estonian National Contest for University Students, Natural Sciences and Engineering, Master's studies, 3rd prize
- 2008 Estonian National Contest for University Students, Bio and Environmental Sciences, Bachelor's studies, 3rd prize
- 2007 AS Hansapank, TTÜ Development Fund, Bachelor's scholarship

SUPERVISED DISSERTATIONS

Doris Pooga, Master's Degree, 2017, (sup) Peep Palumaa, Priit Eek. Crystallisation of Copper-metallothionein 2E. Tallinn University of Technology School of Science, Department of Chemistry and Biotechnology.

Marianna Köster, Master's Degree, 2017, (sup) Priit Eek, Ivar Järving. Crystallization studies of human 15-lipoxygenase-1. Tallinn University of Technology School of Science, Department of Chemistry and Biotechnology.

Kaspar Pöldemaa, Master's Degree, 2016, (sup) Priit Eek, Ivar Järving. Regulation of 11R-lipoxygenase activity: identification of substrate inhibition and dimerisation determinants. Tallinn University of Technology, Faculty of Science, Department of Chemistry.

Janet Tamm, Bachelor's Degree, 2016, (sup) Priit Eek. Quaternary structure studies of 11R-lipoxygenase using chemical cross-linking. Tallinn University of Technology, Faculty of Science, Department of Chemistry.

Marianna Köster, Bachelor's Degree, 2015, (sup) Priit Eek. Expression of mammalian lipoxygenases in bacterial culture. Tallinn University of Technology, Faculty of Science, Department of Chemistry.

Sandra Kaabel, Master's Degree, 2014, (sup) Riina Aav, Priit Eek, Kaja Ilmarinen. Single crystal X-ray diffraction analysis of a chiral isatin derivative with Bruker Smart X2S and Rigaku Compact HomeLab diffractometers. Tallinn University of Technology, Faculty of Science, Department of Chemistry.

Doris Pooga, Bachelor's Degree, 2014, (sup) Peep Palumaa, Priit Eek. Crystallisation of copper-metallothionein 2E. Tallinn University of Technology, Faculty of Science, Department of Gene Technology.

Helian Vunk, Bachelor's Degree, 2014, (sup) Priit Eek. Expression and purification of 11R-lipoxygenase with a proteolytically cleavable His₆-tag. Tallinn University of Technology, Faculty of Science, Department of Chemistry.

Kaspar Pöldemaa, Bachelor's Degree, 2014, (sup) Priit Eek. Mutational analysis of potential substrate channel entrances of 11R-lipoxygenase. Tallinn University of Technology, Faculty of Science, Department of Chemistry.

Mari-Ann Piht, Master's Degree, 2013, (sup) Priit Eek. Arg106–Asp173 bridge — a mediator of allosteric regulation in 11R-lipoxygenase. Tallinn University of Technology, Faculty of Science, Department of Chemistry.

Mari-Ann Piht, Bachelor's Degree, 2011, (sup) Priit Eek, Reet Järving. Cloning and expression of lipoxygenase PLAT domains. Tallinn University of Technology, Faculty of Science, Department of Chemistry.

PUBLICATIONS

Eek, P., Järving, R., Järving, I., Gilbert, N. C., Newcomer, M. E., Samel, N. (2012) Structure of a calcium-dependent 11R-lipoxygenase suggests a mechanism for Ca^{2+} regulation. *J. Biol. Chem.* 287 (26), 22377–22386.

Eek, P., Piht, M.-A., Rätsep, M., Freiberg, A., Järving, I., Samel, N. (2015) A conserved π -cation and an electrostatic bridge are essential for 11R-lipoxygenase catalysis and structural stability. *Biochim. Biophys. Acta. Mol. Cell Biol. Lipids* 1851 (10), 1377–1382.

Eek, P., Pöldemaa, K., Kasvandik, S., Järving, I., Samel, N. (2017) A PDZ-like domain mediates the dimerization of 11R-lipoxygenase. *Biochim. Biophys. Acta. Mol. Cell Biol. Lipids* 1862 (10 Pt A), 1121–1128.

CONFERENCE PRESENTATIONS

Eek, P., Pöldemaa, K., Kasvandik, S., Järving, I., Samel, N. (2016) Investigation of 11R-lipoxygenase quaternary structure. *6th European Workshop on Lipid Mediators*, Frankfurt am Main, Germany.

Eek, P., Järving, R., Järving, I., Newcomer, M.E., Samel, N. (2011) 11R-lipoksügenaasi kristallstruktuuri mudel. *XXXII Eesti keemiapäevad*, Tartu, Estonia.

ELULOOKIRJELDUS

ISIKUANDMED

Nimi Priit Eek
Sünniaeg 24.04.1986
Sünnikoht Tallinn, Eesti
Kodakondsus Eesti
Aadress Keemia ja biotehnoloogia instituut
Tallinna Tehnikaülikool
Akadeemia tee 15, 12618 Tallinn, Eesti
Telefon +372 620 4387
E-post priit.eek@ttu.ee

HARIDUSKÄIK

2011-... Tallinna Tehnikaülikool, keemia ja geenitehnoloogia (keemia), PhD
2008-2011 Tallinna Tehnikaülikool, rakenduskeemia ja biotehnoloogia (biokeemia),
MSc (cum laude)
2005-2008 Tallinna Tehnikaülikool, rakenduskeemia ja biotehnoloogia,
BSc (cum laude)
2002-2005 Viimsi Keskkool (kuldmedal)

KEELTEOSKUS

Eesti (emakeel), inglise (kõrgtase), soome (kesktase), vene (kesktase), saksa (algtase)

TÄIENDUSÕPE

2013 EMBO praktiline kursus „Väikese nurga neutron- ja röntgenhajumine
valgulahuses”
2012 Makromolekulide röntgendifraktsiooni praktiline kursus „RapiData 2012”:
andmekogumine ja struktuuri lahendamine sünkrotronis NSLS

TEENISTUSKÄIK

2017-... Tallinna Tehnikaülikool, keemia- ja biotehnoloogia instituut,
nooremteadur
2015-2016 Tallinna Tehnikaülikool, keemiainstituut, nooremteadur
2009-2010 Louisiana Ülikool (Baton Rouge, LA, USA), bioteaduste osakond,
kaasteadur

ELULOOKIRJELDUS

ORGANISATSIOONILINE TEGEVUS

2008–... Eesti Biokeemia Selts, liige

2005–... Tehnikaülikooli Akadeemiline Meeskoor, liige (teeneline alates 2014)

PREEMIAID JA TUNNUSTUSED

2010 Üliõpilaste teadustööde riiklik konkurs, loodusteadused ja tehnika, magistrirase, III preemia

2008 Üliõpilaste teadustööde riiklik konkurs, bio- ja keskkonnateadused, bakalaureusetase, III preemia

2007 AS Hansapank, TTÜ Arengufond, bakalaureuseõppe stipendium

JUHENDATUD VÄITEKIRJAD

Doris Pooga, magistriraad, 2017, (juh) Peep Palumaa, Priit Eek. Metallotioniini 2E vasevormi kristalliseerimine. Tallinna Tehnikaülikool, Loodusteaduskond, Keemia- ja biotehnoloogia instituut.

Marianna Köster, magistriraad, 2017, (juh) Priit Eek, Ivar Järving. Inimese 15-lipoksügenaasi-1 kristallimise uuringud. Tallinna Tehnikaülikool, Loodusteaduskond, Keemia- ja biotehnoloogia instituut.

Kaspar Põldemaa, magistriraad, 2016, (juh) Priit Eek, Ivar Järving. 11R-lipoksügenaasi aktiivsuse regulatsioon: substraatinhibeerimise ja dimerisatsiooni võtmeelementide tuvastamine. Tallinna Tehnikaülikool, Matemaatika-loodusteaduskond, Keemiainstituut.

Janet Tamm, bakalaureusekraad, 2016, (juh) Priit Eek. 11R-lipoksügenaasi kvaternaarstruktuuri uuringud keemilise ristsidumise meetodil. Tallinna Tehnikaülikool, Matemaatika-loodusteaduskond, Keemiainstituut.

Marianna Köster, bakalaureusekraad, 2015, (juh) Priit Eek. Imetajate lipoksügenaaside ekspresseerimine bakterikultuuris. Tallinna Tehnikaülikool, Matemaatika-loodusteaduskond, Keemiainstituut.

Sandra Kaabel, magistriraad, 2014, (juh) Riina Aav, Priit Eek, Kaja Ilmarinen. Kiraalse isatiini derivaadi monokristall-röntgendifraktsioon analüüs Bruker Smart X2S ja Rigaku Compact HomeLab difraktomeetritega. Tallinna Tehnikaülikool, Matemaatika-loodusteaduskond, Keemiainstituut.

Doris Pooga, bakalaureusekraad, 2014, (juh) Peep Palumaa, Priit Eek. Metallotioniini 2E vasevormi kristalliseerimine. Tallinna Tehnikaülikool, Matemaatika-loodusteaduskond, Geenitehnoloogia instituut.

Helian Vunk, bakalaureusekraad, 2014, (juh) Priit Eek. Proteolüütiliselt eemaldatava His₆-epitoobiga 11R-lipoksügenaasi ekspressioon ning puhastamine. Tallinna Tehnikaülikool, Matemaatika-loodusteaduskond, Keemiainstituut.

Kaspar Põldemaa, bakalaureusekraad, 2014, (juh) Priit Eek. 11R-lipoksügenaasi substraadikanaali potentsiaalsete suudmete mutatsioonanalüüs. Tallinna Tehnikaülikool, Matemaatika-loodusteaduskond, Keemiainstituut.

Mari-Ann Piht, magistrakraad, 2013, (juh) Priit Eek. Arg106–Asp173 sild 11R-lipoksügenaasi allosteerilise regulatsiooni vahendajana. Tallinna Tehnikaülikool, Matemaatika-loodusteaduskond, Keemiainstituut.

Mari-Ann Piht, bakalaureusekraad, 2011, (juh) Priit Eek, Reet Järving. Lipoksügenaaside PLAT domeenide kloonimine ja ekspresseerimine. Tallinna Tehnikaülikool, Matemaatika-loodusteaduskond, Keemiainstituut.

PUBLIKATSIOONID

Eek, P., Järving, R., Järving, I., Gilbert, N. C., Newcomer, M. E., Samel, N. (2012) Structure of a calcium-dependent 11R-lipoxygenase suggests a mechanism for Ca^{2+} regulation. *J. Biol. Chem.* 287 (26), 22377–22386.

Eek, P., Piht, M.-A., Rätsep, M., Freiberg, A., Järving, I., Samel, N. (2015) A conserved π -cation and an electrostatic bridge are essential for 11R-lipoxygenase catalysis and structural stability. *Biochim. Biophys. Acta. Mol. Cell Biol. Lipids* 1851 (10), 1377–1382.

Eek, P., Pöldemaa, K., Kasvandik, S., Järving, I., Samel, N. (2017) A PDZ-like domain mediates the dimerization of 11R-lipoxygenase. *Biochim. Biophys. Acta. Mol. Cell Biol. Lipids* 1862 (10 Pt A), 1121–1128.

KONVERENTSIDE ETTEKANDED

Eek, P., Pöldemaa, K., Kasvandik, S., Järving, I., Samel, N. (2016) Investigation of 11R-lipoxygenase quaternary structure. *6th European Workshop on Lipid Mediators*, Frankfurt am Main, Saksamaa.

Eek, P., Järving, R., Järving, I., Newcomer, M.E., Samel, N. (2011) 11R-lipoksügenaasi kristallstruktuuri mudel. *XXXII Eesti keemiapäevad*, Tartu, Eesti.